ISTANBUL TECHNICAL UNIVERSITY ★ GRADUATE SCHOOL OF SCIENCE ENGINEERING AND TECHNOLOGY

A STUDY ON PRESSURE TRANSIENT TESTING UNDER OIL-WATER FLOW CONDITIONS

M.Sc. THESIS

Gismat VALIYEV

Department of Petroleum and Natural Gas Engineering

Petroleum and Natural Gas Engineering

Thesis Advisor: Prof. Dr. Abdurrahman SATMAN

SEPTEMBER 2014

ISTANBUL TECHNICAL UNIVERSITY ★ GRADUATE SCHOOL OF SCIENCE ENGINEERING AND TECHNOLOGY

A STUDY ON PRESSURE TRANSIENT TESTING UNDER OIL-WATER FLOW CONDITIONS

M.Sc. THESIS

Gismat VALIYEV
(505101500)

Department of Petroleum and Natural Gas Engineering

Petroleum and Natural Gas Engineering

Thesis Advisor: Prof. Dr. Abdurrahman SATMAN

SEPTEMBER 2014

İSTANBUL TEKNİK ÜNİVERSİTESİ ★ FEN BİLİMLERİ ENSTİTÜSÜ

PETROL-SU FAZLI AKIŞ KOŞULLARINDA KARARSIZ BASINÇ TESTİ ÇALIŞMASI

YÜKSEK LİSANS TEZİ

Gismat VALİYEV
(505101500)

Petrol ve Doğal Gaz Mühendisliği Anabilim Dalı

Petrol ve Doğal Gaz Mühendisliği Programı

Tez Danışmanı: Prof. Dr. Abdurrahman SATMAN

EYLÜL 2014

Gismat Valiyev, a **M.Sc.** student of ITU **Graduate School of Science Engineering and Technology** student ID **505101500**, successfully defended the **thesis** entitled "**A STUDY ON PRESSURE TRANSİENT TESTİNG UNDER OIL-WATER FLOW CONDİTİONS**", which he prepared after fulfilling the requirements specified in the associated legislations, before the jury whose signatures are below.

Thesis Advisor : **Prof. Dr. Abdurrahman SATMAN** .....
İstanbul Technical University

Jury Members : **Prof. Dr. Abdurrahman SATMAN** .....
İstanbul Technical University

Assis. Prof. Dr. Ömer İnanç TÜREYEN .....
İstanbul Technical University

Prof. Dr. Ayşe KAŞLILAR .....
İstanbul Technical University

Date of Submission : 3 September 2014
Date of Defense : 26 September 2014

To my family and my friends,

FOREWORD

I would like to thank my adviser Prof. Dr. Abdurrahman SATMAN for his support guidance and voluable advices at my thesis. Also I appreciate help of my teacher Assoc. Prof. Dr. Ömer İnanç TÜREYEN in my work on thesis. In addition I apreciate advices and help of Dr. Turan IBRAHIMOV. I would like to thank my family members and my friends, who supported me morally during the thesis period.

September 2014

Gismat VALIYEV
(Petroleum engineer)

TABLE OF CONTENTS

Page

FOREWORD ..... **ix**
TABLE OF CONTENTS ..... **xi**
ABBREVIATIONS ..... **xiii**
LIST OF TABLES ..... **xv**
LIST OF FIGURES ..... **xvii**
SUMMARY ..... **xix**
ÖZET ..... **xxi**
1. INTRODUCTION **1**
1.1 Evolution of The Basin 3
1.2 Overview of ACG Field Complex 7
2. LITERATURE REVIEW **11**
3. PROBLEM STATEMENT AND MODELING APPROACH **13**
3.1 Problem Statement And Purpose of Thesis 13
3.2 Forming of simple model for the reservoir 13
4. SAPPHIRE ANALYSIS **17**
4.1 Study of The Oil Field Without Aquifer 17
4.1.1 Case 1: μ_o=0.45 cp 18
4.1.2 Case 2: μ_o=4.5 cp 30
4.2 Study of The Oil Field With Aquifer 38
4.2.1 Case 1: μ_o=0.45 cp 40
4.2.2 Case 2: μ_o=4 cp 50
5. CONCLUSIONS **59**
REFERENCES **61**
CURRICULUM VITAE **63**

ABBREVIATIONS

ACG : Azeri Chirag Gunashli
AIOC : Azerbaijan International Oil Company
BOPD : Barrel Oil Per Day
BHT : Bottomhole Temperature
CA : Central Azeri
EA : East Azeri
GTS : Geologic Time Scale
Ma : Million age
MMBO : Million Barrel Oil
PSA : Production Sharing Agreement
SWG : Shallow Water Gunashli
TVD : True Vertical Depth
WA : West Azeri
GTS : Geologic Time Scale

GREEK SYMBOLS

Parameter	***Field Units***	***SI Units***
λ *- Mobility*	*md/cp*	$m^2/Pa{\cdot}s$
μ *- Viscosity*	*cp*	$Pa{\cdot}s$
ϕ *- Porosity*	*fraction*	*fraction*

SUBSCRIPTS

f – formation
g – gas
i – initial
o – oil
t – total
w – water

NAMENCLATURE

Parameter	***Field Units***	***SI Units***
A *- Area*	ft^2	m^2
B *- Formation Volume Factor*	*bbl/STB*	$m^3/st\ m^3$
c *- Compressibility*	psi^{-1}	Pa^{-1}
h *- Thickness*	*ft*	*m*
k *- Permeability*	*md*	m^2
$\boldsymbol{k_r}$ *- Relative Permeability*	*dimensionless*	*dimensionless*
m *- Slope*	*psi/log cycle*	*Pa/log cycle*
P *- Pressure*	*psia*	*Pa*
q *- Production Rate*	*STB/D*	sm^3/s
$\boldsymbol{R_s}$ *- Solution Gas In Oil Ratio*	*Scf/STB*	$m^3/st\ m^3$
$\boldsymbol{R_{sw}}$ *- Solution Gas In Water Ratio*	*Scf/STB*	sm^3/sm^3
S *- Saturation*	*fraction*	*fraction*
s *- Skin Factor*	*dimensionless*	*dimensionless*
$\boldsymbol{S_{wi}}$ *- Initial Water Saturation*	*fraction*	*fraction*
$\boldsymbol{S_{or}}$ *- Irreducible Oil Saturation*	*fraction*	*fraction*
V *- Volume*	ft^3	m^3
$\boldsymbol{V_p}$ *- Pore Volume*	ft^3	m^3
$\boldsymbol{W_w}$ *- Cumulative Volume of Water At Any Time*	ft^3	m^3
$\boldsymbol{W_e}$ *- Cumulative Water Influx Volume*	ft^3	m^3
$\boldsymbol{W_i}$ *- Initial Water Volume*	ft^3	m^3
$\boldsymbol{W_p}$ *- Cumulative Water Production*	ft^3	m^3

LIST OF TABLES

Page

Table 3.1 : Input data that used for model..... 14
Table 4.1 : Data from Rubis model simulation and Sapphire analysis. 26
Table 4.2 : The calculated values of total mobility of system..... 28
Table 4.3 : Calculated $(k)_{sw}$ values..... 29
Table 4.4 : Data from Rubis model simulation and Sapphire analysis 36
Table 4.5 : The calculated values of total mobility of system..... 37
Table 4.6 : Calculated (k_{sw}) values..... 38
Table 4.7 : Data from Rubis model simulation and Sapphire analysis 45
Table 4.8 : Calculated W_w data 48
Table 4.9 : Calculated valumetric averaged total mobility values for piston-like displacement 48
Table 4.10 : Calculation results of equation **(4.15)**..... 49
Table 4.11 : Calculated valumetric averaged total mobility values for $(k_{rw})_{\bar{s}_w}$=0.82 49
Table 4.12 : Calculation results of equation **(4.15)** for $(k_{rw})_{\bar{s}_w}$=0.82..... 50
Table 4.13 : Data from Rubis model simulation and Sapphire analysis 56
Table 4.14 : Calculated W_w data 57
Table 4.15 : Calculated valumetric averaged total mobility values for piston-like displacement 57
Table 4.16 : Calculation results of equation **(4.15)** for piston-like approach..... 57
Table 4.17 : Calculated valumetric averaged total mobility values for $(k_{rw})_{\bar{s}_w}$=0.48. 58
Table 4.18: Calculation results of equation **(4.15)** for $(k_{rw})_{\bar{s}_w}$=0.48..... 58

LIST OF FIGURES

Page

Figure 1.1 : Location of ACG in the South Caspian Basin. 2
Figure 1.2 : Structural elements of the South Caspian Basin..... 3
Figure 1.3 : Structural elements of the South Caspian Basin..... 4
Figure 1.4 : Paleography of the South Caspian Basin (A) prior to the latest Miocene drop 5
Figure 1.5 : Paleography of the South Caspian Basin (B) after the latest Miocene drop. 6
Figure 1.6 : Stratigraphy and lithology. 8
Figure 1.7 : Stratigrapy example. 9
Figure 1.8 : ACG field complex..... 10
Figure 3.1 : 3D geometry plot of the model. 14
Figure 3.2 : Relative permeability curves. 15
Figure 4.1 : 2D geometry plot of the model. 17
Figure 4.2 : The capillary pressure plot of the model. 17
Figure 4.3 : Bottomhole pressure and surface production rate plot for S_w=0. 18
Figure 4.4 : Sapphire buildup analysis in a case of S_w=0. 18
Figure 4.5 : Bottomhole pressure and surface production rate plot for S_w=0.1. 19
Figure 4.6 : Sapphire buildup analysis in a case of S_w=0.1. 19
Figure 4.7 : Bottomhole pressure and surface production rate plot for S_w=0.2. 20
Figure 4.8 : Sapphire buildup analysis in a case of S_w=0.2. 20
Figure 4.9 : Bottomhole pressure and surface production rate plot for S_w=0.3. 21
Figure 4.10 : Sapphire buildup analysis in a case of S_w=0.3. 21
Figure 4.11 : Bottomhole pressure and surface production rate plot for S_w=0.4. 22
Figure 4.12 : Sapphire buildup analysis in a case of S_w=0.4. 22
Figure 4.13 : Bottomhole pressure and surface production rate plot for S_w=0.5. 23
Figure 4.14 : Sapphire buildup analysis in a case of S_w=0.5. 23
Figure 4.15 : Bottomhole pressure and surface production rate plot for S_w=0.6. 24
Figure 4.16 : Sapphire buildup analysis in a case of S_w=0.6. 24
Figure 4.17 : Bottomhole pressure and surface production rate plot for S_w=0.7. 25
Figure 4.18 : Sapphire buildup analysis in a case of S_w=0.7. 25
Figure 4.19 : Comparison of effective permeability from Sapphire to oil relative permeability from Rubis model..... 26
Figure 4.20 : Bottomhole pressure and surface production rate plot for S_w=0. 30
Figure 4.21 : Sapphire buildup analysis in case of S_w=0. 31
Figure 4.22 : Bottomhole pressure and surface production rate plot for S_w=0.1. 31
Figure 4.23 : Sapphire buildup analysis in a case of S_w=0.1. 32
Figure 4.24 : Bottomhole pressure and surface production rate plot for S_w=0.2. 32
Figure 4.25 : Sapphire buildup analysis in a case of S_w=0.2. 33
Figure 4.26 : Bottomhole pressure and surface production rate plot for S_w=0.3. 33

Figure 4.27 : Sapphire buildup analysis in a case of S_w=0.3. 34
Figure 4.28 : Bottomhole pressure and surface production rate plot for S_w=0.4. 34
Figure 4.29 : Sapphire buildup analysis in a case of S_w=0.4. 35
Figure 4.30 : Bottomhole pressure and surface production rate plot for S_w=0.5. 35
Figure 4.31 : Sapphire buildup analysis in a case of S_w=0.5. 36
Figure 4.32 : Comparison of effective permeability from Sapphire with oil the permeability from Rubis model. 37
Figure 4.33 : The capillary pressure plot of the model. 38
Figure 4.34 : 2D geometry plot of the model. 39
Figure 4.35 : Bottomhole pressure and surface production rate plot for t_p=7000 hr. 40
Figure 4.36 : 3D geometry plot of the simulated model. 40
Figure 4.37 : The cross sectional plot of simulated model. 41
Figure 4.38 : Sapphire buildup analysis for t_p=7000 hr. 41
Figure 4.39 : Bottomhole pressure and surface production rate plot for t_p=53 000 hr. 42
Figure 4.40 : 3D geometry plot of the simulated model. 42
Figure 4.41 : The cross sectional plot of simulated model. 43
Figure 4.42 : Sapphire buildup analysis for t_p=53 000 hr. 43
Figure 4.43 : Bottomhole pressure and surface production rate plot for t_p=100 000 hr 44
Figure 4.44 : The cross sectional plot of simulated model. 44
Figure 4.45 : 3D geometry plot of the simulated model. 45
Figure 4.46 : Sapphire buildup analysis for t_p=100 000 hr. 45
Figure 4.47 : Bottomhole pressure and surface production rate plot for t_p=10 000 hr. 50
Figure 4.48 : Sapphire buildup analysis for t_p=10 000 hr. 51
Figure 4.49 : The cross sectional plot of simulated model. 51
Figure 4.50 : 3D geometry plot. 52
Figure 4.51 : Bottomhole pressure and surface production rate plot for t_p=18 000 hr. 52
Figure 4.52 : Sapphire buildup analysis for t_p=18 000 hr. 53
Figure 4.53 : The cross sectional plot of simulated model. 53
Figure 4.54 : 3D geometry plot. 54
Figure 4.55 : Bottomhole pressure and surface production rate plot for t_p=30 000 hr. 54
Figure 4.56 : Sapphire buildup analysis for t_p=30 000 hr. 55
Figure 4.57 : The cross sectional plot of simulated model. 55
Figure 4.58 : 3D geometry plot. 56

A STUDY ON PRESSURE TRANSIENT TESTING UNDER OIL-WATER FLOW CONDITIONS

SUMMARY

Azeri Chirag Gunashli (ACG) field complex is one of the well known hydrocarbon fields of Azerbaijan at the Caspian Sea. ACG is located at the northern margin of the South Caspian Basin. At the end of 70's the first part Gunashli was discovered and at 80's the rest of Azeri and Chirag sectors were confirmed. For extracting the hydrocarbon reserves, a production sharing agreement was established by Azerbaijan International Oil Company (AIOC). BP company is operating the ACG field complex on behalf of the companies, which includes the AIOC. ACG's oil reserves are estimated to be more than 13 billion stock tank barrels. In 2013 the total production from the field was over 239 million barrel.

To determine the reservoir performance different measurements and tests have been conducted. Well transient testing (WTT) provides indirect determination of reservoir and well parameters. It is one of the most important diagnostic tools used by petroleum engineers to characterize hydrocarbon presence and predict their future performance. Well testing is an important tool used in the industry to obtain data representing well/reservoir system under in-situ and dynamic conditions on a larger scale. Well transient test provides knowledge to determine several parameters, such as permeability under in-situ conditions, average reservoir pressure, productivity index, conditions near the wellbore such as skin factor, as well as distances to outher boundaries.

In WTT interpretation and calculation of parameters, usually single phase conditions are assumed. The fluid flow in Azeri field sector is in multiphase state. But WTT interpretations in Azeri are conducted by using single phase interpretation methods. In this thesis studies were conducted to learn how the water presence would influence the permeability value of test interpretations. The results of this study provides us knowledge that would be used in interpretations in the wells of Azeri field sector. The study commenced by creating the simplified model using the Ecrin Rubis software. Rubis software allows us to create field model and divide it into numerous grids. Also it is easy to enter parameter inputs and run different simulations. After simulating the field model the measured pressure and rate data were transferred to the Ecrin Sapphire software. Using Sapphire it is possible to interpret pressure test data and also to investigate the effects of water.

PETROL-SU FAZLI AKIŞ KOŞULLARINDA KARARSIZ BASINÇ TESTİ ÇALIŞMASI

ÖZET

Azeri Çırag Güneşli (AÇG) petrol sahası Azerbaycan Cumhuriyetinin Hazar denizindeki tanınmış sahalarından bir tanesidir. AÇG sahası Güney Hazarın kuzey sınırlarında yerleşmiştir. İlk olarak 70'lerin sonlarında AÇG sahasının Güneşli kısmı keşfedilmiş, daha sonra 80'lerin ikinci yarısında diğer Azeri ve Çırag kısımları keşf edilmiş ve onaylanmıştır. Hidrokarbon rezervlerinin üretimi için altı farklı ülkeden yerli ve yabancı petrol şirketlerinden kurulu "Azerbaijan International Oil Company" (AIOC) şirketi kurulmuştur. Bu şirketler birliğinin üyesi olan BP şirketi AÇG sahasının operatörü olarak yapılan ve planlanan işleri yürütmektedir. AÇG sahasının petrol rezervleri 13 milyardan fazla olarak değerlendirilmektedir. 2013 yılında AÇG'den elde edilen petrol üretimi 239 milyon varil olmuştur.

Rezervuar performansını değerlendirmek için bir çok farklı yöntemler ve testler yapılmaktadır. Petrol endüstrisinde kuyu testleri rezervuar ve kuyu parametrelerinin değerlendirilmesinde geniş bir şekilde uygulanmaktadır. Aynı zamanda kuyu testleri petrol mühendislerinin rezervuarda geniş ölçeklerde dinamik ortamlarda araştırmalar yapabilmesi için en önemli araçlardan bir tanesidir. Kuyu testleri bir sıra parametrelerin ölçülmesi ve hesaplanması için olanaklar yaratılmaktadır. Bunlara örnek olarak geçirgenliğin, ortalama rezervuar basıncının ve verimliliğin hesaplanmasını, kuyu civarının değerlendirilmesini, zar faktörünün hesaplanmasını ve kuyudan drenaj sınırlarına kadar olan uzaklığın tahminini gösterebiliriz.

Genellikle kuyu testlerinde, parametrelerin hesaplanması ve sistemin yorumlanması bir fazlı akış sistemlerine dayanmaktadır. Bilindiği gibi AÇG rezervuarında akış çok fazlı ortamda olmaktadır. Su fazının kuyu testi değerlendirilmesini nasıl etkilediğini bilmek son derece önemlidir. Bu bakımdan bu tezde su durumunun test değerlendirmesine etkileri incelenmektedir. Bu amaçla "Ecrin Rubis" bilgisayar programında basitleştirilmiş saha modeli kurulmuştur. "Rubis" programı kuyu ve rezervuar özelliklerini yansıtan parametrelerin kolay dahil edilmesi, sahanın gridlenmesi, rezervuarın bulunduğu koşulları da göz önüne alarak petrol sahasının modelinin kurulmasına olanak yaratmaktadır. "Rubis'de" kurulan basitleştirilmiş saha modeli çalıştırıldıktan sonra sahada ölçülen kuyu dibi basıncı ve üretim debisi verileri değerlendirilmiştir. "Rubis'ten" alınan basınç ve debi verilerinin analizi için "Ecrin Sapphire" bilgisayar programı kullanılmıştır. "Sapphire" programı genel olarak kuyu testlerinin yorumlanmasında kullanılan bilgisayar programlarından biridir. Tek fazlı sistemlerin testlerinin değerlendirilmesinin dışında "Sapphire" programında, program dahilinde sisteme su fazını da eklemek mümkündür. "Rubis" programından elde edilen veriler "Sapphire" programına aktarılmış ve değerlendirilmiştir.

Bu tezde iki durum için araştırma yapılmıştır. Birinci durumda "Rubis" kullanılarak sınırları kapalı olan petrol-su akışlı iki fazlı bir rezervuar modeli kurulmuştur. Su

doymuşluğu sıfırdan başlayarak 0.7'ye kadar yükseltilmiş ve elde edilen kuyu dibi basıncı ve kuyu başı üretim debisi verileri "Sapphire" programında analiz edilmiştir. "Sapphire"de analizin nasıl yapıldığına dair açıklamalar tezde gösterilmiştir. Genellikle her iki durum için yapılan araştırmalarda "Sapphire"de basınç analizleri bir fazlı akış varsayımına göre yapılmıştır. Birinci durum için yapılan araştırmada "Rubis"de rezervuar modeli kurulurken petrol akmazlığı 0.45 cp ve su akmazlığı 0.35 cp olarak varsayılmıştır. Araştırma sonucunda elde edilmiş sonuçlar Perrine yaklaşımına göre analiz edilmiştir. Çok fazlı akış sistemleri için Perrine'nin yaklaşımı tez içeriğinde verilmiştir. Bununla ilgili olarak uygun su doymuşluğuna göre sistemin toplam mobiliteleri hesaplanmış ve bu çalışmada önerdiğimiz ilişkiyle veriler analiz edilmiştir.

Akifersiz sistemin araştırılmasından çıkan genel sonuçta iki fazlı petrol-su akışlı sistemlerinden elde edilen basınç verilerinin bir fazlı akış modeline göre analiz edildiğinde elde edilen geçirgenlik değerinin aslında tek fazlı sistemin geçirgenliğini vermediğini, iki fazlı sistemin petrol-su karışımının efektif gecirgenliğini verdiği görüldü. Aynı zamanda sistem dahilinde su doymuşluğunun yükselmesinin basınç testi analizinden elde olunan geçirgenlik değerine etki ettiği görüldü. Fazların akmazlık değerlerindeki değişikliğin araştırma sonucuna olan etkisini öğrenmek için ayni araştırma prosedürleri farklı akmazlık değerlerinde yeniden yapılmıştır. Bu sefer petrolün akmazlığı 0.45'ten 4.5 cp'e çıkarılırken suyun akmazlığı aynı 0.35 cp olarak modele girilmiştir. Fazlar arasındaki yüksek akmazlık farkının oluşması, akmazlığı daha düşük olan su fazının sistem dahilinde daha mobil olmasına ve sonuç olarak da su doymuşluğunun daha küçük değerlerinde su üretiminin yükselmesine sebep olduğu gözlemlenmiştir.

İkinci durumda akifer olduğu zaman için araştırma yapılmıştır. "Rubis" programı kullanılarak iki fazlı petrol-su akışlı rezervuar modeli rezervuarın doğu tarafına akifer yerleştirilerek kurulmuştur. Rezervuara bir sınırdan su girişi olduğu için, sistemin su doymuşluğu akifersiz sistemin araştırılmasındaki gibi tüm rezervuar içinde eşit olarak yayılmamaktadır. Bu durumda sistem kısmen su ile doymuş olmaktadır.

Akiferli sistemin araştırılması üç koşula göre yapılmıştır. Birinci koşulda su fazı çok az miktarda rezervuara girmekte, ama henüz üretim kuyusuna varmamış durumdadır. İkinci koşulda akiferden rezervuara giren olan su üretim kuyusuna kadar ulaşıyor, ama rezervuardan üretilen suyun debisi çok küçük miktarlarda oluyor. Üçüncü koşulda akiferden rezervuara giren olan su üretim kuyusuna varıyor ve üretilen suyun miktarı yüksek seviyelere ulaşmış oluyor. Bu koşullarda çalıştırılan rezervuar modelinden elde olunan kuyu dibi basıncı ve kuyu başı üretim debisi verileri "Sapphire"e aktarılmış ve bir fazlı akış sistemine göre varsayım yapılarak analiz edilmiştir. Akiferli sistemin araştırılmasından elde olunan sonuçlar hacimsel denge yaklaşımıyla yorumlanmıştır. Bununla ilgili olarak ortalama hacimsel mobiliteleri hesaplamak için bir ilişki önerilmiştir. Bu araştırmada da akifersiz sistemde olduğu gibi akmazlık değerinde olan değişimin sonuçlara olan etkisine bakılmıştır.

Akifersiz sistemin araştırılmasından elde edilen genel sonuç; iki fazlı petrol-su akışlı sistemlerin verilerinin bir fazlı sisteme göre varsayım yapılarak basınç testi analizi yapılmasından bulunan geçirgenlik değerinin aslında iki fazlı sistemin geçirgenlik değerini vermediğidir. Basınç testi analizinden alınan geçirgenliğin aslında iki fazlı sistemdeki petrol-su karışımı için toplam bir geçirgenlik değeri olduğu sonucuna varılmıştır.

Hem akifersiz ve hem de akiferli sistemin araştırılmasında su fazının basınç testi analizine olan etkisine dair ayrıntılı açıklamalar tezde verilmiştir.

1. INTRODUCTION

The Azeri-Chirag-Gunashli (ACG) field complex is located 100 km South East of Baku, in the South Basin of offshore Azerbaijan (**Figure 1.1**). This entire field complex for development purposes is divided into Azeri, Chirag, Gunashli areas. Gunashli is also divided into two areas: Deep-Water Gunashli (DWG) and Shallow-Water Gunashli (SWG). The water depth where the ACG locates is in 120-350 m. Firstly in 1978 Gunashli was discovered. During 1985-87, Chirag and Azeri have been confirmed as an extention of Gunashli. The first production began from SWG in 1980. In Soviet Union times there was a lack of deep-water technology, hence this caused SWG first to be developed first. Until the end of 1991, the cumulative production from SWG had reached 244 MMBO. In 1986 to maintain high production rates water injection was started. As the result of water injection application in 1991 production had reached its peak value, approximately 130 000 barrel oil per day (BOPD) (C&C Reservoirs, 2005).

In December 1994, ten different oil companies from six different countries established the Azerbaijan International Oil Company (AIOC). These oil companies agreed the Production Sharing Agreement (PSA) terms with Azerbaijan. BP company operates the field on behalf of the shareholders. Following companies have shares in ACG: BP 35.8%, SOCAR 11.6%, Chevron 11.3%, INPX 11%, Statoil 8.6%, ExxonMobil 8%, TPAO 6.8%, ITOCHU 4.3%, ONGC Videsh Limited (OVL) 2.7% (Url-1, 2014).

From that time knowing in common as an ACG field the first production was realised at Chirag in 1997. Chirag is an offshore production, drilling and quarters (PDQ) platform. The facilities of Chirag consist of: 24 slot PDQ platform with water injection equipment, 176 km long 24-inch oil pipeline to the receiving terminal at Sangachal, 48 km long 16-inch gas pipeline to the oil rocks, 12 km long 18-inch gas pipeline to Central Azeri. At the end of 2013, Chirag produced on average 69 670 BOPD and had 13 oil producer and 5 water injector wells. There are three offshore production, drilling and quarters (PDQ) platforms at the Azeri area: Central Azeri,

West Azeri and East Azeri. The facilities of Central Azeri (CA) consist of: 48 slot production, drilling and quarters (PDQ) platform, 30-inch oil pipeline from CA to the Sangachal Terminal, 28-inch gas pipeline from CA to the Sangachal Terminal, expansion of the existing onshore terminal at Sangachal. At the end of 2013, Central Azeri produced on average 151 760 BOPD and had 17 oil producer, 1 water injector and 6 gas injector wells (Url-1, 2014).

The facilities of West Azeri (WA) consist of: 48 slot production, drilling and quarters (PDQ) platform, 30-inch oil pipeline from WA to the Sangachal Terminal. At the end of 2013, WA produced on average 151 760 BOPD and had 20 oil producer and 6 water injector wells (Url-1, 2014).

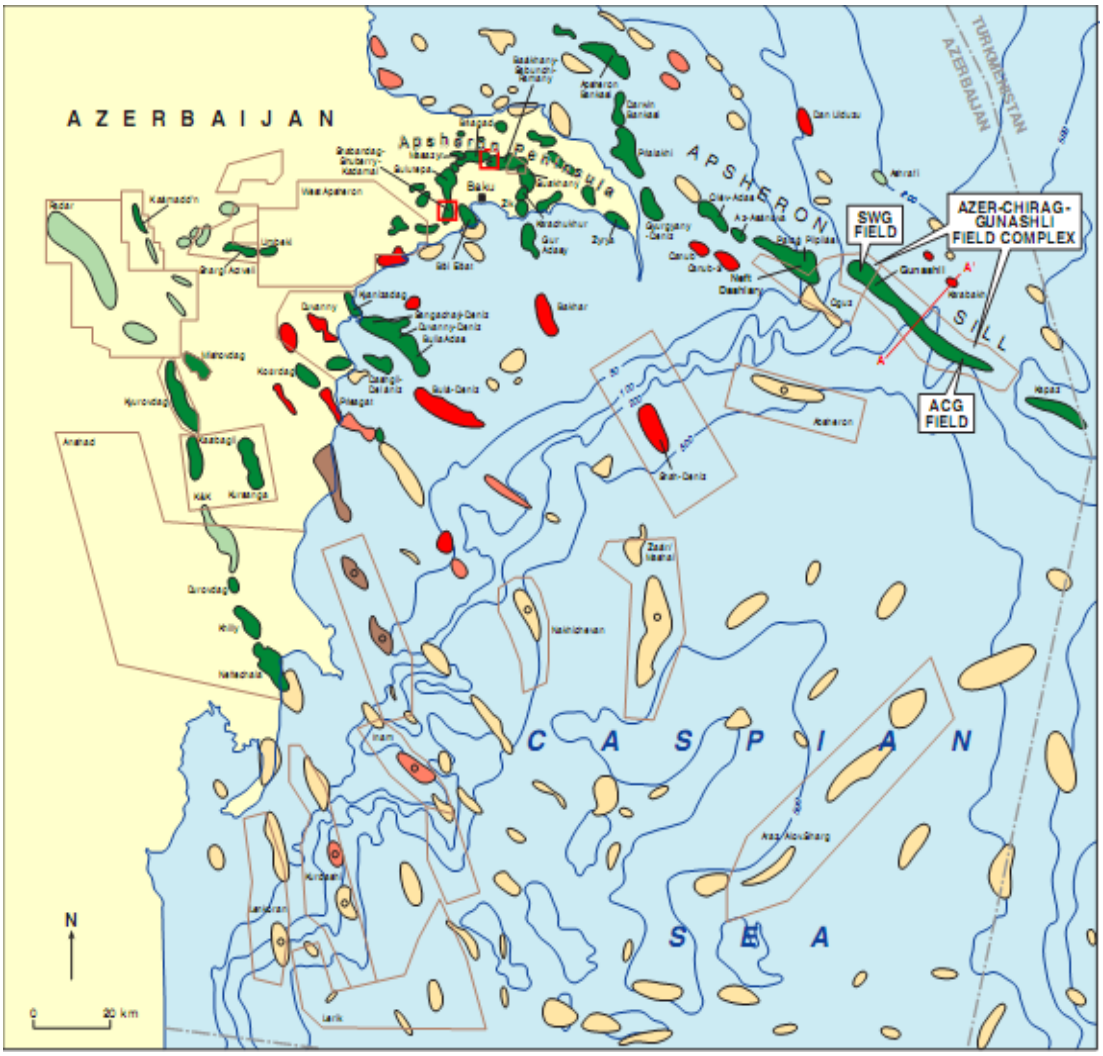

Figure 1.1 : Location of ACG in the South Caspian Basin (C&C Reservoirs, 2005).

The facilities of the East Azeri (EA) consist of: 48 slot production, drilling and quarters (PDQ) platform, 22-inch gas pipeline from EA directed to Central Azeri platform, 30-inch oil pipeline from Central Azeri to Sangachal Terminal. At the end

of 2013 year East Azeri produced on average 106 700 BOPD and had 15 oil producer, 5 water injector wells (Url-1, 2014).

The first oil production from Deepwater Gunashli (DWG) complex occurred in 2008. DWG complex consists of two bridge-linked platforms: 48 slot drilling, utilities, and quarters (DUQ) platform, a process, gas compression, water injection and utilities (PCWU) platform. At the end of 2013, DWG produced on average 139 080 BOPD, 16 oil producer and 14 water injector wells exist in DWG.

In 2013, average production from ACG was 655 370 BOPD. In total over 239 million barrels of oil has been produced (Url-1, 2014).

1.1 Evolution of The Basin

The ACG field Complex is located on the Apsheron Ridge at the northern margin of the South Caspian Basin. The Basin is surrounded by mountain belts. The South Caspian Basin from the north are limited by the West North-West trending lineament of the Great Caucasus Mountains, Apsheron Ridge and Balkan/Kopet Dag Mountains **(Figure 1.2)**.

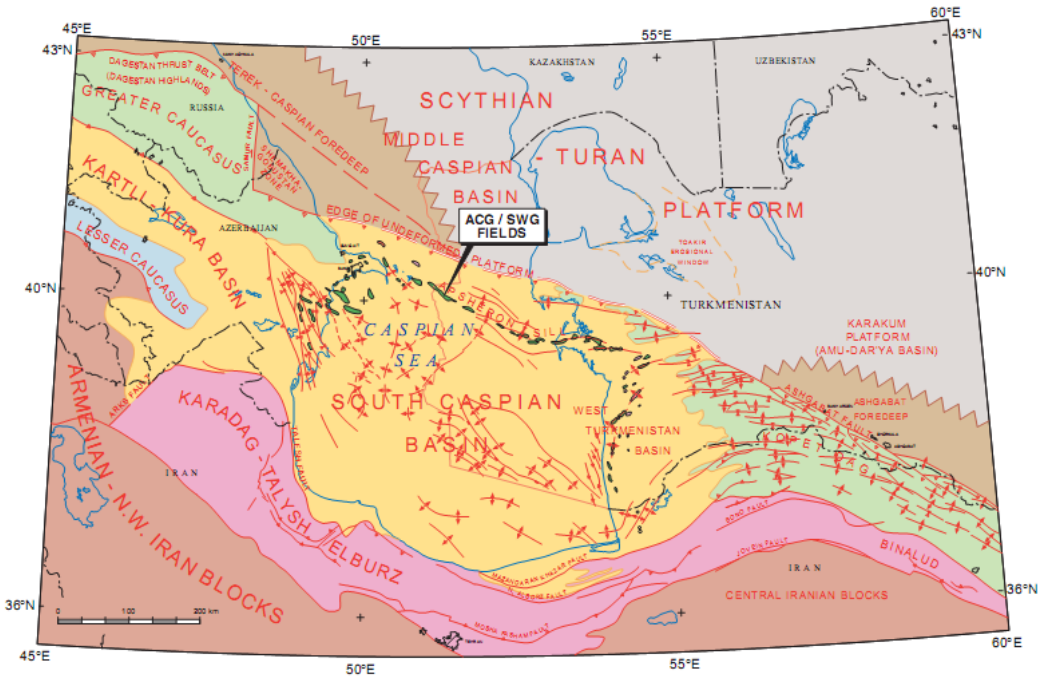

Figure 1.2 : Structural elements of the South Caspian Basin (C&C Reservoirs, 2005).

In **Figure 1.3** the geologic time scale (GTS) is shown.

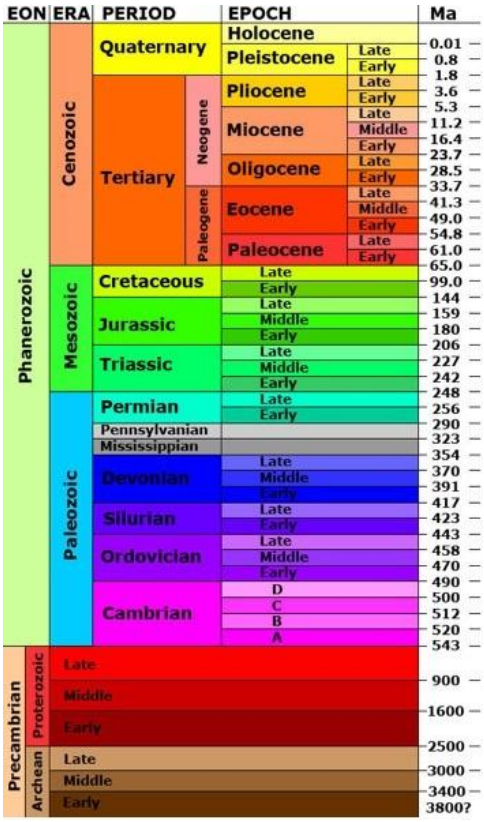

Figure 1.3 : Structural elements of the South Caspian Basin (Url-2, 2014).

In the deepest and central areas of the basin there is a fragment of oceanic crust, which is related to Mesozoic-Recent sediments that overlie basaltic basement. The thickness of that Mesozoic-Recent sediment is 25 km. When Iran and Eurasia continental plates collapsed, the collision triggered activity pushing down that oceanic crust. In Tertiary period during the rapid subsidence, the basin filled approximately 15 km of sediments (C&C Reservoirs, 2005). In Pliocene-Recent time the sediment accumulating increased up to 7 km in just 5 million age (Ma). The north edge lineament of South Caspian Basin is also the deformed southern margin of the stable Scytion-Turan Platform, which is a part of the Eurasion plate (**Figure 1.2**). That area also shows the joint line of the former Paleo-Tethys Ocean. The merging of the Iran and Turan continental blocks, which happened in the Late Triassic period, closed that ocean. In the Early Jurassic period at the Basin of the prior joint line, which referred to Para-Tethys, created a narrow marin. In the Paleocene-Eocene period, new extensions in the same merge line caused a crack line, which generated the oceanic crust in the Central South Caspian Basin. This basin in the Baku and Apsheron areas filled with up to 1250 m of Upper Cretaceous-Paleocene marine shales, marls and limestones with discountinous sandy and conglomeratic layers.

Because of poor reservoir quality, these units are miner producers in onshore areas. During the Oligocene period compressional norrowing and massive eustatic sea level created anoxic circumstances in Para-Tethys and formation of the main hydrocarbon source rock of the Maikop Series. Miocene deposits are dominantly organic rich and the thickness of these deposits reach 1000 m (C&C Reservoirs, 2005). In the latest Miocene, new compression with a massive eustatic sea level drop, caused a sharp drop in base level, with a range between 600-1500 m in 5.5 Ma. The South Caspian became isolated in a semi-arid climate. Major rivers fed the basin with the vast volumes of sediments, which were subsided very rapidly. In **Figures 1.4** and **1.5** the difference in the base area prior to and after the latest Miocene drop is shown.

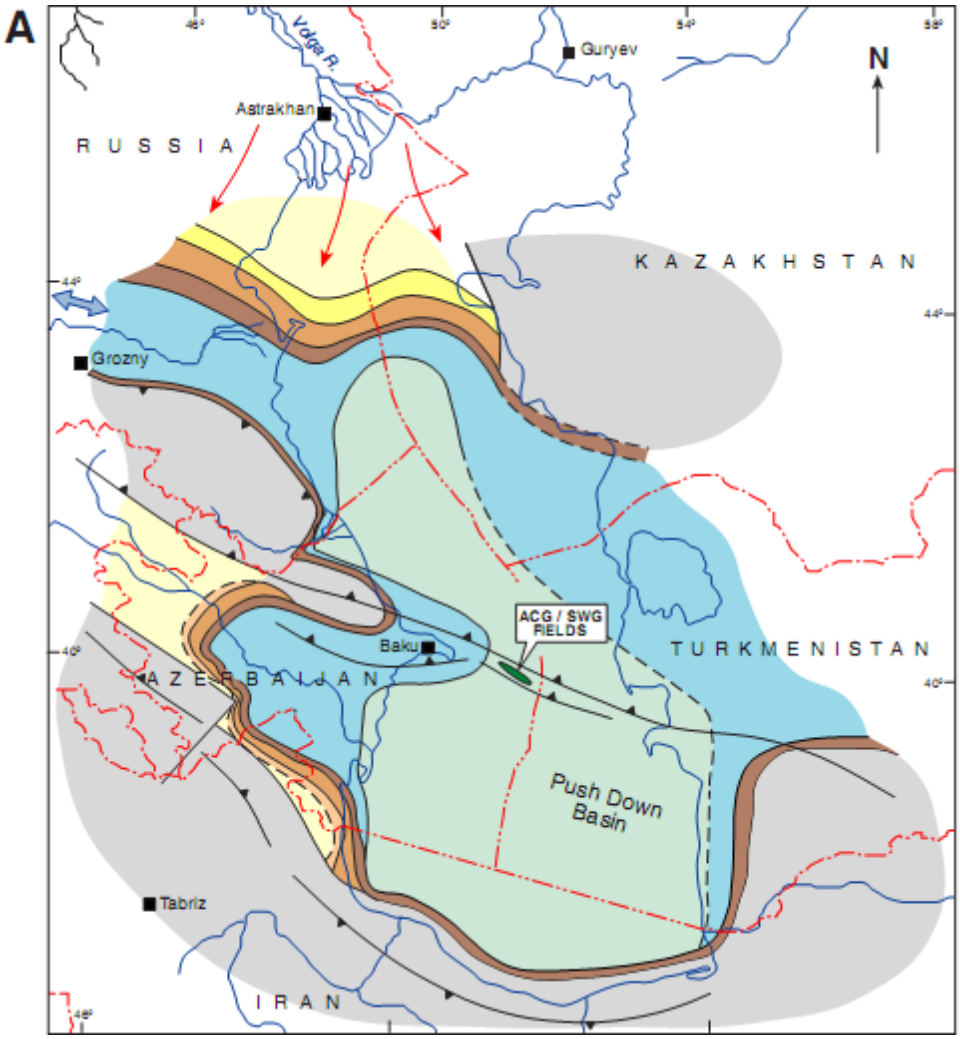

Figure 1.4 : Paleography of the South Caspian Basin (A) prior to the latest Miocene drop (C&C Reservoirs, 2005).

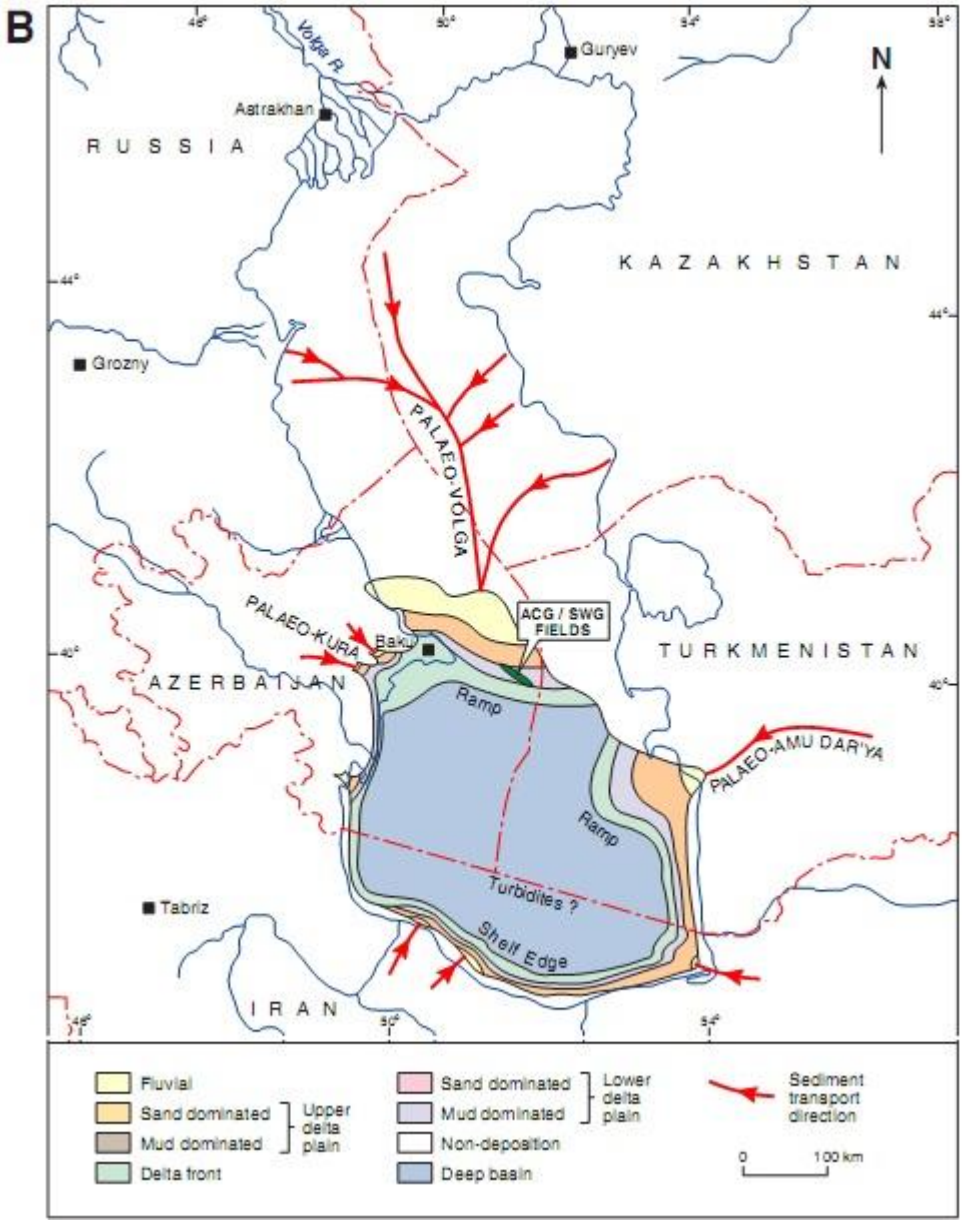

Figure 1.5 : Paleography of the South Caspian Basin (B) after the latest Miocene drop (C&C Reservoirs, 2005).

From the south-flowing Paleo-Volga River, the sediment came and created a vast alluvial plain and delta complex in Apsheron and Baku area. Due to that migration the productive series shales and quartz-rich sandstones were deposited. In just 2 Ma the thickness of deposit was 5-7 km, which was lied down at the basin centre of the South Caspian area. The main regional seal were laid down by the Late Pliocene, and the Akchagyl shales, when a marine connection via the Black Sea was restablished, and together with Apsheron marine shales and minor sandstones, they created 2500 m of thickness. In Late Pliocene period, the convergence of the Turan platform with the combined Arabian-Iran Plate caused compression of older layers and created new

ones. There was extreme reduction in the Kopet Dag and Greater Caucasus fold. In the same area the Apsheron Ridge and other North West-inclining high relief anticlines formed. In many zones of the basin similar faulted anticlines with a diversity of orientations formed. Seismically active Quaternary continental sediments deposited between the growing layers. The deposits are molasse type ones and their thickness is up to 1500 m. The source rocks of Apsheron Ridge oils referred to Oligocene Maikop Series (C&C Reservoirs, 2005). There is a possibility that there was contribution from the Miocene Diatom Series. Apsheron Ridge source rocks are in common with most other hydrocarbon deposits, which are in the South Caspian Basin (**Figure 1.6**). The thicknesses of the Maikop mudstones are greater than 1000 m. In Pliocene-Quaternary periods the bulk of oil generation occurred.

1.2 Overview of ACG Field Complex

ACG field complex is a thrusted anticline with three peaks. The southern flank dip of the thrusted anticline is approximately 25°, whereas the northern flank is sharper than southern one, it is approximately up to 40°. ACG structure lies towards the North West inclining line. Length of the structure is about 54 km long and width is up to 5 km. The total area of ACG field complex is approximately 56 km^2 (13760 ac). In four places mud volcano vents impale the entire field (C&C Reservoirs, 2005). Folding and faulting began in the late Pliocene. The natural drive mechanisms are strong aquifer, solution gas and only in Azeri sector of the field complex exists a gas-cap. In intermediate reservoirs, oil exists, while shallow and deep reservoirs contain gas. The API of the produced fluid is about 32°API.

5.5 Ma ago in the uppermost Miocene the productive series sedimentation started. In the Apsheron onshore and offshore, the productive series are composed of nine formations (**Figure 1.6**). We can divide productive series into two groups; the lower productive series and the upper productive series. The lower productive series are Kalin, Pre-kirmaky, Kirmaky, Post Kirmaky Sand, and Post Kirmaky Clay formations. The upper productive series are Pereriva, Balakhany, Sabunchi, and Surakhany formations C&C Reservoirs, 2005). All these formations have hydrocarbon bearing reservoirs. The thickness of the Pereriva formation in the ACG is up to 170 m. The Pereriva B and D sands are the most important producers (**Figure 1.7**).

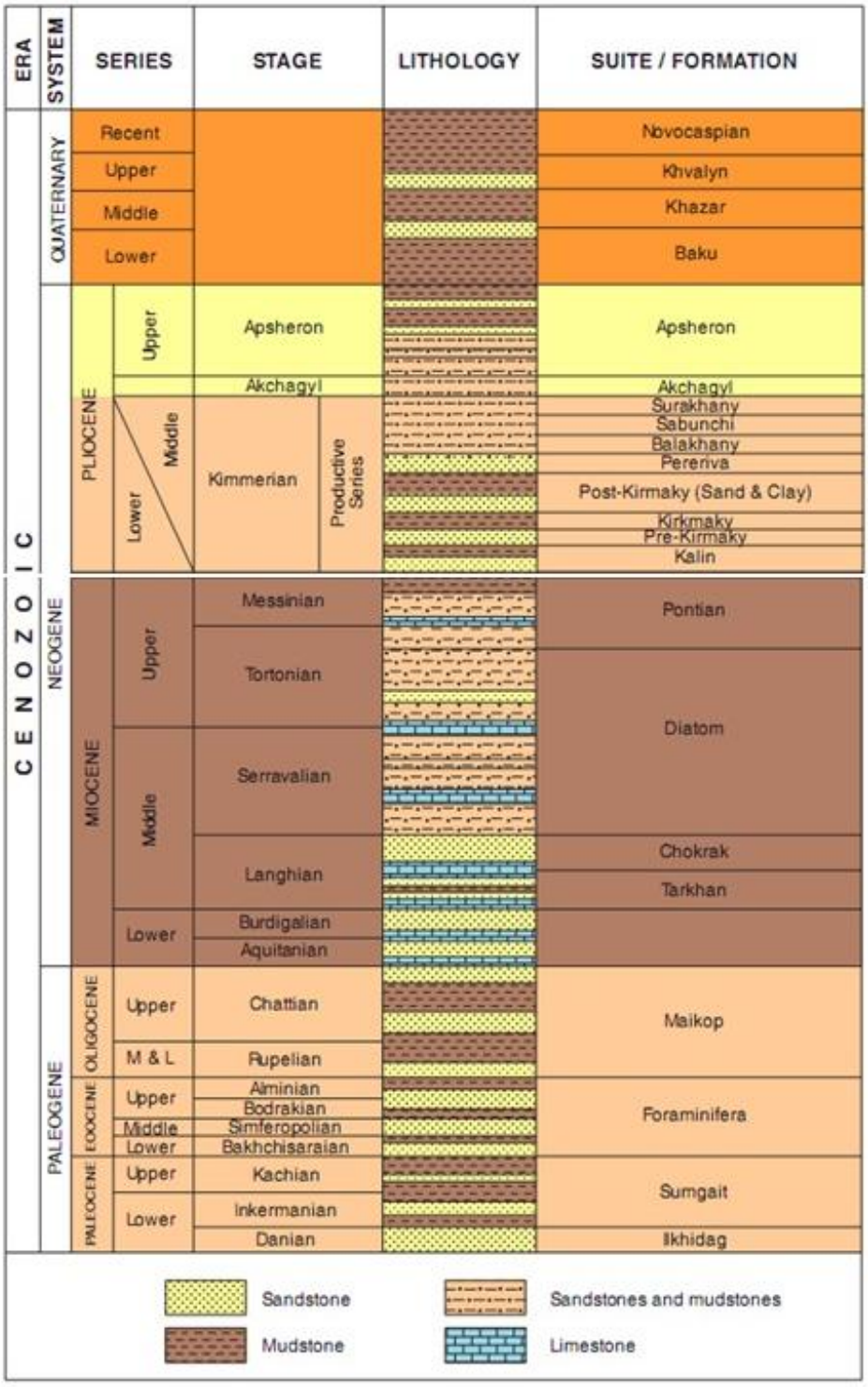

Figure 1.6 : Stratigraphy and lithology (C&C Reservoirs, 2005).

The Pereriva and Balakhany sediments record sand-prone and shale-prone stacking patterns associated with alternation between more proximal and distal environments of deposition. For the Pereriva B the probable averaging net pay thickness is greater than 38 m and for the Pereriva D it is more than 23 m. Generally, the Pereriva B and D units are very extensive (Wethington W. B. et al, 2002).

The continuity of them is high, and also they have excellent horizontal connectivity. In **Figure 1.8** a geological map of ACG field complex is shown.

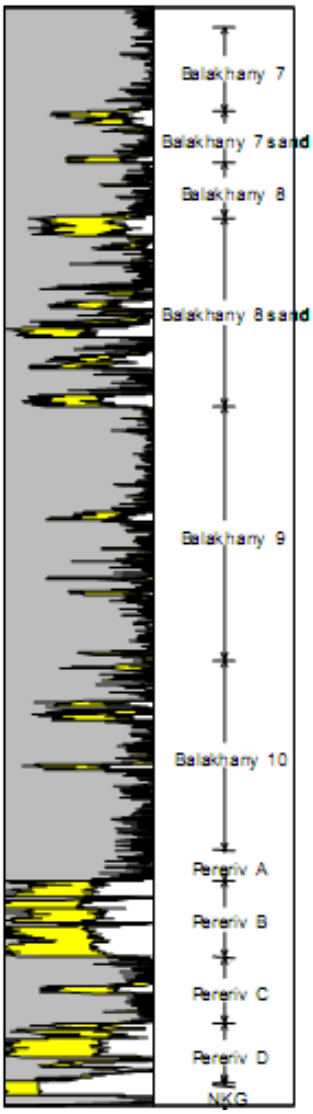

Figure 1.7 : Stratigrapy example (Wethington et al., 2002).

Average porosity of the Pereriva reservoirs is 20% and permeabilities are between 50 and 300 md, with average initial water saturation of 25 – 30%.

The thickness of the Balakhany formation in the ACG is 350 – 600 m. The Balakhany sandstone formation is divided into 6 units, from V to X. Thickness of unit intervals is varying from 10 to 60 m. The Balakhany VIII and X are the most significant reservoir units. In the Balakhany formation the Net:Gross (N:G) is in the range of 0.2 – 0.64. At Chirag sector of the field the average porosity of the Balakhany X is 20% and permeability is in the range of 100 - 300 md. At Azeri sector of the structure, the permeability measured is 10 – 200 md. Initial water

saturation for the Balakhany X is 25% (Wethington W. B. et al., 2002). Close to mud volcanos the reservoir quality becomes worse. There are thin clay layers in each formation units. These clay layers are ruptured in many places, hence they are spread discontinuously.

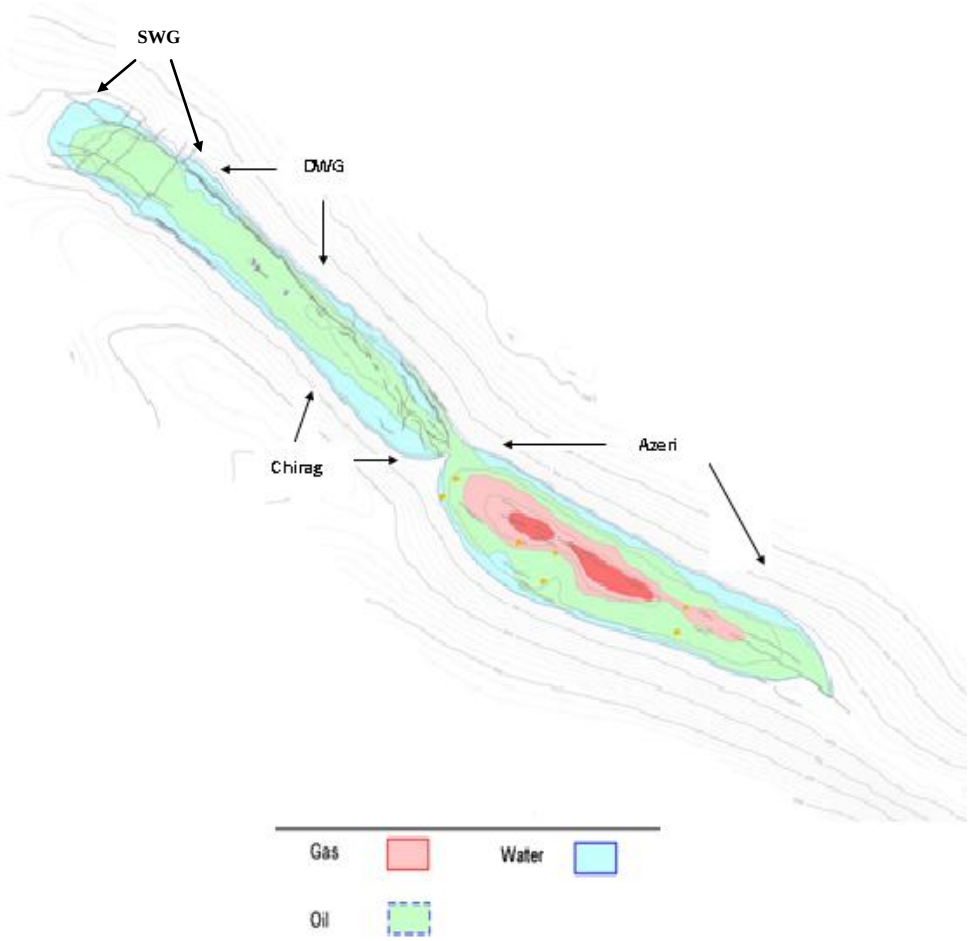

Figure 1.8 : ACG field complex (Ibrahimov, 2014).

.

.

2. LITERATURE REVIEW

Several different methods have been proposed for the interpretation of well tests. These methods are discussed in the literature; Perrine (1956), Martin (1959), Raghavan (1989), Al-Khalifah et al. (1987) Bourdet (2002), Horne (1995), Zeng and Xu (2009), and Kamal and Pan (2010, 2011).

The Perrine's method (or sometimes it is called the Perrine-Martin method) is a modified single phase method. Perrine proposed replacing the single phase mobility by the sum of the mobilities of the fluids and also the single phase compressibility by the multiphase compressibility in the single phase flow theory. According to Perrine a total fluid mobility is defined as :

$$\lambda_t = \left(\frac{k}{\mu}\right)_t = \frac{k_o}{\mu_o} + \frac{k_g}{\mu_g} + \frac{k_w}{\mu_w} = k \cdot \left(\frac{k_{ro}}{\mu_o} + \frac{k_{rg}}{\mu_g} + \frac{k_{rw}}{\mu_w}\right) \quad \textbf{(2.1)}$$

The total compressibility is expressed by Martin (1959) as:

$$c_t = c_f + S_o c_o + S_w c_w + S_g c_g + \frac{S_o B_g}{5.615 \cdot B_o}\left(\frac{\partial R_s}{\partial P}\right) + \frac{S_w B_g}{5.615 \cdot B_w}\left(\frac{\partial R_{sw}}{\partial P}\right) \quad \textbf{(2.2)}$$

The assumptions in Perrine's method are (Escobar and Montealegre, 2008):

1. The saturation gradients must be small and independent of the pressure.
2. The pressure gradients must be small.
3. The capillary pressures between the phases must be negligible.

In this approach it is also necessary to use the total fluid production rate, that is defined as:

$$(qB)_t = q_o B_o + q_w B_w + [1000 \cdot q_{sg} - q_o R_s] \cdot B_g \quad \textbf{(2.3)}$$

When performing type curve analysis the multiphase dimensionless pressure and time are defined as:

$$P_D = \frac{\lambda_t h}{141.2 \cdot (qB)_t} \Delta P \qquad \textbf{(2.4)}$$

$$t_D = \frac{0.000264 \cdot \lambda_t t}{\phi \cdot c_t \cdot r_w^{\ 2}} \qquad \textbf{(2.5)}$$

The slope m of the semilog analysis is expressed by:

$$m = \frac{162.6 \cdot (qB)_t}{\lambda_t h} \qquad \textbf{(2.6)}$$

The skin effect is given by:

$$s = 1.151 \cdot [\frac{P_i - P_{1hr}}{m} - \log \frac{\lambda_t}{\phi \cdot c_t \cdot r_w^{\ 2}} + 3.227] \qquad \textbf{(2.7)}$$

Most of the literature on the effects of multiphase flow on the interpretation of pressure-buildup tests discuss the analysis of buildup test involving oil and gas multiple phases. Since the purpose of this thesis is to analyse the oil and water multiphase flow, literature on oil and gas multiphase flow is not covered in this report. However, the detailed discussion on oil and gas multiphase analysis can be found in references section of this report (Al-Khalifah et al., 1989; Ayan and Lee, 1988a, 1988b; Chu et al., 1986; Vo Dyung and Raghavan, 1991; Weller, 1966).

3. PROBLEM STATEMENT AND MODELING APPROACH

3.1 Problem Statement And Purpose of Thesis

Azeri and Chirag fields are being developed with gas and water injection. Wells historically started with zero watercut. During several years watercut increased in wells. Some of the wells currently reached to a water cut more than 40%. There were conducted regular well transient tests and measurements in the wells. The interpretations of the tests were done assuming only the oil phase flow. There is a need to study how this assumption would effect the interpretation of permeability values, if high value water cut impaction is taken into consideration. The main aim of the proposed project is to investigate the water effects on permeability value that obtained from buildup test analysis, which is conducted assuming conventional single phase flow method. This study is carried out by creating a simplified software field model. The investigations are conducted for two cases. In the first case, the simulated model is bounded with no flow sealing boundaries. In the second case, the field model is assumed to be bounded with an aquifer from the east side of the model. In both cases the investigation is conducted by increasing water saturation in the simulated model, then the simulated bottomhole pressure and surface production rate data are transferred to another software for interpretation of well test data. For creating simplified field model the Ecrin Rubis (Ecrin v4.30, 2013) software is used and for analyzing pressure data from the model the Ecrin Sapphire (Ecrin v4.30, 2013) software is used

3.2 Forming of simple model for the reservoir

A model was simulated using the Ecrin Rubis software. Study was conducted in a simplified field model. A rectangular field area was assumed and a vertical well was considered. Well radius was taken 0.3 ft, the thickness of the reservoir as 125 ft and the perforation was set along the whole vertical thickness. The grid number in x direction consists of 22 blocks and in z direction consists of 10 blocks. The top of the

reservoir is set at 8000 ft. The reservoir model parameters, used in simulating of model are given in **Table 3.1**.

Table 3.1 : Input data used for model

Properties	Value
Length of Reservoir	10 000 ft
Width of Reservoir	10 000 ft
Thickness of Reservoir	125 ft
Top of the Reservoir	8000 ft
Reservoir Pressure	5000 psia
Reservoir Temperature	142 °F
Absolute Reservoir Permeability	400 md
Porosity	0.22
Grid in x Direction	22
Grid in z Direction	10
Net to Gross Thickness Ratio	1
Tubing Roughness	0.0012 in
Thermal Gradient in Well	0.0149999 °R/ft
Well ID	3.6 in
Wellbore Storage	0.01 bbl/psi
Salinity of Water	10 000 ppm
Formation Volume Factor of Water	1.03069 bbl/STB
Gravity of Oil	35 °API
Formation Volume Factor of Oil	Standing Correlation
Oil Compressibility	1.01198E-5 psi^{-1}
Formation Compressibility	3E-6 psi^{-1}
Skin	0
Total Production (Oil+Water) Rate	35 000 STB/D

Figure 3.1 shows the 3D geometry plot of the field.

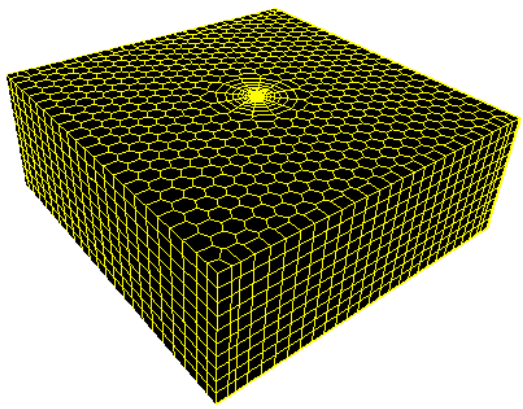

Figure 3.1 : 3D geometry plot of the model.

The relative permeability curve plot, used in model is given in **Figure 3.2**. As it is noticed in **Figure 3.2**, the irreducible water saturation (S_{wi}) is assumed to be 0.1 and the residual oil saturation (S_{or}) is 0.1. Thus k_{ro}=1.0 at S_{wi} and k_{rw}=1.0 at S_{or} points represent the end points at the relative permeability curves.

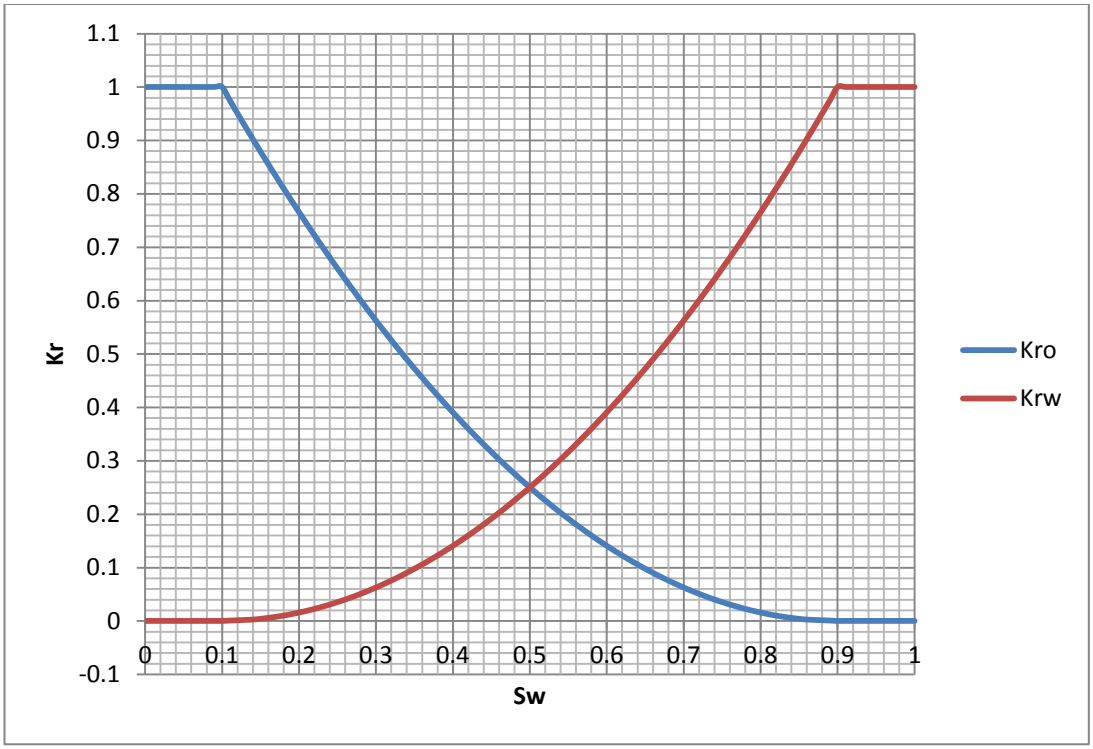

Figure 3.2 : Relative permeability curves.

Study was conducted to investigate to understand how water phase affects the transient analysis data. Ecrin Sapphire software is used to interpret the pressure tests. Two cases were studied. In the first case there is a rectangular field with no flow sealing boundaries. The gravity effects are not accounted in this case. The study is conducted by increasing the water saturation from zero to 0.7 in the system for the oil viscosity of 0.45 and 4.5 cp whereas the water viscosity is kept the same, 0.35 cp. In the second case the same rectangular field is simulated, but in that case there is an aquifer breakthrough from the east side of the model.

4. SAPPHIRE ANALYSIS

4.1 Study of The Oil Field Without Aquifer

A rectangular reservoir with no flow sealing boundaries was assumed in the first case. The gravity effects are not accounted during the simulation. The 2D geometry plot of the field is given in **Figure 4.1**.

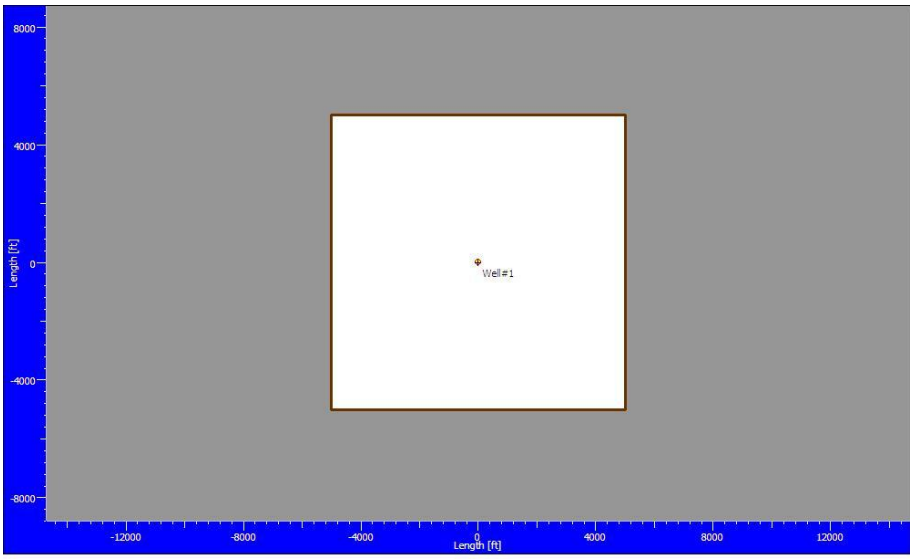

Figure 4.1 : 2D geometry plot of the model.

The relative permeability curve plot is the same as in **Figure 3.2**. The capillary pressure plot, used in this field model is shown in **Figure 4.2**.

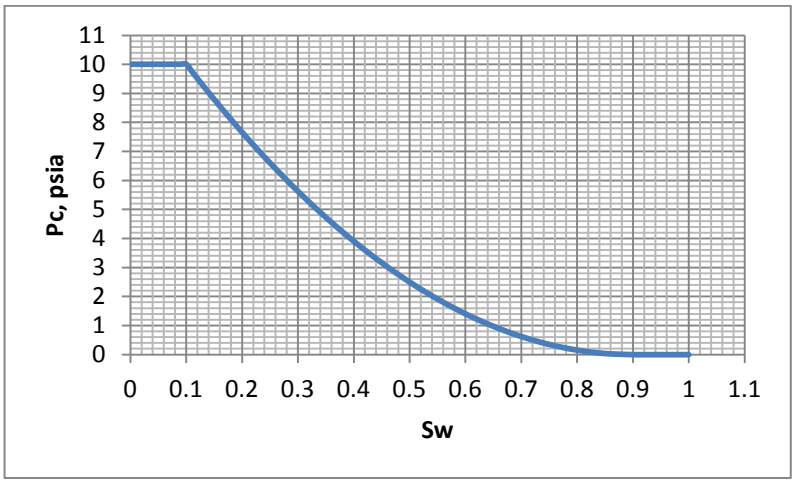

Figure 4.2 : The capillary pressure plot of the model.

4.1.1 Case 1: μ_o=0.45 cp

The first case also consists of two parts. In the first part the viscosity of water is equal to 0.35 cp and the viscosity of oil is equal to 0.45 cp. The total production from system is 35000 STB/D. The well is produced for 2000 hr before shut-in. The shut-in time is 200 hr. The plot of pressure and production rate data from Rubis in the case of no water saturation *(S_w)* in the system is zero is shown in **Figure 4.3**.

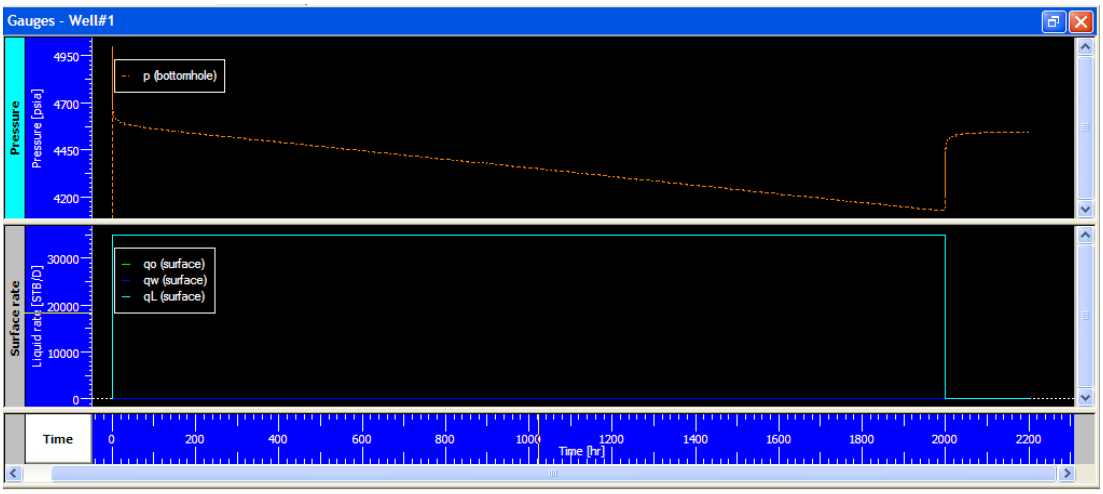

Figure 4.3 : Bottomhole pressure and surface production rate plot for S_w=0.

The plot of the model matching the buildup data in Ecrin Sapphire for S_w=0 is shown in **Figure 4.4**.

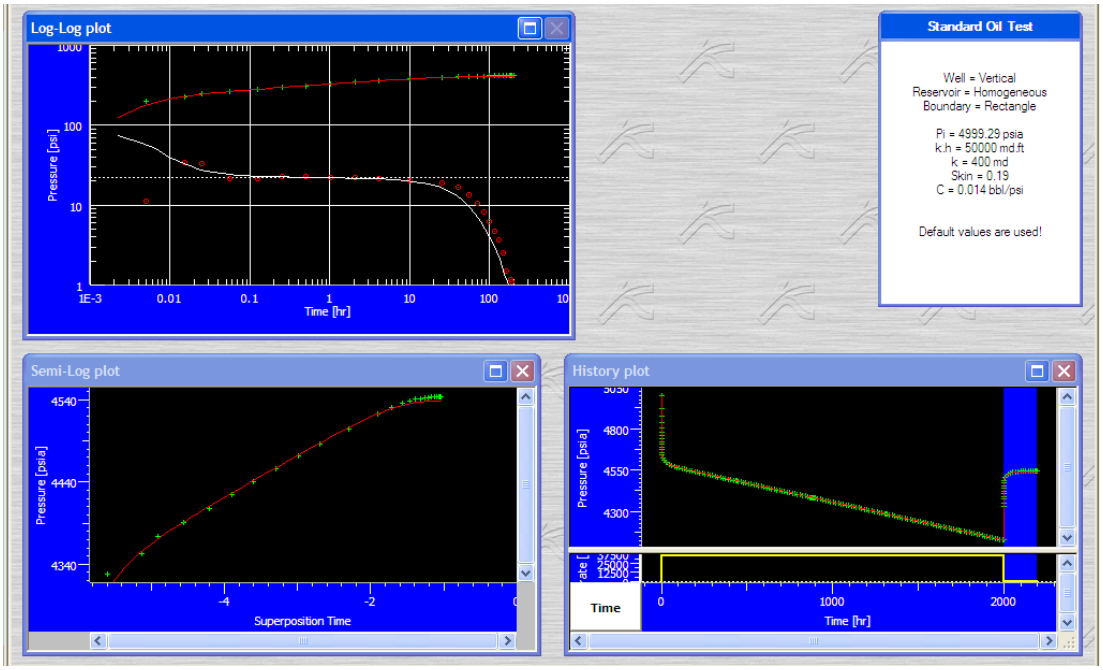

Figure 4.4 : Sapphire buildup analysis in a case of S_w=0.

According to this analysis we can see that there is not any change in permeability value (400 md), which is same as in Rubis model.

Figure 4.5 shows the Rubis pressure and production rate outcome plot for the case when S_w=0.1.

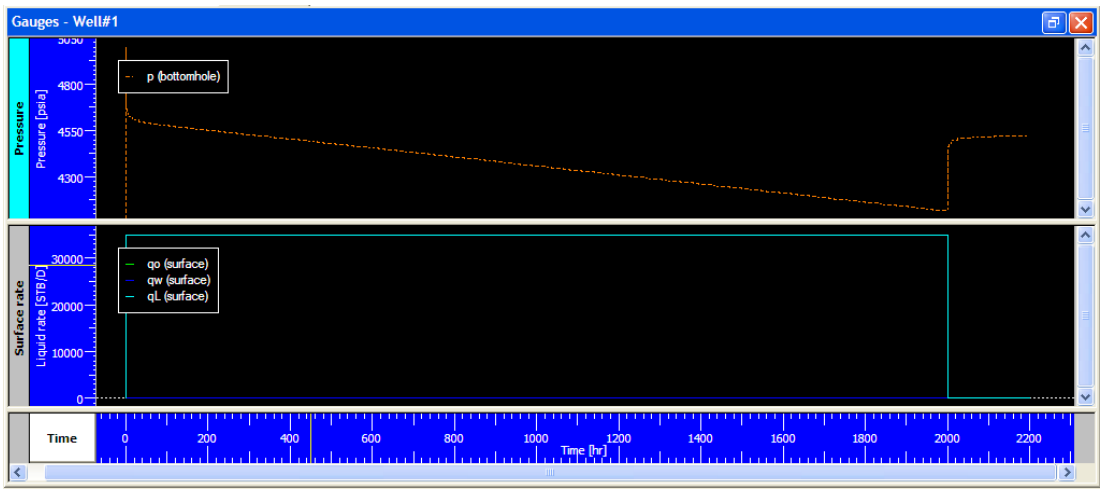

Figure 4.5 : Bottomhole pressure and surface production rate plot for S_w=0.1.

Figure 4.6 shows the plot of the model matching the pressure-time data in Ecrin Sapphire for S_w=0.1.

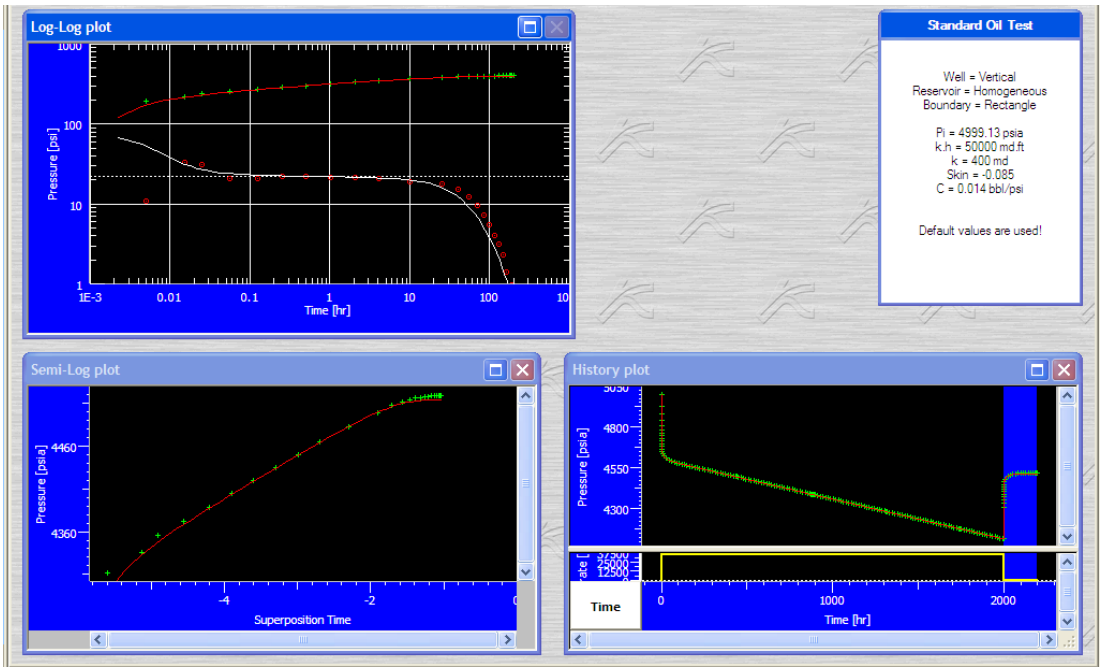

Figure 4.6 : Sapphire buildup analysis in a case of S_w=0.1.

Although the water saturation reached to 0.1 values, the water is still immobile in system *(S_w=S_{wi})* and therefore there is not water production. The permeability value still remains the same (400 md).

The plot of the pressure and production rate for S_w=0.2 is shown in **Figure 4.7**.

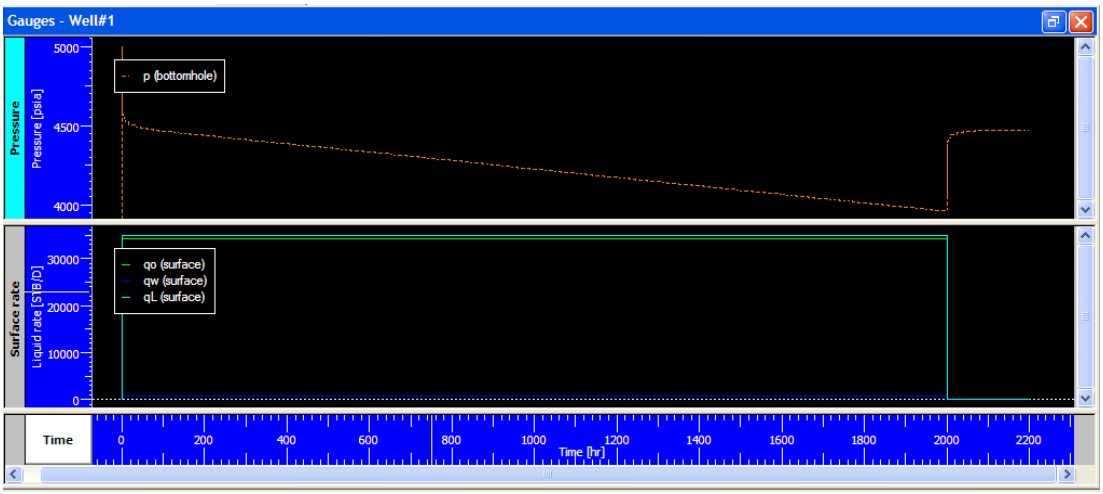

Figure 4.7 : Bottomhole pressure and surface production rate plot for S_w=0.2.

When the water saturation reaches to 0.2 *(S_w>S_{wi})* , there is a water production about 866 STB/D.

Figure 4.8 shows the plot of the model match on data distribution in Ecrin Sapphire for S_w=0.2.

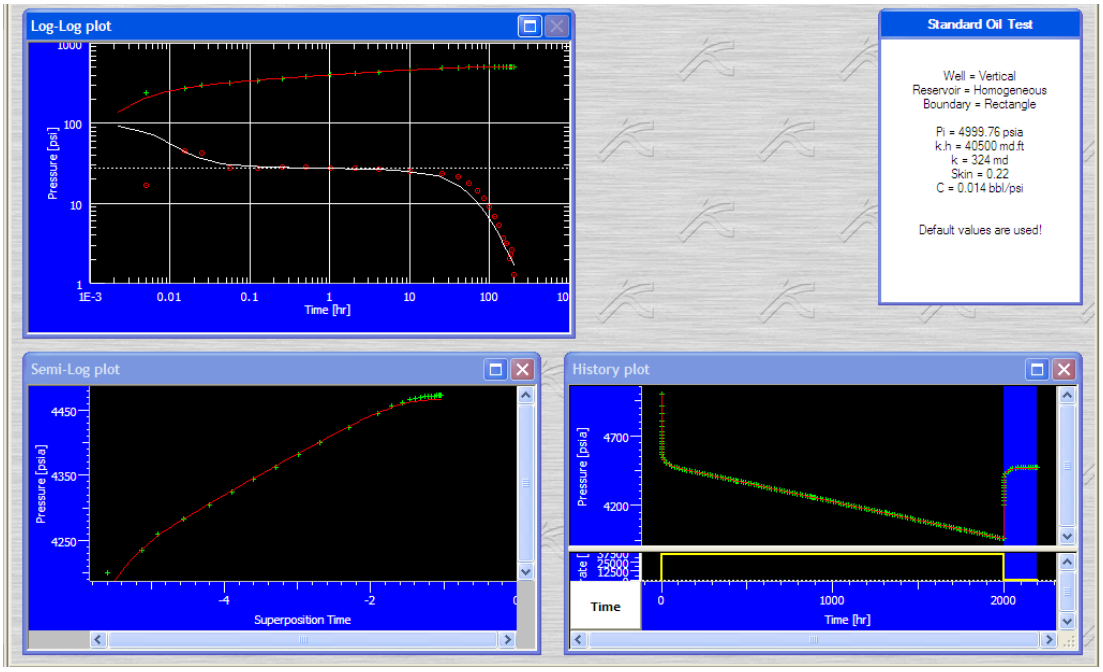

Figure 4.8 : Sapphire buildup analysis in a case of S_w=0.2.

In the case of S_w=0.2 permeability obtained from the match is 324 md.

Figure 4.9 shows the pressure and production data plot for S_w=0.3.

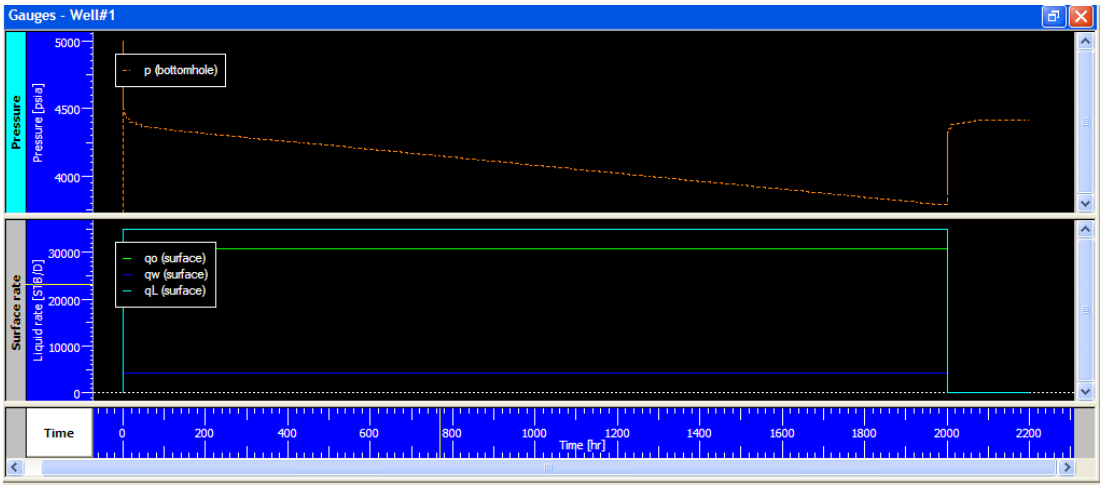

Figure 4.9 : Bottomhole pressure and surface production rate plot for S_w=0.3.

In this case the water production reached to 4221 STB/D.

The Sapphire buildup analysis for S_w=0.3 is shown in **Figure 4.10** as well.

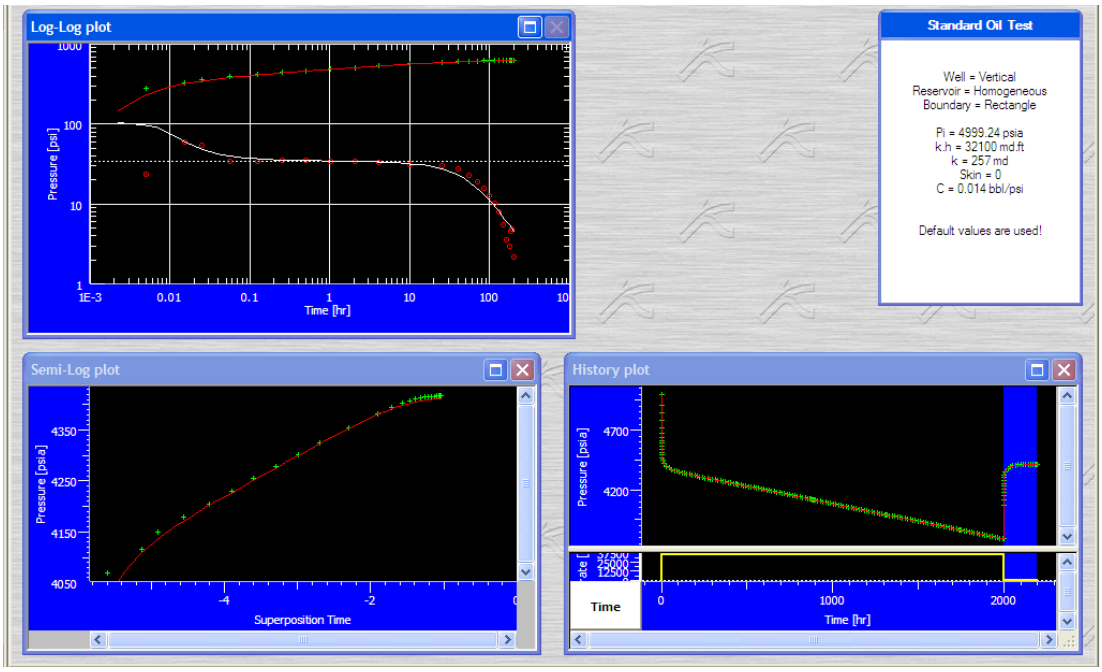

Figure 4.10 : Sapphire buildup analysis in a case of S_w=0.3.

In the case of S_w=0.3, decrease in permeability is continuing. The value of permeability is 257 md.

The pressure and production rate plot for S_w=0.4 is given in **Figure 4.11**. Because of increase in water saturation the water production rate is also increasing.

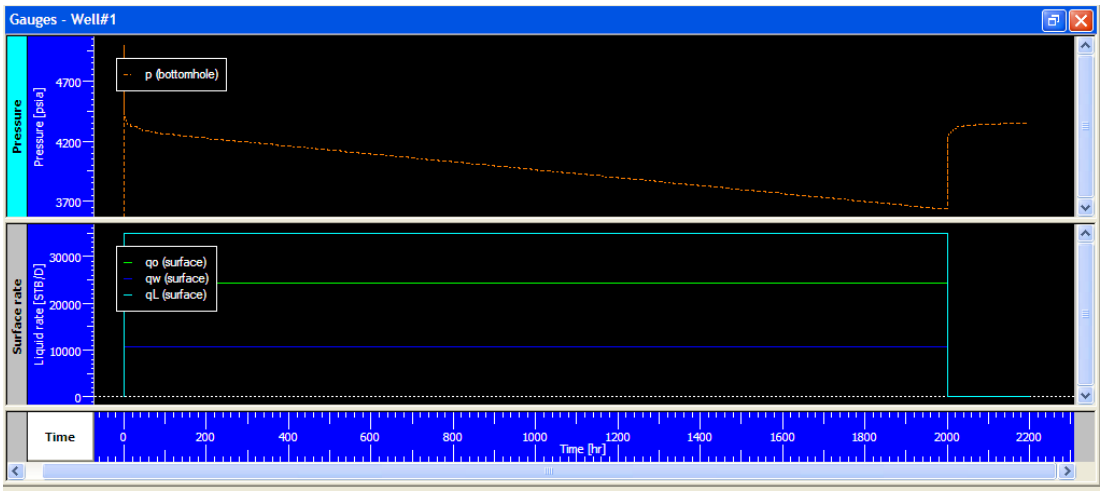

Figure 4.11 : Bottomhole pressure and surface production rate plot for S_w=0.4.

In S_w=0.4 case water production rate reached to 10 704 STB/D. So, the water cut value is about 30.58%. The Sapphire buildup analysis for this case is shown in **Figure 4.12**.

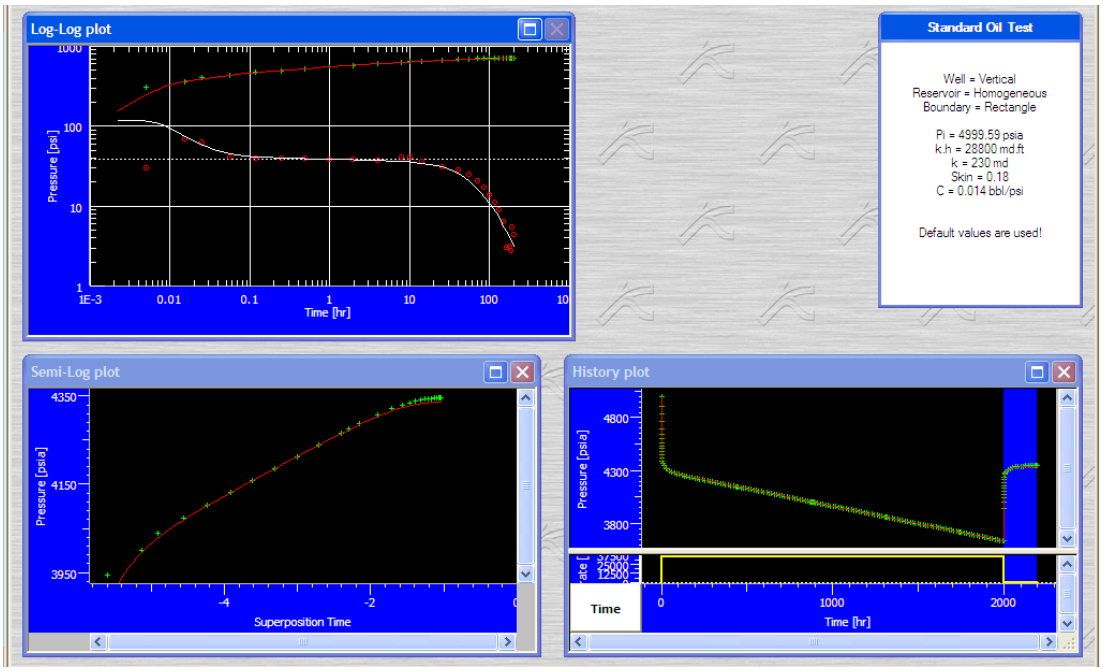

Figure 4.12 : Sapphire buildup analysis in a case of S_w=0.4.

According to buildup analysis decline in permeability is continuing and it is determined to be 230 md.

The plot for pressure and production rate data for S_w=0.5 is given in **Figure 4.13**.

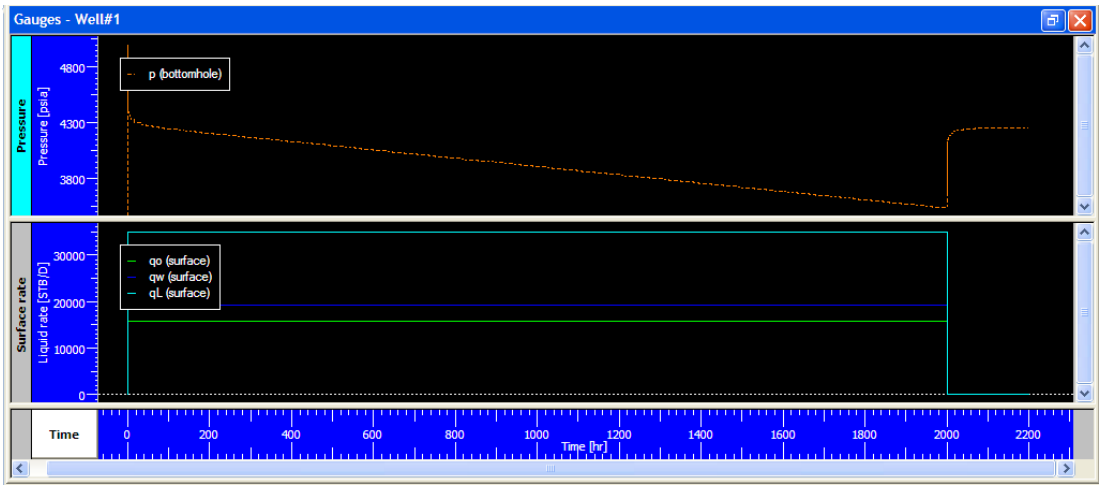

Figure 4.13 : Bottomhole pressure and surface production rate plot for S_w=0.5.

In the case of S_w=0.5 water production rate exceeds oil production rate and it becomes 19 157 STB/D. Water cut value is 54.73%.

The buildup analysis for S_w=0.5 case is given in **Figure 4.14**.

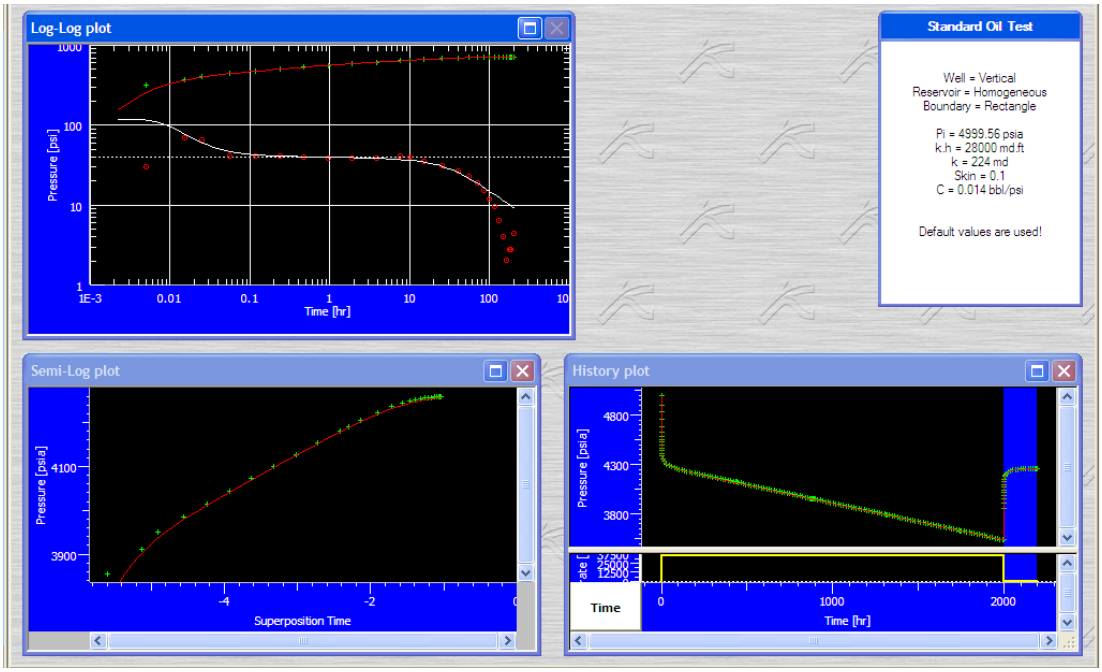

Figure 4.14 : Sapphire buildup analysis in a case of S_w=0.5.

In S_w=0.5 value decline in permeability occurs as expectedly and the value of permeability is 224 md.

Figure 4.15 shows the pressure and production rate data plot for S_w=0.6.

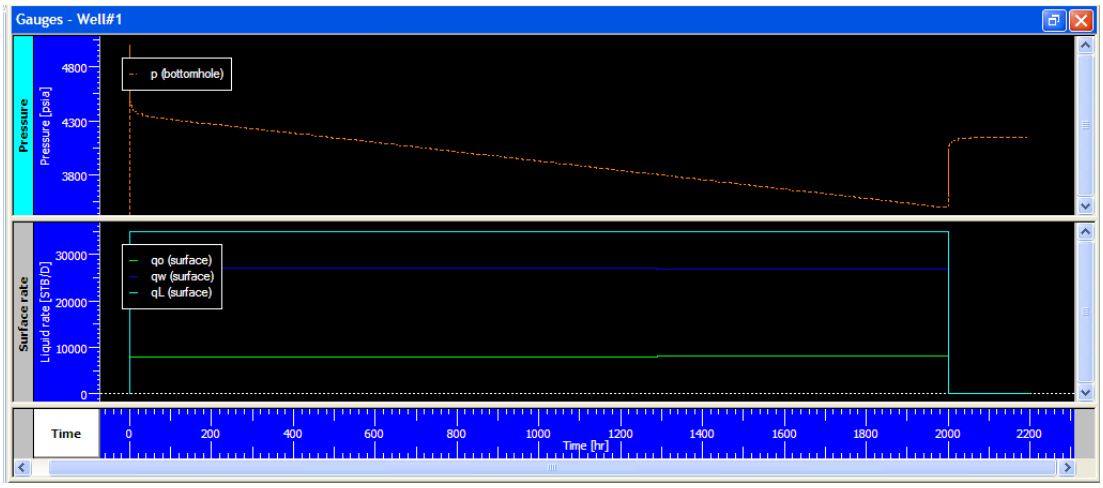

Figure 4.15 : Bottomhole pressure and surface production rate plot for S_w=0.6.

At S_w=0.6 the water production reaches to 26 903 STB/D and water cut becomes 76.86%.

The Sapphire buildup analysis for this case is shown in **Figure 4.16**.

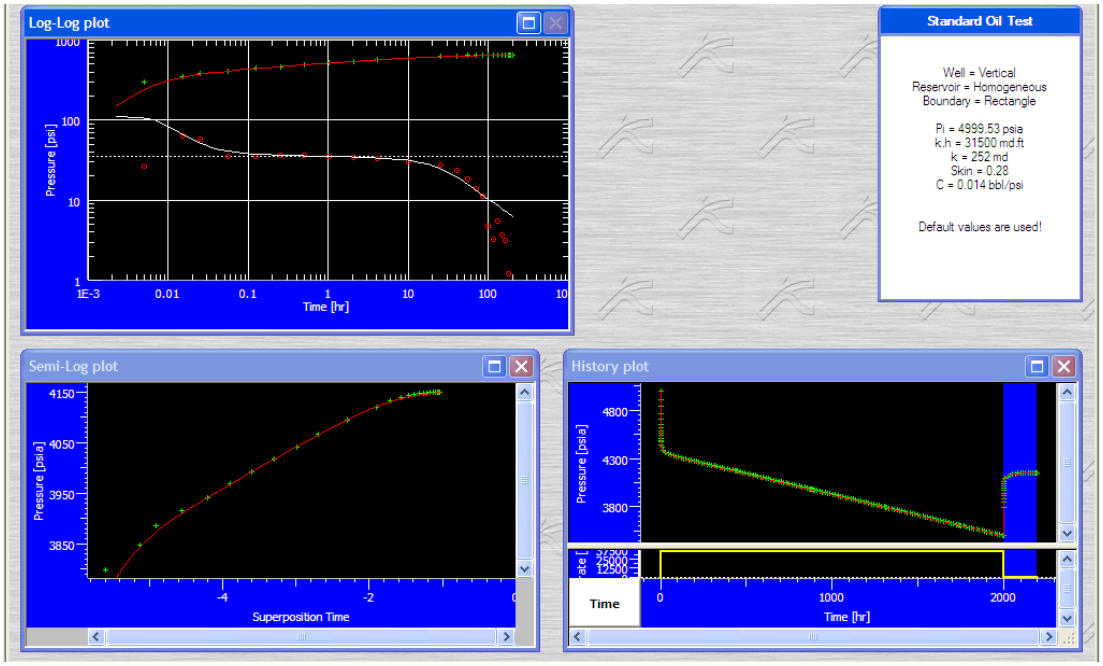

Figure 4.16 : Sapphire buildup analysis in a case of S_w=0.6.

In the buildup analysis for S_w=0.6 value there is an increase in permeability value as compared to S_w=0.5 case. The value of permeability is 252 md.

The next plot of pressure and production rate data for S_w=0.7 case is shown in **Figure 4.17**.

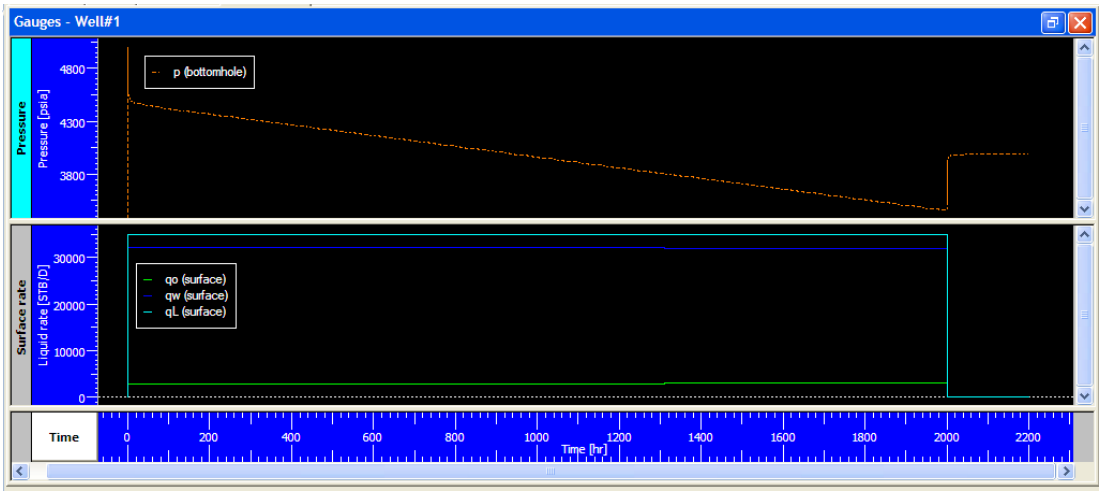

Figure 4.17 : Bottomhole pressure and surface production rate plot for S_w=0.7.

For the case of S_w=0.7 the water production reaches to 32 000 STB/D and the water cut for this case is 91.43%.

The buildup analysis for the S_w=0.7 is given in **Figure 4.18**.

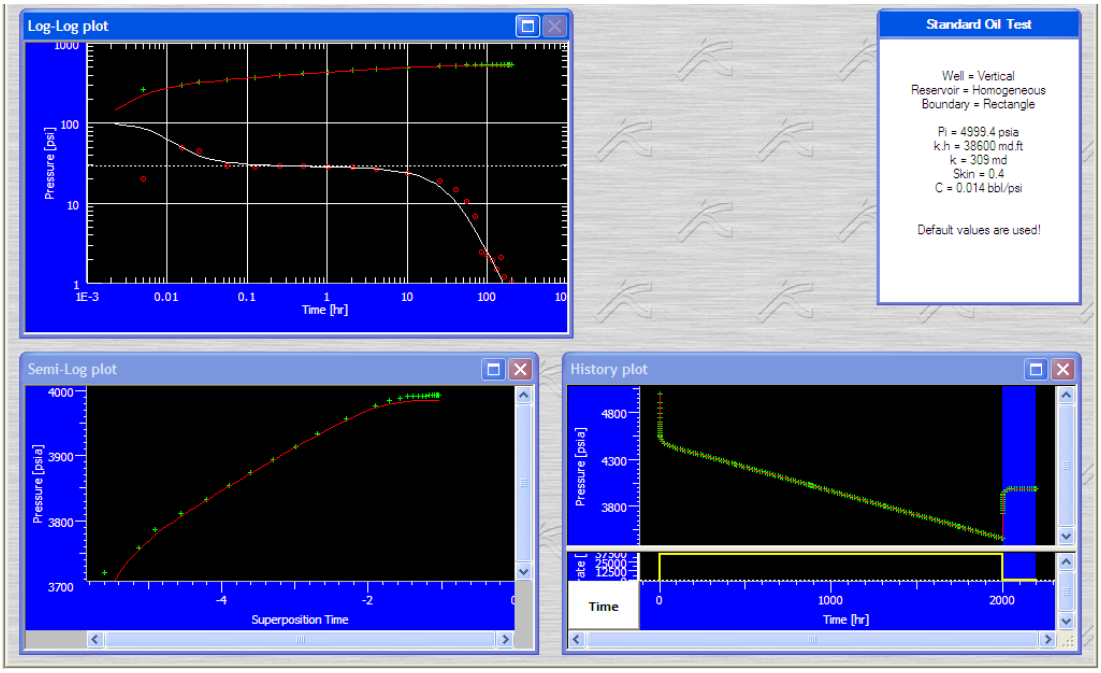

Figure 4.18 : Sapphire buildup analysis in a case of S_w=0.7.

In this case of S_w=0.7 permeability reaches to 309 md.

The obtained parameters from Rubis and Sapphire analysis for various S_w case are given in **Table 4.1**. In **Table 4.1** $P_{wf,s}$ represents the wellbore flowing pressure at shut-in.

Table 4.1 : Data from Rubis model simulation and Sapphire analysis.

Water Saturation, S_w	Bottomhole Pressure, $P_{wf,s}$, psia	Water Production, q_w, STB/D	Initial Pressure, P_i, psia	Permeability–Thickness, *kh*, md-ft	Permeability, *k*, md	Skin, *s*	Wellbore storage, *C*, bbl/psi
0	4127.86	0	4999.29	50 000	400	0.19	0.014
0.1	4116.83	0	4999.13	50 000	400	-0.085	0.014
0.2	3961.46	866	4999.76	40 500	324	0.22	0.014
0.3	3789.29	4221	4999.24	32 100	257	0	0.014
0.4	3634.08	10 704	4999.59	28 800	230	0.18	0.014
0.5	3538.25	19 157	4999.56	28 000	224	0.1	0.014
0.6	3501.48	26 903	4999.53	31 500	252	0.28	0.014
0.7	3458.77	32 000	4999.4	38 600	309	0.4	0.014

From **Table 4.1** we can see the change in permeabilities, obtained from Sapphire buildup analysis. As mentioned before the interpretation in Sapphire is conducted using the single phase interpretation method. Although the actual system in Rubis simulation contains two phases, Sapphire interprets the pressure and production rate data as if there is only one phase but not a two phase in system. Therefore Sapphire yields the permeability parameters as if they are the absolute permeability of whole system, but in reality we know that the obtained permeability parameters from Sapphire buildup analysis are not the real absolute permeability data of system. Since there is more than one phase in our system, permeability should correspond to the effective permeability. In fact the permeability data from the Sapphire analysis represent the total effective permeability of the water-oil mixture. Comparison of the obtained permeability data from Sapphire analysis, which actually are effective permeability, with the oil effective permeability from Rubis field model, is shown in **Figure 4.19**.

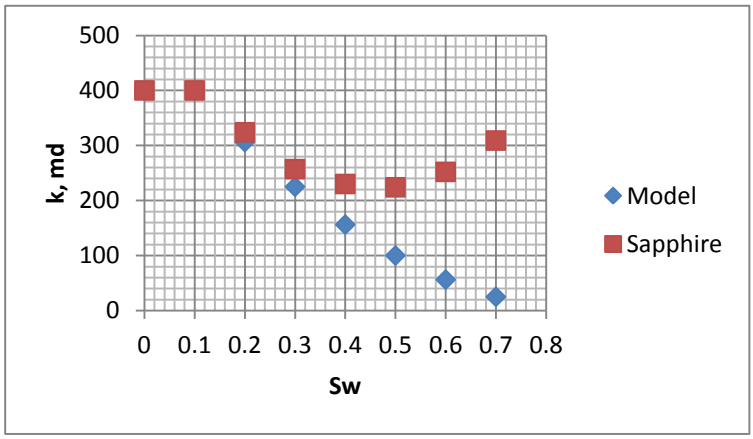

Figure 4.19 : Comparison of effective permeability from Sapphire to oil relative permeability from Rubis model.

From **Figure 4.19** it seems that the total effective permeability of the system fluid mixture decreases until a certain value of the water saturation (S_w), afterwards it starts to increase.

As the interpretation of the system is conducted as it is a single phase, it is necessary to check the change of whole system total mobility value as a function of water saturation.

We can calculate the total mobility of two phase system by the Perrine's correlation, which is given below:

$$\lambda_t = \left(\frac{k}{\mu}\right)_t = \lambda_o + \lambda_w = k \cdot \left(\frac{k_{ro}}{\mu_o} + \frac{k_{rw}}{\mu_w}\right) = \frac{162.6}{mh}(qB)_t \quad \textbf{(4.1)}$$

We can define the total flow rate as:

$$(qB)_t = q_o B_o + q_w B_w \quad \textbf{(4.2)}$$

In the special case of 100% oil flow and no water flow, then Perrine's equation becomes:

$$\lambda_t = \left(\frac{k}{\mu}\right)_t = \left(\frac{k}{\mu}\right)_o = \lambda_o \quad \textbf{(4.3)}$$

From two phase flow Perrine's equation, equation **(4.1)**, we can determine absolute permeability. For this we need to know slope (m) from the semilog interpretation plot and the relative permeability data at the corresponding water saturation value. We know that the relative permeability is a function of saturation ($k_{ro}, k_{rw} = f(S_w)$). The equation of absolute permeability is shown below:

$$k = \frac{162.6}{mh}(qB)_t \cdot \frac{1}{\left(\frac{k_{ro}}{\mu_o} + \frac{k_{rw}}{\mu_w}\right)_{S_w}} \quad \textbf{(4.4)}$$

The oil viscosity in the system is 0.45 cp and the water viscosity is 0.35 cp. From Rubis model simulation we know the value of absolute permeability (k) as an input is 400 md. At corresponding water saturation (S_w), oil and water relative permeabilities are taken from **Figure 3.2**, which is used in model simulation. The water saturation changes from zero to 0.7. **Table 4.2** shows the relative permeability values as a function of water saturation and also the total system mobilities are calculated by

using equation **(4.1)**. Water cut gives the ratio of water production rate in total production rate in persentages.

Table 4.2 : The calculated values of total mobility of system.

Water Saturation, S_w	Water Cut, %	Oil Relative Permeability, k_{ro}	Water Relative Permeability, k_{rw}	The Total Mobility of Fluid Mixture, λ_t, md/cp
0	0	1	0	888.889
0.1	0	1	0	888.889
0.2	2.47	0.765	0.0156	697.829
0.3	12.06	0.5625	0.0625	571.429
0.4	30.58	0.3907	0.1407	508.089
0.5	54.73	0.25	0.25	507.937
0.6	76.86	0.14	0.3906	570.844
0.7	91.43	0.062	0.5625	697.968

An example of calculation in the case of S_w=0.2 is shown below:

$$\lambda_t = k \cdot \left(\frac{k_{ro}}{\mu_o} + \frac{k_{rw}}{\mu_w}\right) = 400 \cdot \left(\frac{0.765}{0.45} + \frac{0.0156}{0.35}\right) = 697.829 \frac{md}{cp}$$

In S_w=0.2 the oil relative permeability from the **Figure 3.2** is 0.765 and the water relative permeability from the same figure is 0.0156. The absolute permeability (k) is 400 md.

The following expression can be used to determine of the relationship between the change of permeabilities and the total mobilities:

$$\frac{k_{sw}}{k_{sw_i}} = \frac{(\lambda_t)_{S_w}}{(\lambda_t)_{S_{wi}}} \qquad \textbf{(4.5)}$$

In equation **(4.5)** k_{sw} represents the permeability value obtained from Sapphire at corresponding water saturation. The parameter k_{swi} represents the permeability value at the initial water saturation value, which is 400 md. The initial water saturation (S_{wi}) is 0.1. $(\lambda_t)_{sw}$ and $(\lambda_t)_{swi}$ are the total mobility values at the corresponding the water saturation and the initial water saturation, respectively. As it seems from equation **(4.5)** the proportionality of the ratios must be equal. There is a calculation example for S_w=0.3 below:

$$\frac{k_{sw}}{k_{sw_i}} = \frac{257}{400} = 0.642$$

$$\frac{(\lambda_t)_{S_w}}{(\lambda_t)_{S_{wi}}} = \frac{571.429}{888.889} = 0.642$$

So, the proportionality of the ratios, given by equation **(4.5)** is confirmed. Thus by using equation **(4.5)** we can find the permeability values analytically. We can rewrite equation **(4.5)** as below:

$$(k)_{sw} = (k)_{sw_i} \cdot \frac{(\lambda_t)_{S_w}}{(\lambda_t)_{S_{wi}}} \qquad \textbf{(4.6)}$$

Table 4.3 shows the calculated $(k)_{sw}$ values from equation **(4.6)**.

Table 4.3 : Calculated $(k)_{sw}$ values.

S_w	$(k)_{sw}$
0	400
0.1	400
0.2	314.023
0.3	257.143
0.4	228.64
0.5	228.5716
0.6	256.8798
0.7	314.0856

As we see the calculated permeability values in **Table 4.3** are very close to the permeability values in **Table 4.1** which are obtained from Sapphire interpretations.

According to **Table 4.2** we can see the changes in obtained mobility values as a function of S_w and water cut. In detail, we see a decline in mobility values until the water saturation reaches to 0.5, afterwards the mobility values are increasing, showing a similar behavior of permeability in **Table 4.1** that were obtained from Sapphire buildup analysis. A detailed investigation of the data in **Table 4.1** and **4.2** shows that when the water cut exceeds 70% the water phase dominates the flow system and water mobility becomes higher than oil mobility and thus increases the whole system permeability and the total mobility. According to this phenomenon, the total system mobility value and the permeability of the total fluid mixture of system are related to each other. In other words, as the total mobility increases, then total fluid mixture effective permeability also increases, and as mobility decreases, then fluid effective permeability value decreases too, accordingly.

According to Perrine's two phase analysis, the skin equation is given below:

$$s = 1.151 \cdot [\frac{P_{1hr} - P_{wf(\Delta t=0)}}{m} - log \frac{\left(\frac{k}{\mu}\right)_t}{\phi \cdot c_t \cdot r_w^2} + 3.23] \quad \textbf{(4.7)}$$

P_{1hr} is taken from the Horner straight line, whereas $(P_{wf})_{\Delta t=0}$ is the wellbore flowing pressure at the end of production period.

The slope (m) of the semilog straight line is also given below:

$$m = 162.6 \cdot \frac{(qB)_t}{\left(\frac{k}{\mu}\right)_t \cdot h} \quad \textbf{(4.8)}$$

In calculating skin values, Sapphire does not employ equation **(4.7)**. Instead it treats the multiphase flow as it is a single phase oil flow. Thus the skin values obtained from Sapphire single-phase pressure analysis (**Table 4.1**) is different from the input value of zero provided to Ecrin Rubis simulator. The difference in skin value could be due to the difference of c_t values used in Ecrin and Sapphire softwares.

4.1.2 Case 2: μ_o=4.5 cp

In this case we change the oil phase viscosity to 4.5 cp. As a result the mobility difference between phases becomes higher. The results of Sapphire buildup analysis and Rubis pressure and production rate simulations are presented below.

Figure 4.20 shows the plot of bottomhole pressure and surface production rate for the case of S_w=0 obtained from the Rubis software.

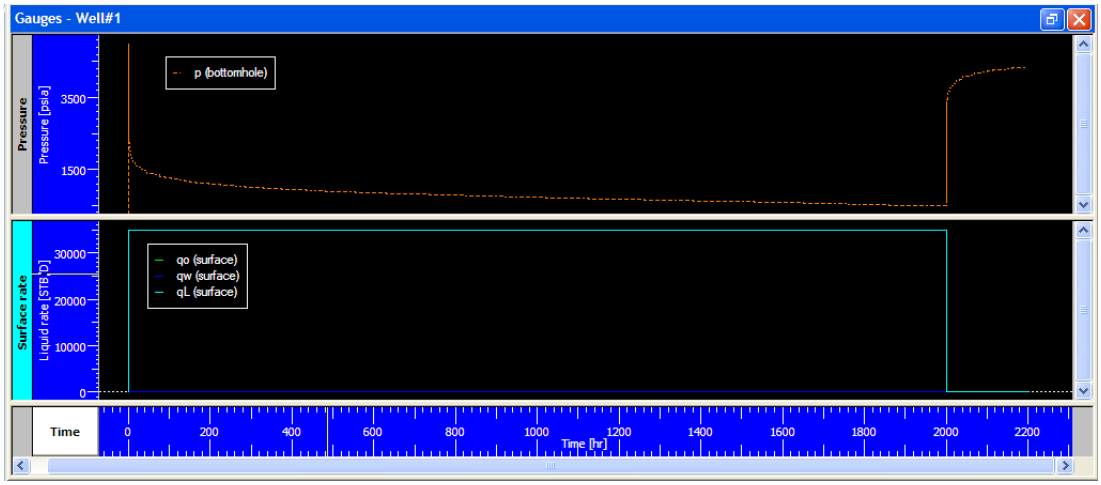

Figure 4.20 : Bottomhole pressure and surface production rate plot for S_w=0.

Because water saturation is zero, there is not any water production. Sapphire buildup analysis using the pressure and time data obtained from Rubis simulator is given in **Figure 4.21**.

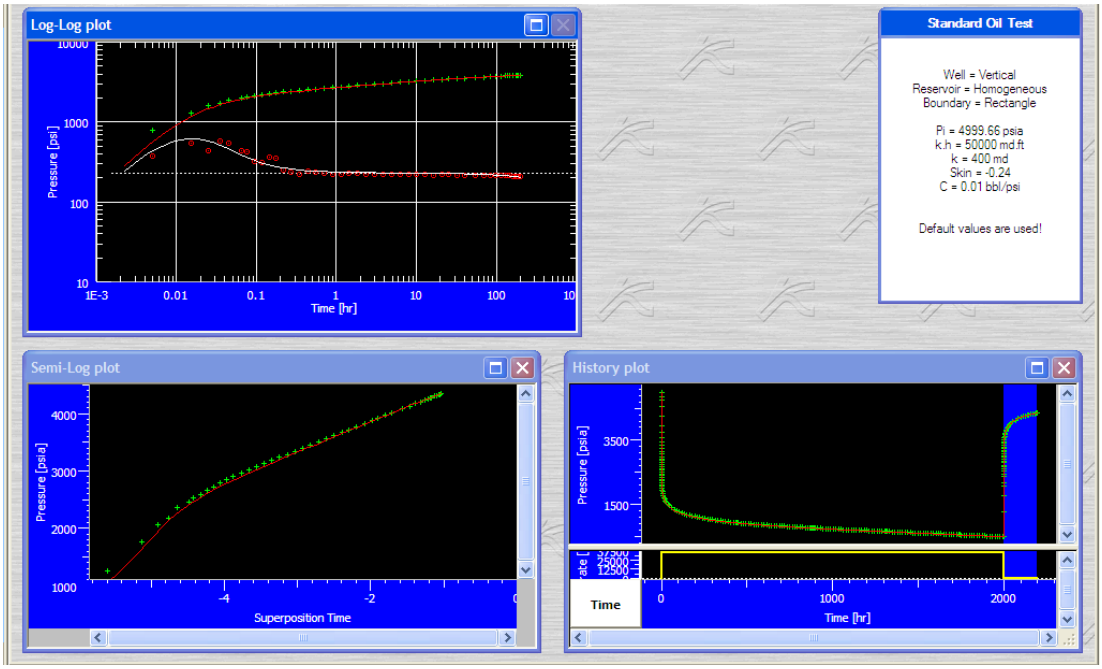

Figure 4.21 : Sapphire buildup analysis in case of S_w=0.

According to this analysis we can see that there is not any change in permeability value, which is same as in Rubis model (400 md).

Figure 4.22 shows pressure and production rate plot for S_w=0.1 obtained from the Rubis software.

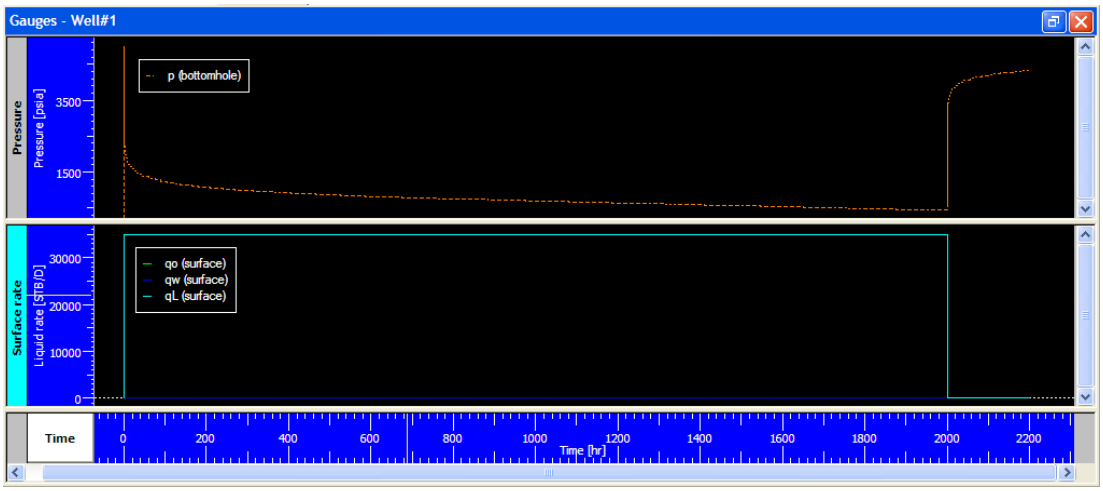

Figure 4.22 : Bottomhole pressure and surface production rate plot for S_w=0.1.

Since S_w=S_{wi} there is not any water production in S_w=0.1 case yet.

The Sapphire buildup analysis for S_w=0.1 is shown in **Figure 4.23**.

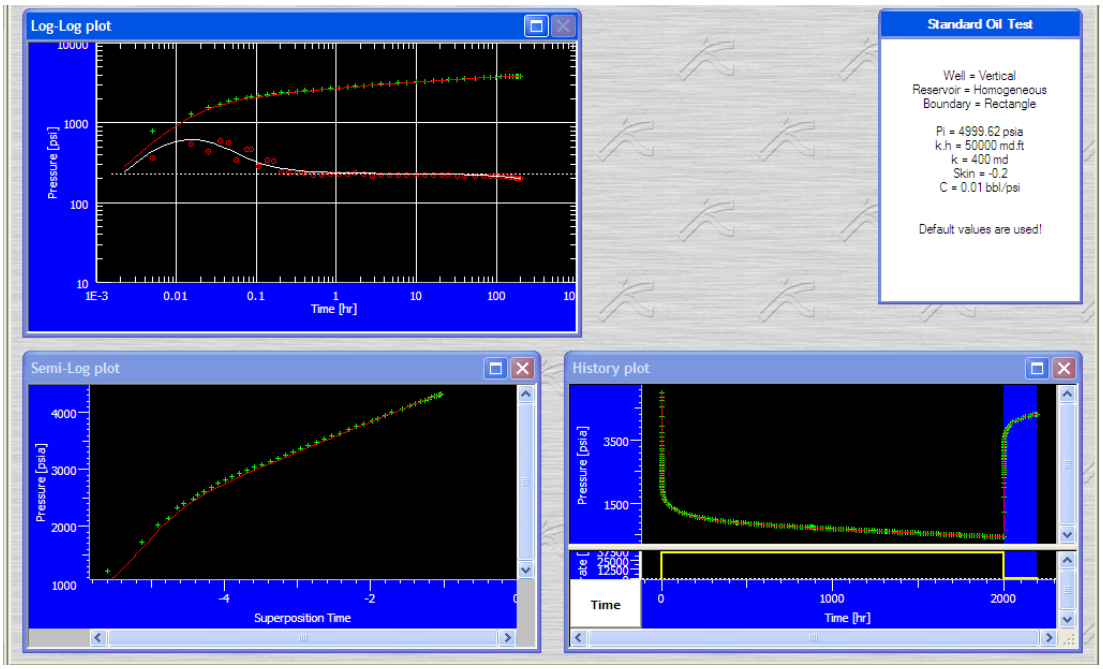

Figure 4.23 : Sapphire buildup analysis in a case of S_w=0.1.

The permeability value still remains the original input value of 400 md.

Next the plot of pressure and production rate data for S_w=0.2 is given in **Figure 4.24**.

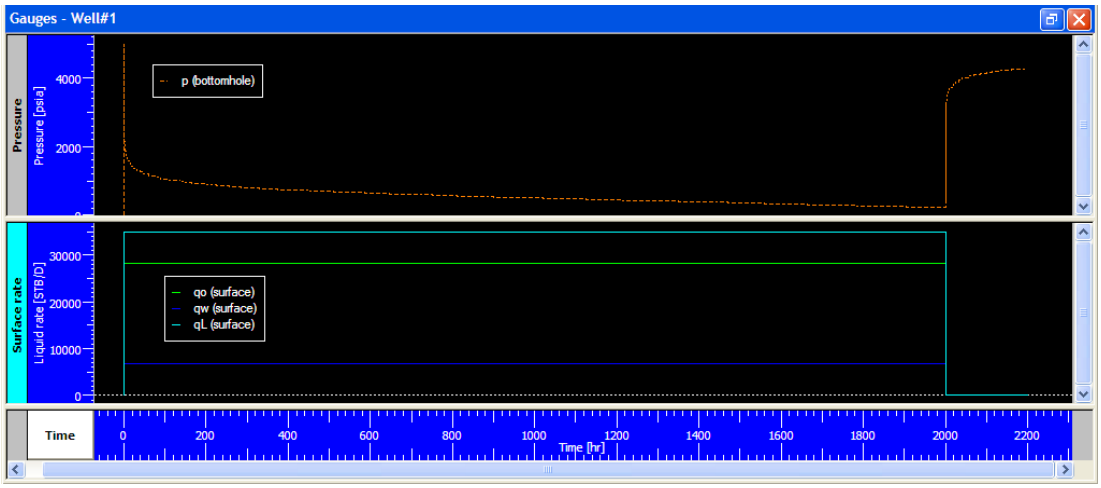

Figure 4.24 : Bottomhole pressure and surface production rate plot for S_w=0.2.

As observed in **Figure 4.24** as soon as water saturation reaches to 0.2 there is a water production about 6853 STB/D. Compare to the case of S_w=0.2 for μ_o=0.45 cp, the water cut value is higher; it is 19.58% as compared to 2.47%. The high value of water production is due to the fact that water becomes more mobile than oil phase.

Figure 4.25 shows the Sapphire buildup interpretation of this case.

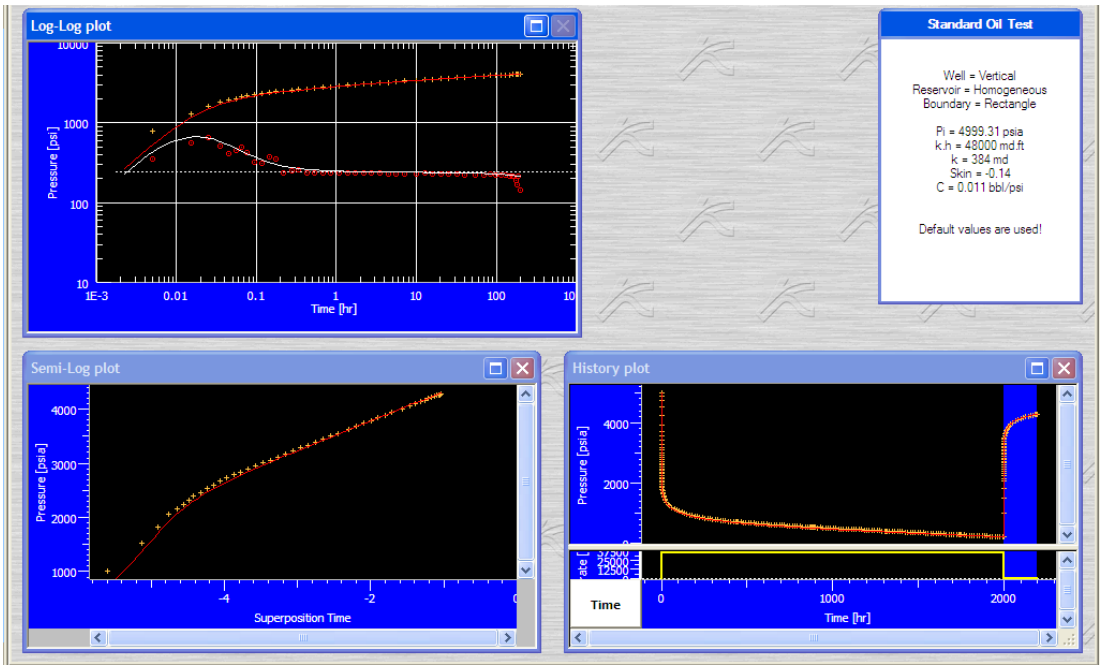

Figure 4.25 : Sapphire buildup analysis in a case of S_w=0.2.

From buildup analysis shown in **Figure 4.25** the permeability is obtained to be 384 md that is slightly less than the input value of 400 md.

Figure 4.26 shows the pressure and production rate plot for S_w=0.3.

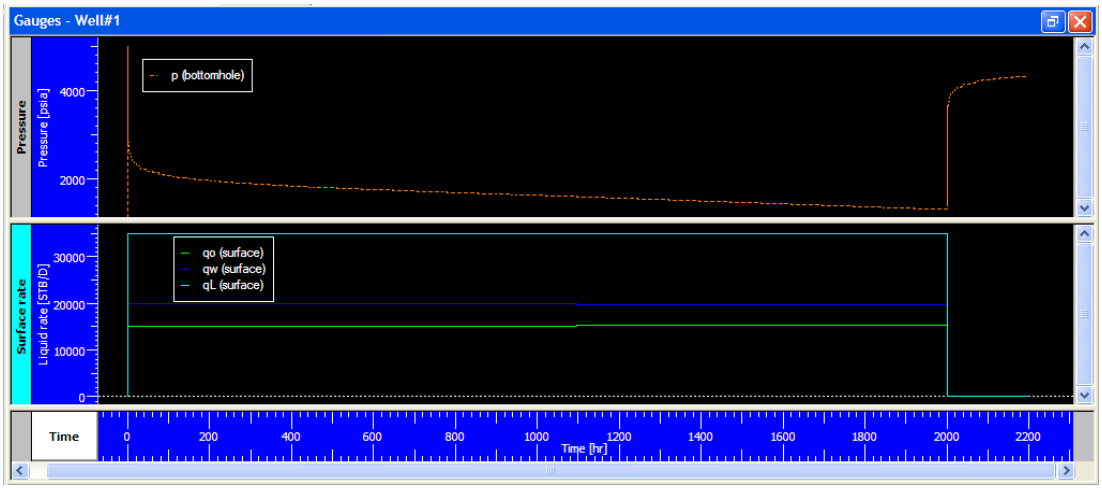

Figure 4.26 : Bottomhole pressure and surface production rate plot for S_w=0.3.

In S_w=0.3 case the production of water has exceeded the oil production. The water cut is 56.35%.

Sapphire buildup interpretation for S_w=0.3 is shown in **Figure 4.27**.

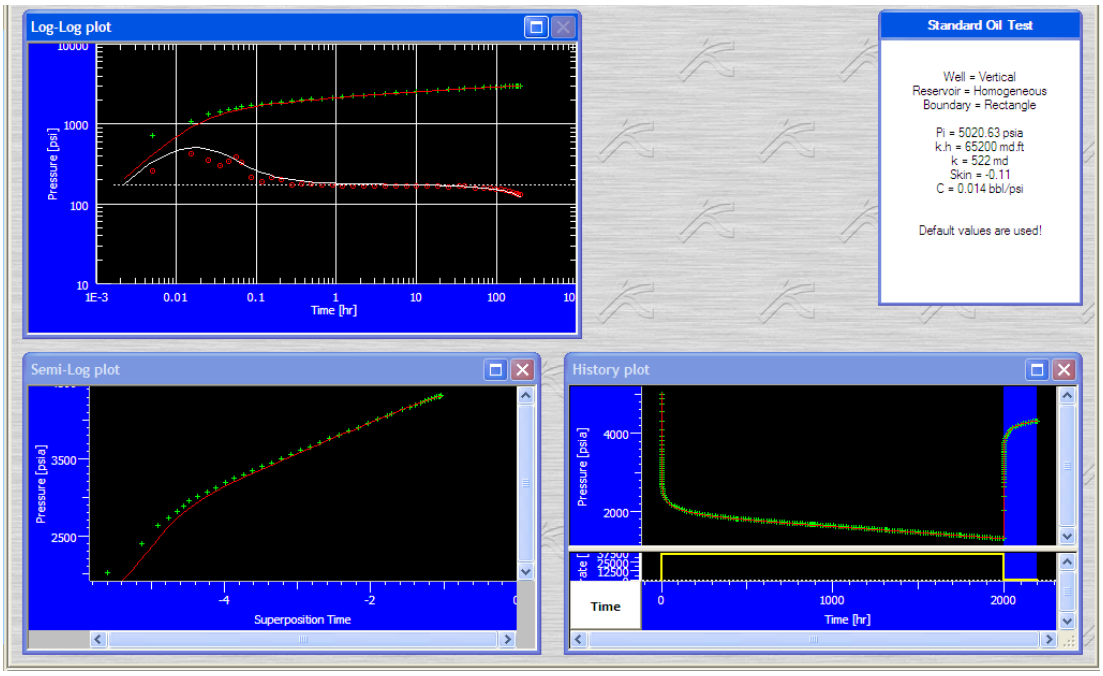

Figure 4.27 : Sapphire buildup analysis in a case of S_w=0.3.

As soon as water phase flow becomes dominant in the system, the fluid mixture becomes more mobile. Then Sapphire buildup analysis results in higher permeability (522 md) than the input value of 400 md.

Figure 4.28 shows the pressure and production rate plot for S_w=0.4.

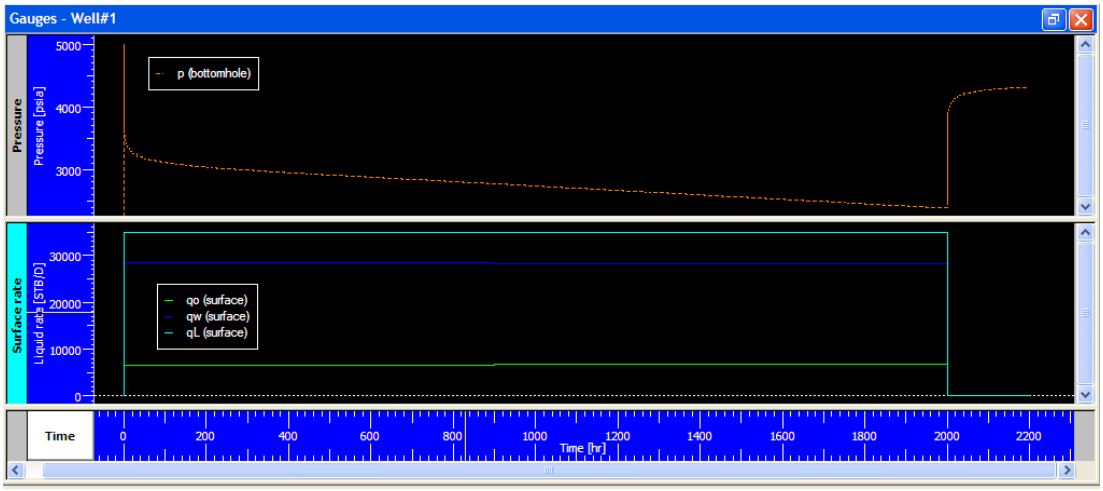

Figure 4.28 : Bottomhole pressure and surface production rate plot for S_w=0.4.

As the water saturation increases, the water production also increases. Water cut in this case is 80.73%.

Sapphire buildup analysis is given in **Figure 4.29**.

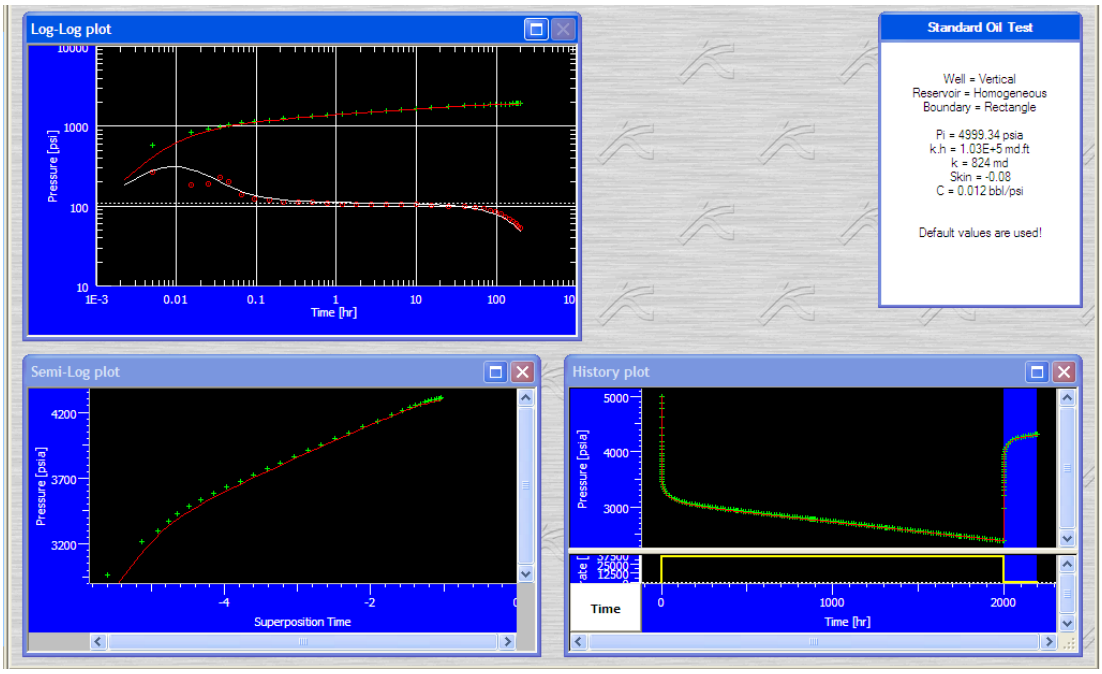

Figure 4.29 : Sapphire buildup analysis in a case of S_w=0.4.

Permeability in this case is 824 md, as expectedly due to much higher mobility of water phase.

Figure 4.30 shows another pressure and production rate plot for S_w=0.5.

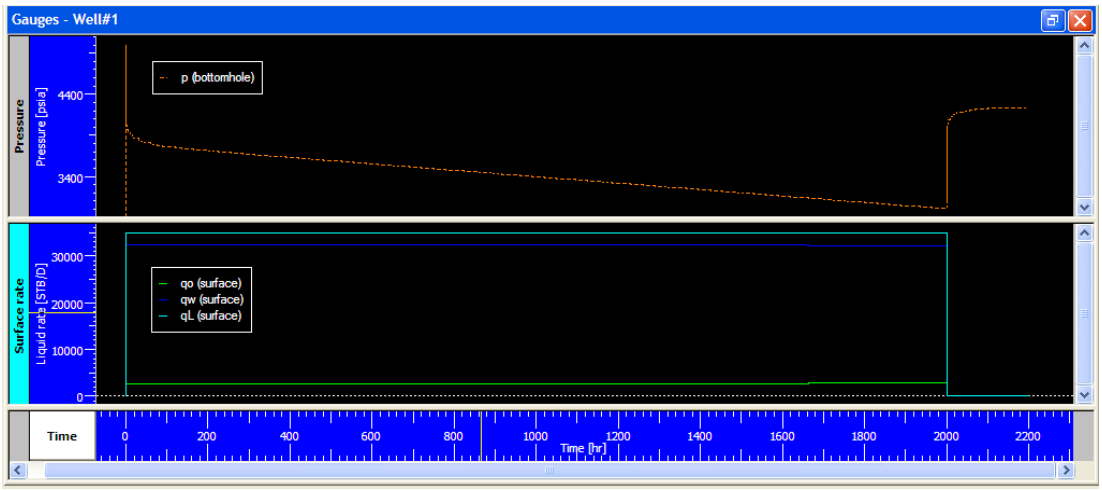

Figure 4.30 : Bottomhole pressure and surface production rate plot for S_w=0.5.

As we see from the plot the water production reached to considerably higher values. Water cut value reached 92.12%.

Figure 4.31 shows the Sapphire buildup interpretation of S_w=0.5 case.

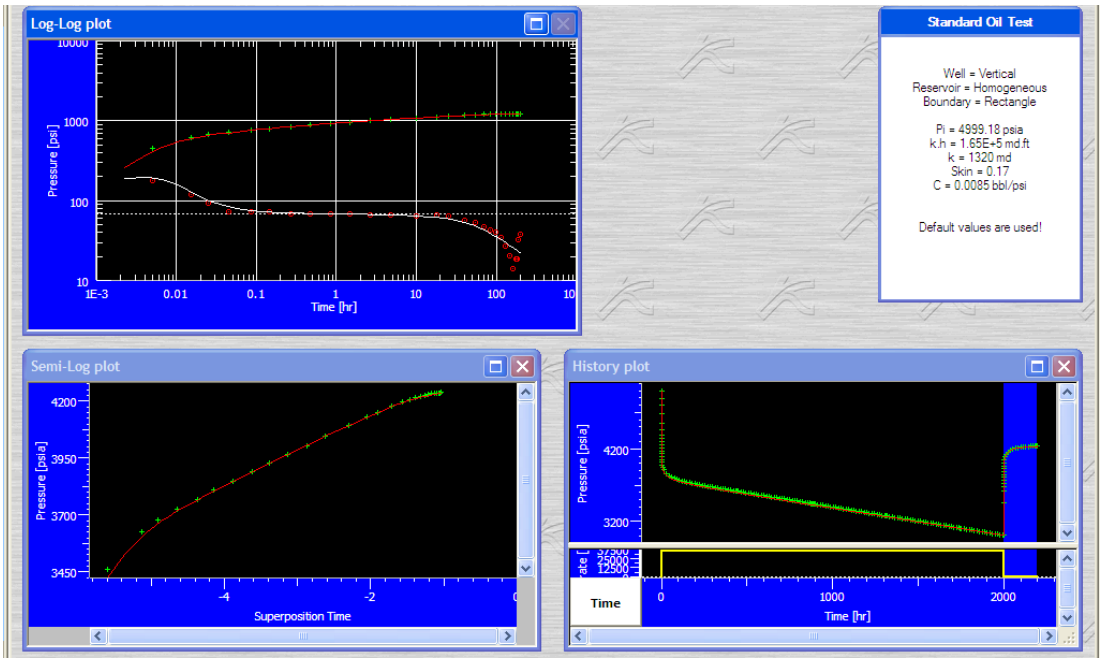

Figure 4.31 : Sapphire buildup analysis in a case of S_w=0.5.

Permeability from the Sapphire analysis is obtained to be 1320 md.

The parameters obtained from Rubis and Sapphire analysis are listed in **Table 4.4**.

Table 4.4 : Data from Rubis model simulation and Sapphire analysis.

Water Saturation, S_w	Bottomhole Pressure, $P_{wf,\,s}$, psia	Water Production, q_w, STB/D	Initial Pressure, P_i, psia	Permeability–Thickness, kh, md-ft	Permeability, k, md	Skin, s	Wellbore storage, C, bbl/psi
0	479.992	0	4999.66	50 000	400	-0.24	0.01
0.1	438.085	0	4999.62	50 000	400	-0.2	0.01
0.2	216.249	6853	4999.31	48 000	384	-0.14	0.01
0.3	1312.38	19724	4999.69	65 200	522	-0.11	0.014
0.4	2385.54	28256	4999.34	103 000	824	-0.08	0.012
0.5	3007.93	32241	4999.18	165 000	1320	0.17	0.0085

We know that the permeability data obtained from the Sapphire analysis are the total effective permeabilities of oil-water fluid mixture. When we increase the oil viscosity to 4.5 cp, we have shown how the water cut and permeability values change. By increasing the oil viscosity, as a result the high mobile water phase production increased the effective fluid permeability obtained from Sapphire analysis.

Figure 4.32 shows the comparison of the oil effective permeability from simulated Rubis model and the total average effective permeability data of the fluid mixture obtained from Sapphire analysis.

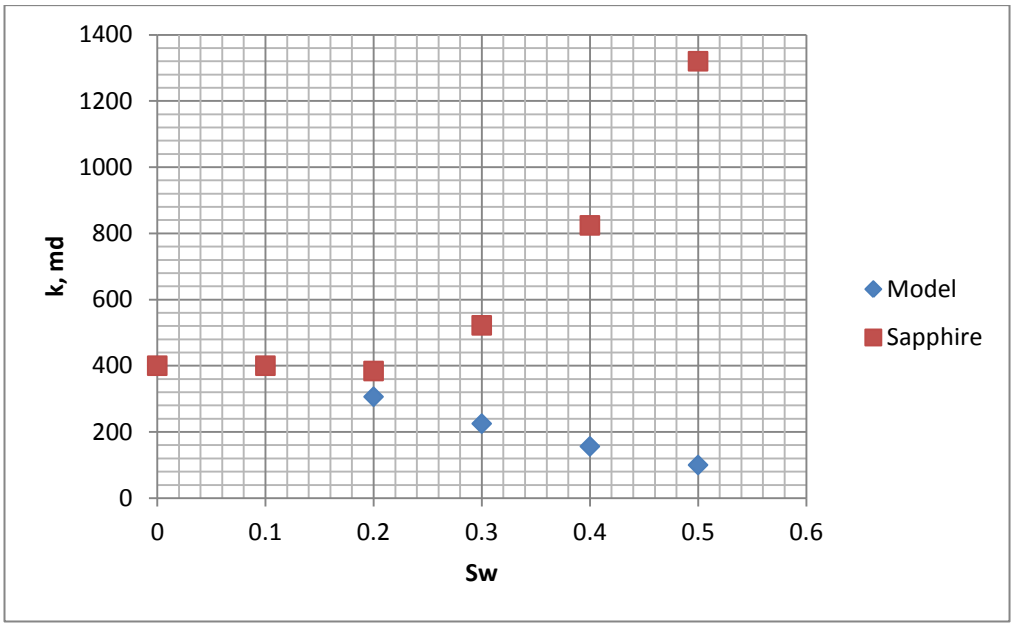

Figure 4.32 : Comparison of effective permeability from Sapphire with oil the permeability from Rubis model.

Using again equation **(4.1)** and same calculation procedures as in section 4.1.1, we can calculate the simulated model total mobility values for the corresponding water saturation values. **Table 4.5** shows the results of these calculations.

Table 4.5 : The calculated values of total mobility of system.

Water Saturation, S_w	Water Cut, %	Oil Relative Permeability, k_{ro}, md	Water Relative Permeability, k_{rw}, md	The Total Mobility of Fluid Mixture, λ_t, md/cp
0	0	1	0	88.889
0.1	0	1	0	88.889
0.2	19.58	0.765	0.0156	85.829
0.3	56.35	0.5625	0.0625	121.429
0.4	80.73	0.3907	0.1407	195.529
0.5	92.12	0.25	0.25	307.937

As in the case of μ_o=4.5 cp, here also we see the same behavior. Calculated total mobility (λ_t) initially declines and then increases from the certain value of the appropriate water saturation value. This total mobility behavior in **Table 4.5** is similar to the fluid mixture permeability behavior obtained from Sapphire in **Table 4.4**. Here we also can check the equality in proportionality of ratios that is given by equation **(4.5)**. For example we can calculate for S_w=0.4:

$$\frac{k_{sw}}{k_{sw_i}} = \frac{824}{400} = 2.06$$

$$\frac{(\lambda_t)_{s_w}}{(\lambda_t)_{s_{wi}}} = \frac{195.529}{88.889} = 2.19$$

As we see the proportionality between the ratios above is almost equal. By using equation **(4.6)**, we can find the permeability values that we found from Sapphire buildup interpretations. **Table 4.6** shows the results of the $(k)_{sw}$ calculations.

Table 4.6 : Calculated $(k)_{sw}$ values.

S_w	$(k)_{sw}$
0	400
0.1	400
0.2	386.23
0.3	546.4298
0.4	879.8794
0.5	1385.715

We can come out with the conclusion that when using the conventional single phase interpretation method by using the Sapphire commercial software for interpreting the two phase oil-water system pressure-time data, the permeability obtained from the single phase interpretation is the total effective permeability of the fluid mixture in the system. Increase in mobility increases the permeability, and decrease in mobility yields a decrease in the permeability.

4.2 Study of The Oil Field With Aquifer

A rectangular oil reservoir with an aquifer, bounded from the east side of the field, was assumed in this second case. The other three boundaries are no flow sealing type. The capillary pressure plot, which is used in this field model, is shown below in **Figure 4.33**.

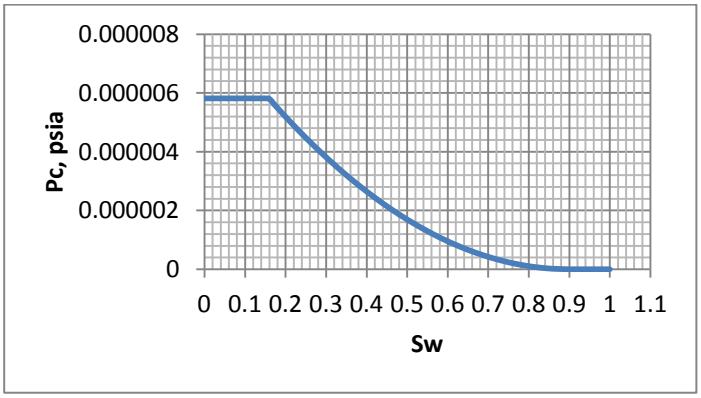

Figure 4.33 : The capillary pressure plot of the model.

The gravity effects are accounted during the simulation of it. The 2D geometry plot of it is given in **Figure 4.34**.

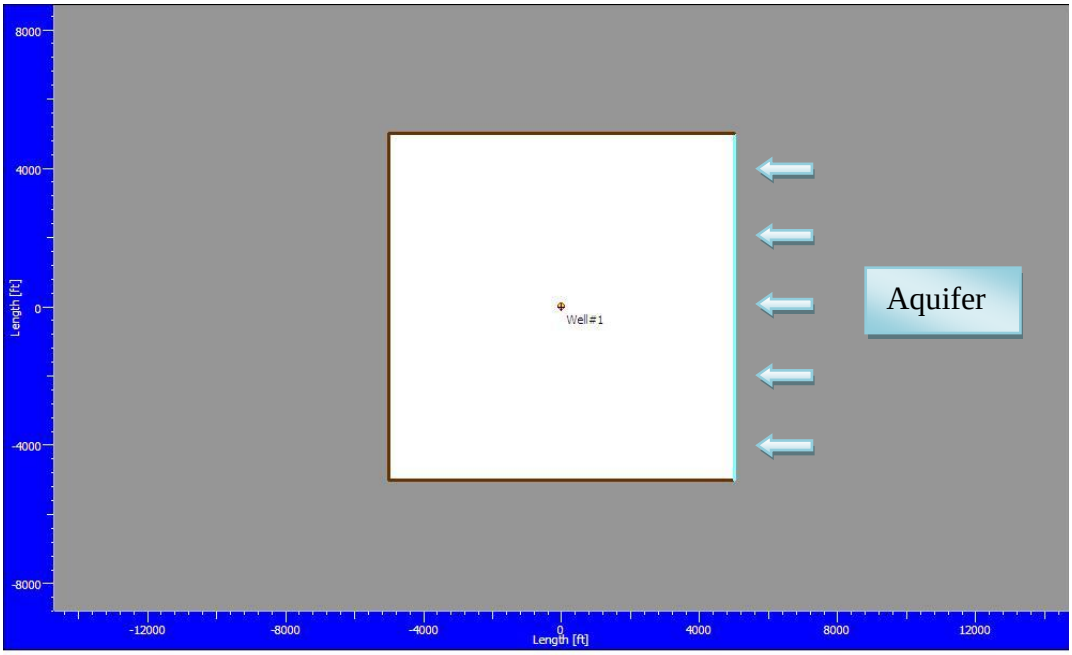

Figure 4.34 : 2D geometry plot of the model.

The relative permeability curve plot is the same as in **Figure 3.2**.

The aquifer properties are represented by Schiltuis constant, in this model it is 204.973 B/D/psi. Schilthuis (1936) proposed a method to determine the water influx from an aquifer into an oil reservoir assuming that the flow is at steady-state. The flow behavior is described below:

$$\frac{dW_e}{dt} = e_w = C(P_i - P) \qquad \textbf{(4.9)}$$

Where W_e is water influx (bbl), e_w is rate of water influx (bbl/day), C is the water influx constant (Schilthuis constant) (bbl/day/psi), P_i is the aquifer pressure, and P is the oil reservoir average pressure.

The study consists of simulating the model in Ecrin Rubis software and then transferring the bottomhole pressure and total surface production rate data to Ecrin Sapphire software. Interpretation in Ecrin Sapphire is conducted for conventional single phase method. The aim is to investigate the aquifer impact on system permeability value.

4.2.1 Case 1: μ_o=0.45 cp

The study is conducted at three conditions. At the first condition (t_p=7000 hr) the water of aquifer has not reached to the well located in the center of the reservoir. At the second condition (t_p=53 000 hr) the aquifer water has reached to the well assuming there is a slight water breakthrough, so the water production is not much. At the third condition (t_p=100 000 hr) the water breakthrough has happened and the water cut value is quite high. The total fluid production is 35 000 STB/D. The shut-in time of buildup tests ($t_{shut\text{-}in}$) is 200 hr. The initial water saturation (S_{wi}) is 0.1. The oil viscosity is 0.45 cp and the water viscosity is 0.35 cp.

For the first condition the bottomhole pressure and surface production rate are shown in **Figure 4.35**. For this condition the production time (t_p) is 7000 hr.

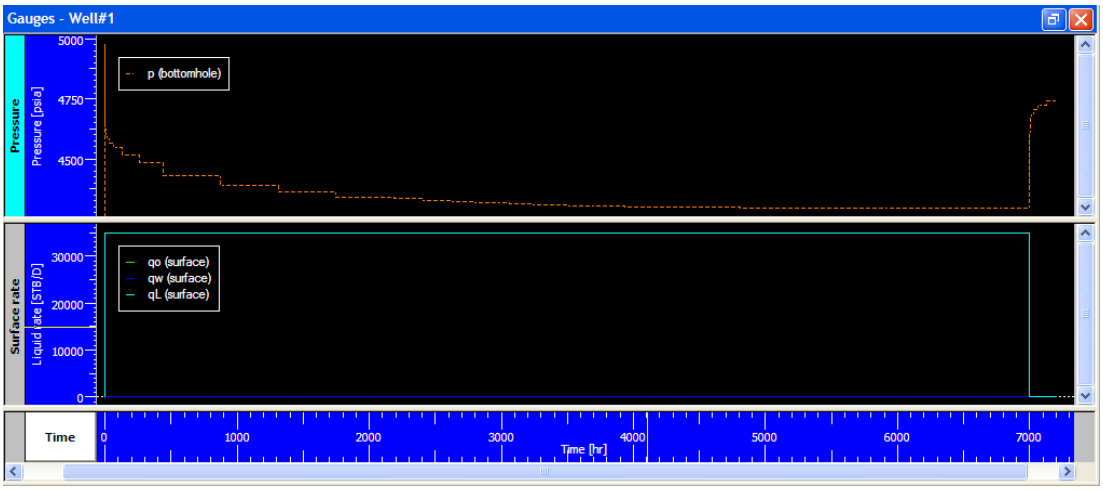

Figure 4.35 : Bottomhole pressure and surface production rate plot for t_p=7000 hr.

As we mentioned at the first condition the water breakthrough has not happened yet, therefore there is not any water production.

The 3D geometry plot of simulated field model is given in **Figure 4.36** below.

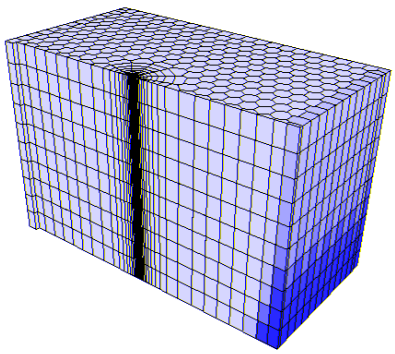

Figure 4.36 : 3D geometry plot of the simulated model.

Figure 4.37 shows the cross sectional saturated map of this condition.

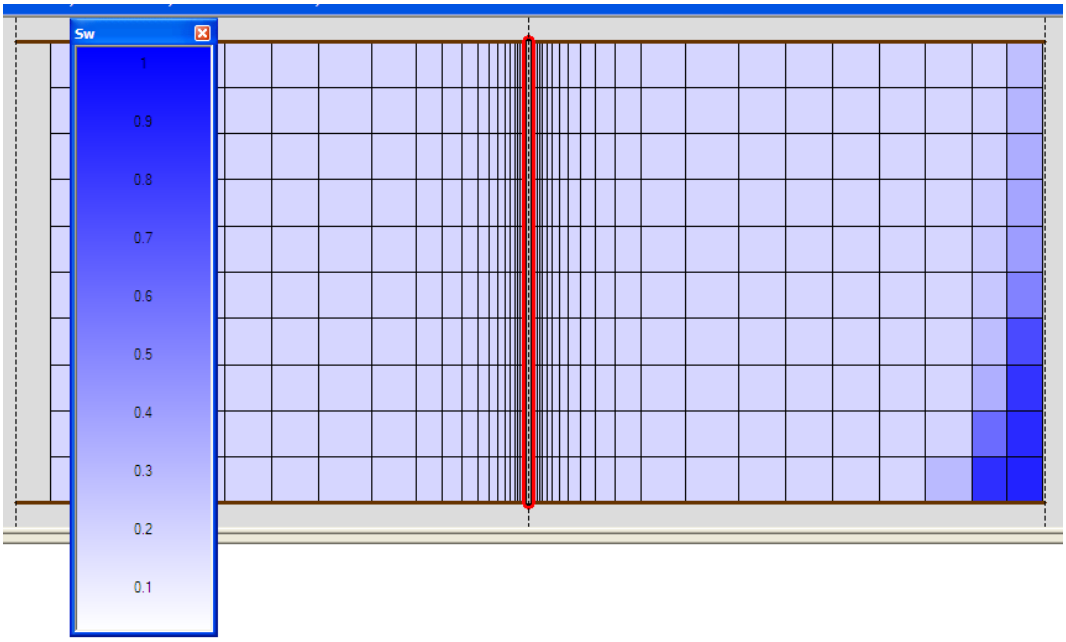

Figure 4.37 : The cross sectional plot of simulated model.

As we see from the plot, the water is entering to reservoir from the east side where the aquifer is located. The Sapphire buildup test interpretation is shown in **Figure 4.38**.

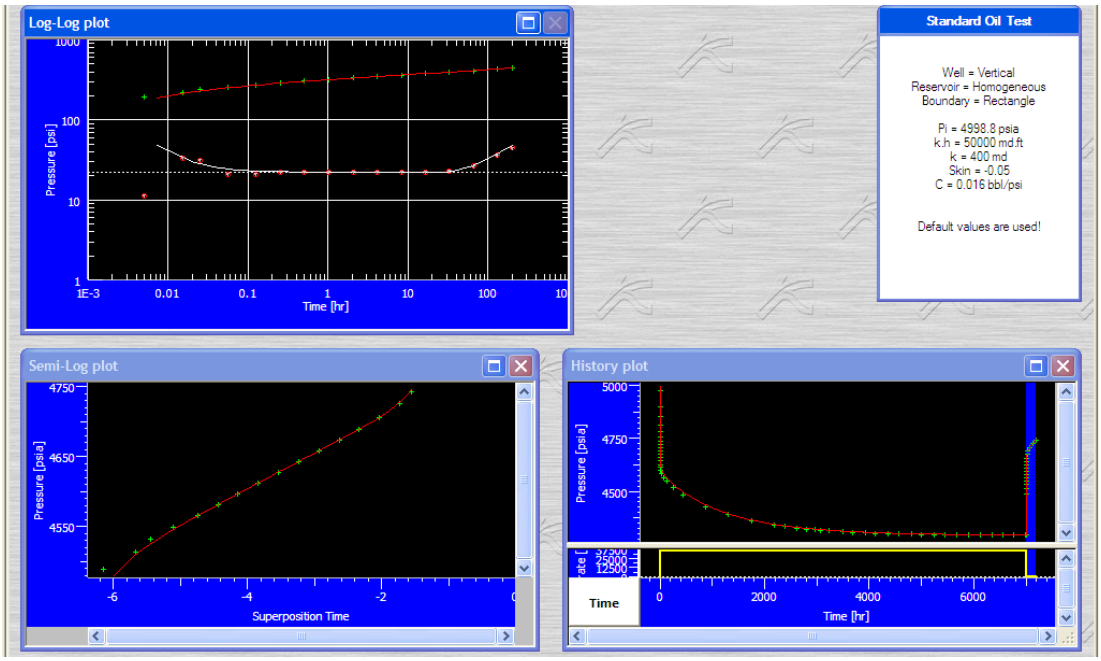

Figure 4.38 : Sapphire buildup analysis for t_p=7000 hr.

From **Figure 4.38** we see that the Sapphire interpretation model does not fully match on the drawdown part of the pressure distribution data in the history plot. It is due to the fact that the eastern part of the field contains a two phase flow system whereas

the western part has only single phase oil system. Analysing this complex system pressure behavior with the Sapphire model which is based on the single phase flow formulation is believed to cause the difference in drawdown part of the pressure-time data. Our emphasis here is to use the Sapphire interpretation model to match the buildup pressure data. According **Figure 4.38** we see that the permeability obtained 400 md which indicates that amount of water influx occured in 7000 hr production time does not affect the overall system permeability.

Figure 4.39 shows the pressure and production rate data plot for the second condition, where the water breakthrough happens, but the water cut value is very small. At the second condition the production time is 53 000 hr.

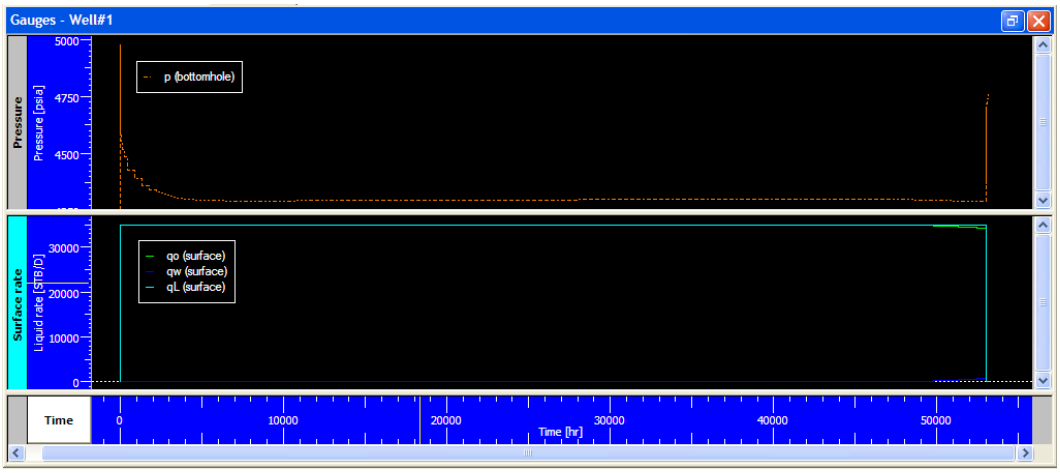

Figure 4.39 : Bottomhole pressure and surface production rate plot for t_p=53 000 hr.

From the plot above we see the water breakthrough has happened approximately after the 50 000 hr of production. The water production rate is 775 STB/D and the water cut value is 2.21%. The 3D geometry plot of simulated field model for this condition is given in **Figure 4.40**.

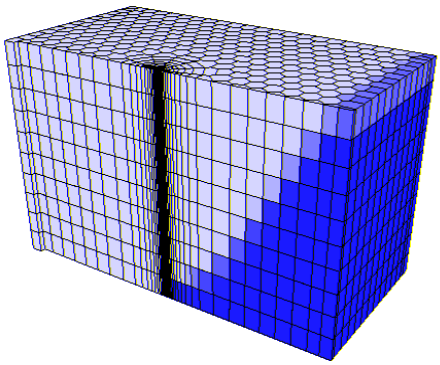

Figure 4.40 : 3D geometry plot of the simulated model.

The water front exhibits a gravity under riding behavior due to higher gravity of water and thus water flows in downward direction in the reservoir. **Figure 4.41** shows the cross sectional plot of the second condition.

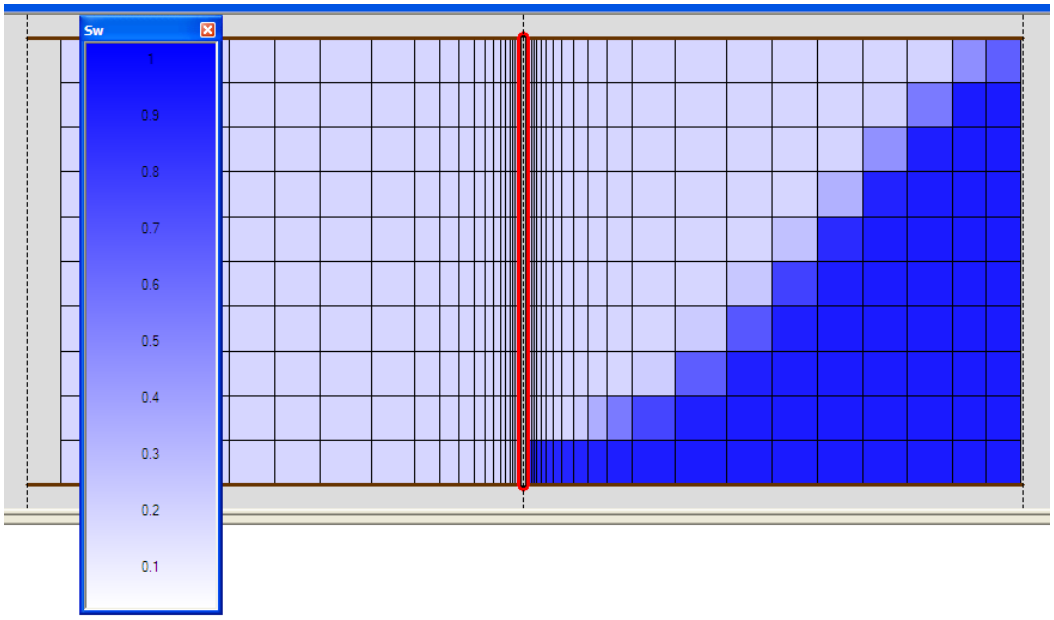

Figure 4.41 : The cross sectional plot of simulated model.

From cross section plot of the field (**Figure 4.41**) the water breakthrough is observed.

The buildup interpretation analysis of the second condition is shown in **Figure 4.42**.

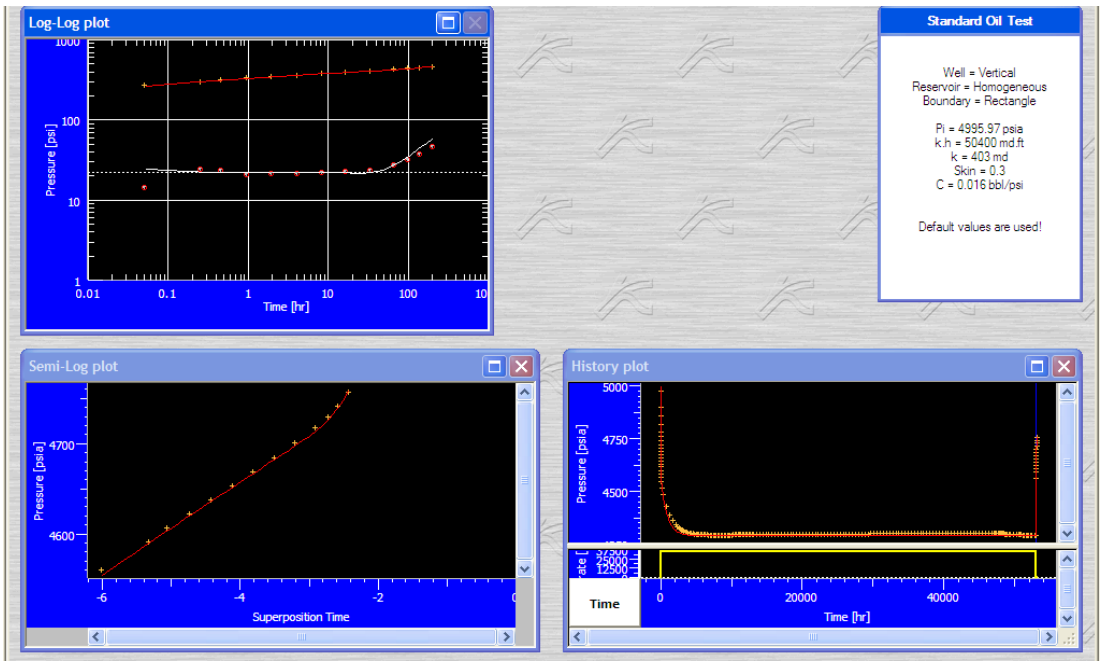

Figure 4.42 : Sapphire buildup analysis for t_p=53 000 hr.

From the interpretation plot we see that little change in permeability value is observed. The permeability is 403 md.

Figure 4.43 shows the pressure and production rate data plot of the third condition, where a considerable water breakthrough has occurred and the water production rate is quite high. The production time for the third condition is 100 000 hr.

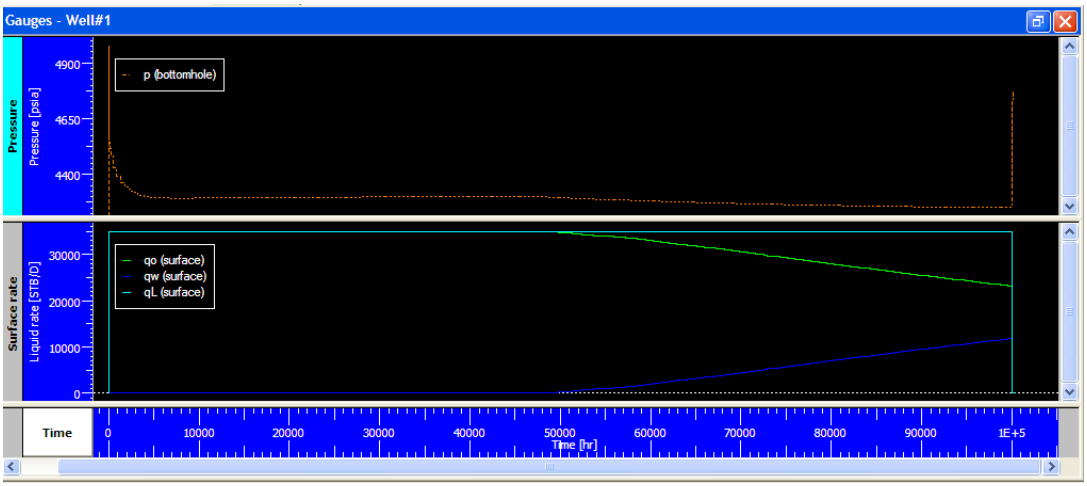

Figure 4.43 : Bottomhole pressure and surface production rate plot for t_p=100 000 hr.

At the third condition the water production reached to 11 768 STB/D and the water cut is 33.62%. **Figure 4.44** shows the cross sectional plot of the model.

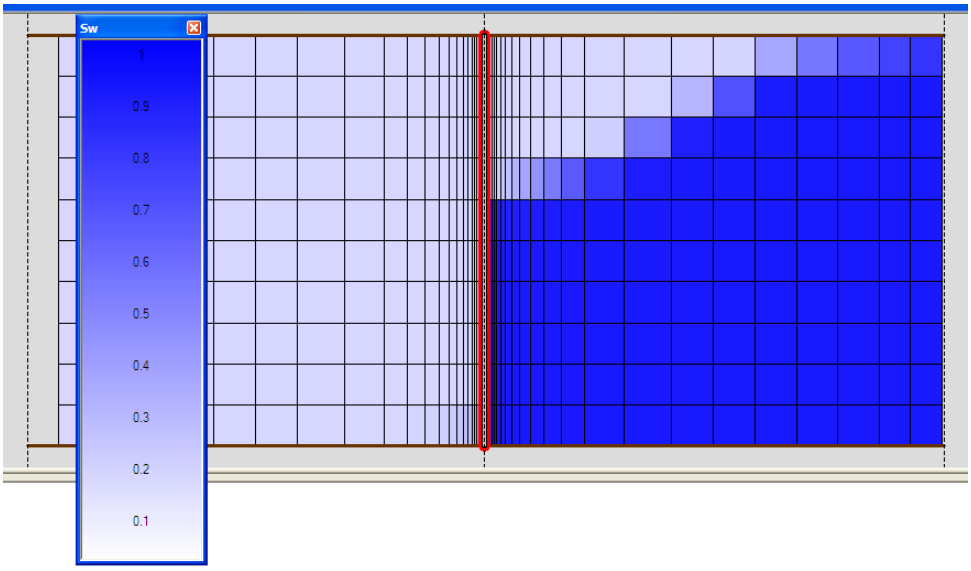

Figure 4.44 : The cross sectional plot of simulated model.

Figure 4.45 shows the 3D geometry plot of the model for this condition.

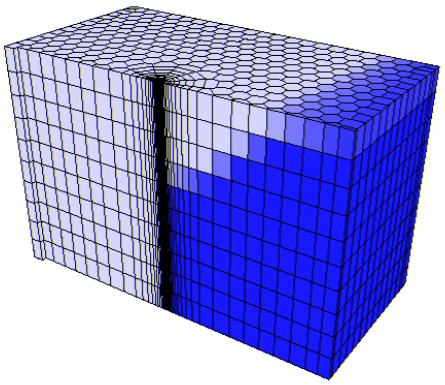

Figure 4.45 : 3D geometry plot of the simulated model.

The Sapphire buildup analysis for the third condition is given in **Figure 4.46**. From **Figure 4.46** we see a slight increase in permeability at third condition. As the amount of the water cut becomes higher, it affects the permeability value.

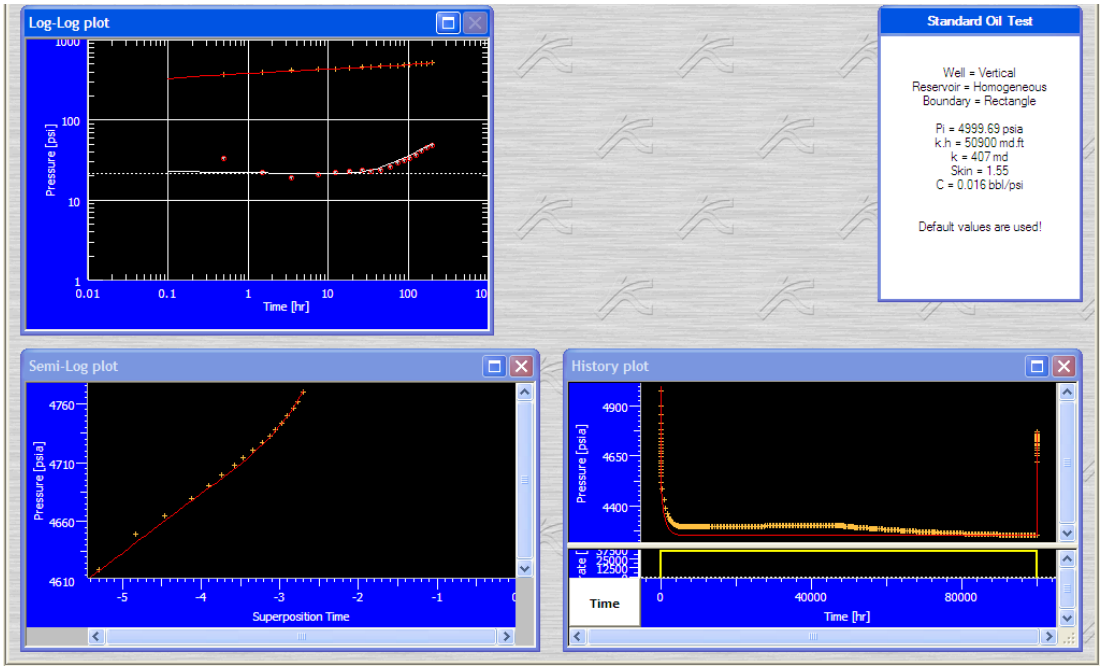

Figure 4.46 : Sapphire buildup analysis for t_p=100 000 hr.

Results obtained from Rubis simulation model and from Sapphire buildup interpretations are given in **Table 4.7**:

Table 4.7 : Data from Rubis model simulation and Sapphire analysis.

Production Time, t_p, hr	$P_{wf,s}$, psia	Water Production, q_w, STB/D	Initial Pressure, P_i, psia	Permeability-Thickness, kh, md-ft	Permeability, k, md	Skin, s	Wellbore Storage, C, bbl/psi
7000	4293.35	0	4998.8	50 000	400	-0.05	0.016
53 000	4289.57	775	4895.97	50 400	403	0.3	0.016
100 000	4250.79	11768	4999.69	50 900	407	1.55	0.016

As mentioned before our system is simulated in Rubis as a two phase system, but in Sapphire it was interpreted using single phase method. Sapphire assumes the whole system as if there is only oil phase in it, and in this case the obtained permeability data from Sapphire are the total effective permeability of oil-water fluid mixture.

From **Table 4.7** we see that the permeability increases as water influx increases. The mobility difference between the phases plays an important role. Because the water phase is more mobile compare to oil, it impacts the system parameters. At the first condition we know that the water breakthrough has not occurred and there is not any water production and the obtained total fluid mixture effective permeability is as same as the absolute permeability that is used in Rubis model simulation. At the second condition the water breakthrough occurred, and it increased permeability slightly. At the third condition the water cut is at considerably high levels. This considerable increase affects the permeability data, as we see from **Table 4.7**.

In this case for analyzing the system we cannot use equation **(4.1)**. In the case without an aquifer the water saturation is equally distributed through the system, but here one side of the field is invaded by the water so, the water saturation is not equally distributed. Our system is partially composite. The initial water saturation is 0.1. The reservoir is consisted of two zones. The first zone is the oil zone, where $S_o=1-S_w$ and oil relative permeability (k_{ro}) is 1. The volume of the oil zone we can define as V_{oz}. The second zone is the water invaded zone, where the water saturation is greater than initial water saturation ($S_w>S_{wi}$) and the water relative permeability (k_{rw}) is less than 1. The volume of the water invaded zone is defined as V_{ow}. The sum of oil and water zone volume yield the total reservoir volume, respectively ($V=V_{oz}+V_{wz}$).

To analyze the system properly we propose a new term; the volumetric averaged total mobility. The reason that we use a volumetric average for the total mobility representing the reservoir is simple, because the permeability (which is effective) determined from the well test analysis represents the permeability of the reservoir tested by a transient pressure test. We can find the volumetric averaged total mobility as:

$$\bar{\lambda}_t = \left(\frac{V_{oz}}{V}\right) \cdot \frac{k}{\mu_o} + \left(\frac{V_{wz}}{V}\right) \cdot \frac{k k_{rw}}{\mu_w} \qquad \textbf{(4.10)}$$

We know that in water invaded zone the water relative permeability is less than one ($k_{rw}<1$), but we do not know the exact value of the relative water permeability value. Therefore if we assume that in water invaded zone the invasion is going as piston-like displacement, then the water relative permeability becomes one ($k_{rw}=1$) and $S_w=1-S_{or}$.

To use equation **(4.10)** we need to know V_{oz}, V_{wz}, V values. We can find V_{wz} and V_{oz} as:

$$V_{wz} = \frac{W_w}{\phi} \tag{4.11}$$

$$V_{oz} = V - V_{wz} \tag{4.12}$$

W_w is volume of water for the water invaded zone in reservoir at any time. We can describe it as:

$$W_w = \begin{bmatrix} Water\ Volume \\ Initially\ in \\ The\ Reservoir \end{bmatrix} + \begin{bmatrix} Cumulative\ Amount \\ of\ Water\ Influx \end{bmatrix} - \begin{bmatrix} Cumulative\ Amount \\ of\ Water\ Produced \end{bmatrix}$$

We can calculate W_w as below:

$$W_w = W_i + W_e - W_p \tag{4.13}$$

W_i, W_e and W_p are the initial volume of water in the reservoir, cumulative water influx and cumulative water production, respectively. Water influx values we can get from Rubis simulation model. We can calculate the volume of the initial water as:

$$W_i = V_p S_{wi} \tag{4.14}$$

Our reservoir is rectangular and we know the length (10 000 ft) and the width (10000 ft) of it. So the area (A) of our field yields 10^8 ft^2. The reservoir thickness (h) is 125 ft. Then the bulk volume of reservoir is:

$$V = Ah = 10^8 \cdot 125 = 1.25 \cdot 10^{10}\ ft^3$$

We know the reservoir porosity (ϕ) is 0.22. So then the pore volume is:

$$V_p = V\phi = 0.22 \cdot 1.25 \cdot 10^{10} = 2.75 \cdot 10^9\ ft^3$$

So, W_i is $2.75 \cdot 10^8$ ft^3. In the first condition (t_p=7000 hr) 1/35 part of reservoir is invaded by water, so in this case we need to multiply W_i to 1/35. In the second condition (t_p=53 000 hr) the water invasion is 1/4 part of whole reservoir, in the third condition (t_p=100 000 hr) this value is 1/3 part of the reservoir. The cumulative water production (W_p) data are obtained from Ecrin simulator.

Table 4.8 shows the calculated W_w data for this case.

Table 4.8 : Calculated W_w data.

Production Time, t_p, hr	Water Cut, %	Water Influx, W_e, MM ft^3	Cumulative Water Production, W_p, MM ft^3	Volume of Water At Corresponding Time, W_w, MM ft^3
7000	0	46.51	0	54.37
53 000	2.21	407.8	0.1201	476.4
100 000	33.62	779.5	67.65	803.5

Afterwards we can calculate the V_{wz} and V_{oz} values. The absolute permeability (k) from model is 400 md. Now we have all parameters that we need for equation **(4.10)**. The obtained volumetric averaged total mobility values for the piston-like approach are given in **Table 4.9**.

Table 4.9 : Calculated volumetric averaged total mobility values for piston-like displacement.

Production Time, t_p, hr	Water Invaded Zone Volume, V_{wz}, MM ft^3	Oil Zone Volume, V_{oz}, MM ft^3	The Volumetric Averaged Total Mobility of Fluid Mixture, $\bar{\lambda}_t$, md/cp
7000	247.1	12253	893.910
53 000	2166	10334	932.888
100 000	3652	8847.7	963.095

By using equation **(4.15)** we can apply the proportionality equality of ratios:

$$\frac{(k)_t}{(k)_{t=0}} = \frac{(\bar{\lambda}_t)_t}{(\bar{\lambda}_t)_{t=0}} \qquad \textbf{(4.15)}$$

Where: $(k)_t$ – permeability from Sapphire test analysis, $(k)_{t=0}$ – permeability at initial state (400 md), $(\bar{\lambda}_t)_t$ – the volumetric averaged total mobility, $(\bar{\lambda}_t)_{t=0}$ - total mobility at initial state, here it is 888.889 md/cp.

Table 4.10 shows the calculation results of equation **(4.15)** for each three conditions.

Table 4.10 : Calculation results of equation **(4.15)**.

Production Time, t_p, hr	$\frac{(k)_t}{(k)_{t=0}}$	$\frac{(\bar{\lambda}_t)_t}{(\bar{\lambda}_t)_{t=0}}$
7000	1	1.006
53 000	1.0075	1.049
100 000	1.0175	1.083

The piston-like displacement approach is an idealized case. In reality the water relative permeability value of the water invaded zone is less than one, as we mentioned above. Because in reality there remain oil in water invaded zone. In this case the water saturation will not be equal to (1-S_{or}), such as $S_w \neq (1 - S_{or})$, the value of water saturation will be the average water saturation behind the front ($S_w = \bar{S}_w$) and the water relative permeability will increase as the invasion time increases. The volumetric averaged total mobility for this case is written below:

$$\bar{\lambda}_t = \left(\frac{V_{oz}}{V}\right) \cdot \frac{k}{\mu_o} + \left(\frac{V_{wz}}{V}\right) \cdot \frac{k(k_{rw})_{\bar{s}_w}}{\mu_w} \qquad \textbf{(4.16)}$$

As we see from equation **(4.16)**, the value of the water relative permeability must be evaluated at the average water saturation. The average water saturation ($\bar{S}_w$) value can be found from Buckley – Leverett analysis. In this topic the calculation of average water saturation value due to Buckley – Leverett is not within our scape. If we assume that the value of $(k_{rw})_{\bar{s}_w} = 0.82$, then we can use equation **(4.16)** for the real case. The results of these calculations are in **Table 4.11**.

Table 4.11 : Calculated volumetric averaged total mobility values for $(k_{rw})_{\bar{s}_w}$=0.82.

Production Time, t_p, hr	Volumetric Averaged Total Mobility, $\bar{\lambda}_t$, md/cp
7000	889.843
53 000	897.249
100 000	902.988

By using equation **(4.15)** to check the equality in proportionality of ratios are given in **Table 4.12**.

Table 4.12 : Calculation results of equation **(4.15)** for $(k_{rw})_{\bar{s}_w}$=0.82.

Production Time, t_p, hr	$\frac{(k)_t}{(k)_{t=0}}$	$\frac{(\bar{\lambda}_t)_t}{(\bar{\lambda}_t)_{t=0}}$
7000	1	1.001
53 000	1.0075	1.009
100 000	1.0175	1.016

In **Table 4.12** the obtained ratios are better than the ratios in **Table 4.10**. This fact is also proves that the relative water permeability in the water invaded zone is less than one.

The main difference between the oil field without aquifer case and the the oil field with aquifer case is, in the first study case the water phase exists uniformly in the whole system, but in the second case the water is entering from outside, namely from aquifer.

4.2.2 Case 2: μ_o=4 cp

To study how the oil viscosity affects the results, we conducted the same investigation that we did in section 4.2.1 this time oil viscosity is 4 cp. The total fluid production rate is the same 35 000 STB/D. Buildup shut-in time is 200 hr.

The pressure and production rate data of the first condition when the water breakthrough has not occurred is shown in **Figure 4.47**. The production time is 10000 hr.

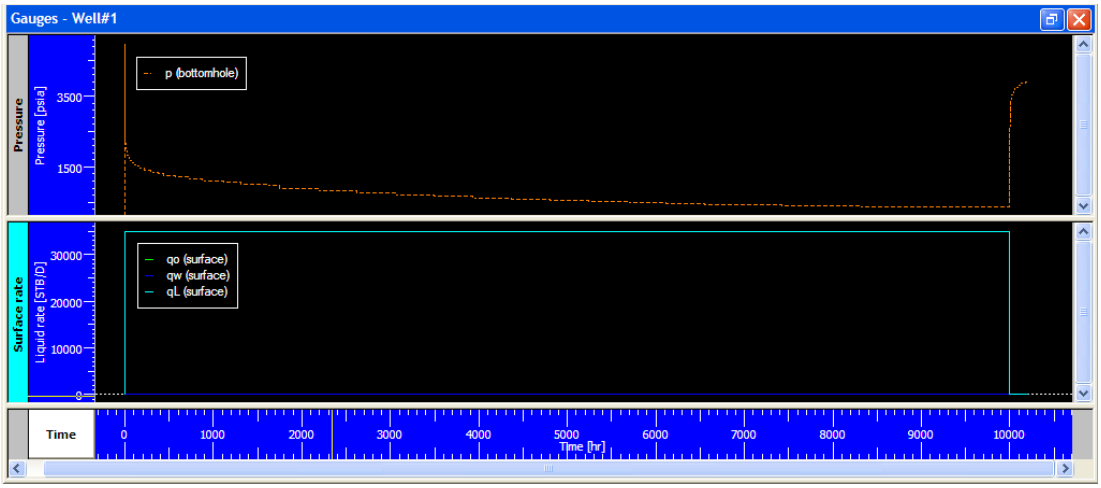

Figure 4.47 : Bottomhole pressure and surface production rate plot for t_p=10 000 hr.

As we see there is not any water production, because the water from aquifer has not reached to well yet.

Sapphire buildup analysis of this condition is shown in **Figure 4.48**.

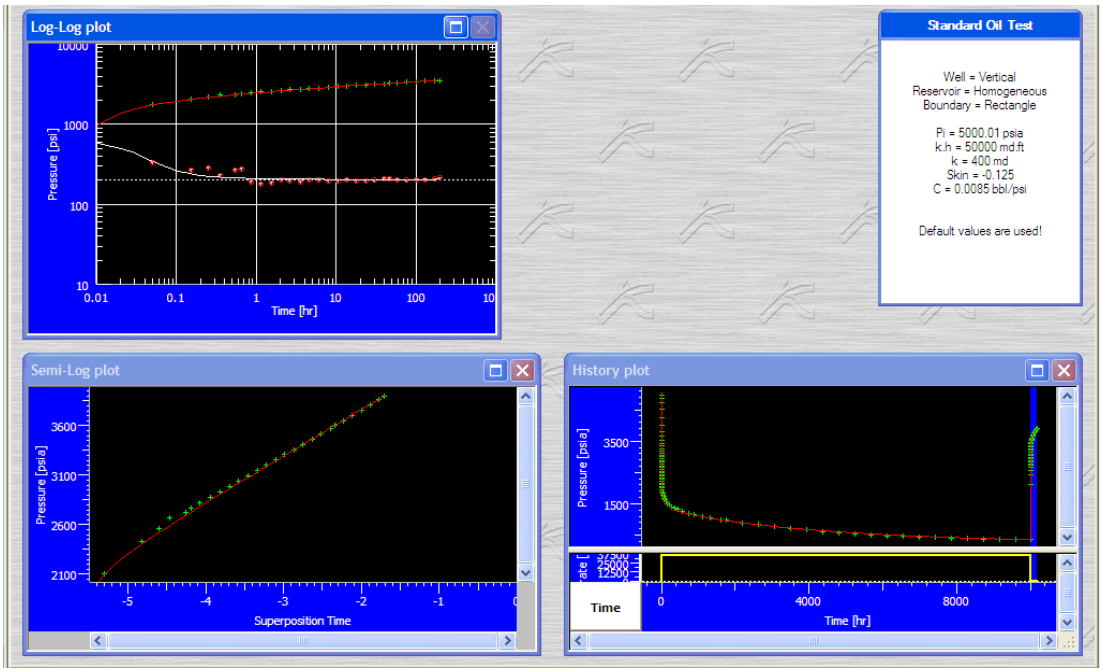

Figure 4.48 : Sapphire buildup analysis for t_p=10 000 hr.

Just like in the first condition of section 4.2.1, here also there is no change in permeability. **Figure 4.49** shows the cross sectional plot of the first condition.

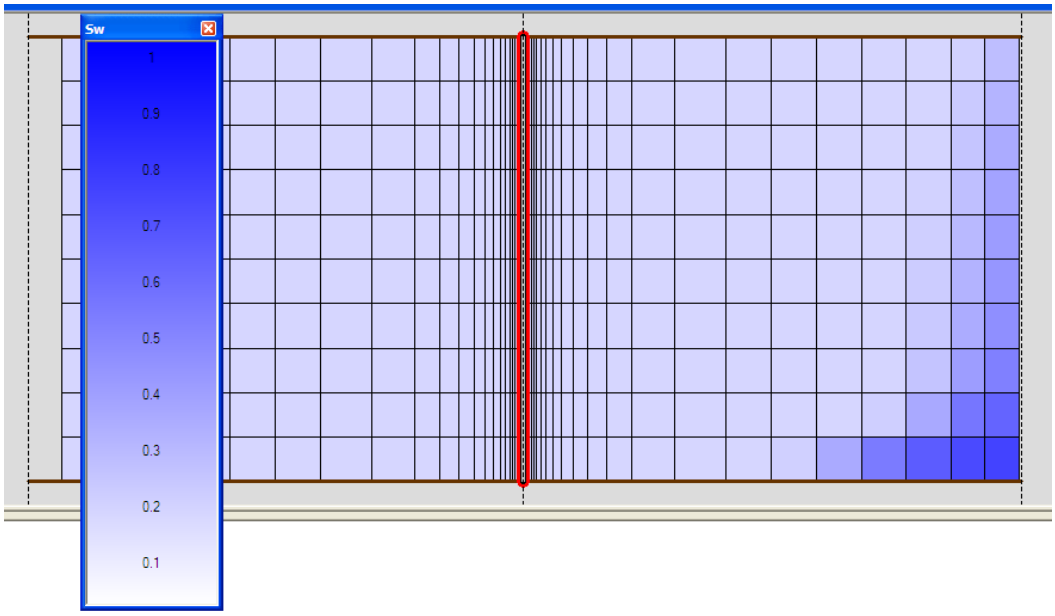

Figure 4.49 : The cross sectional plot of simulated model.

Figure 4.50 shows the 3D geometry plot of the model related to this condition.

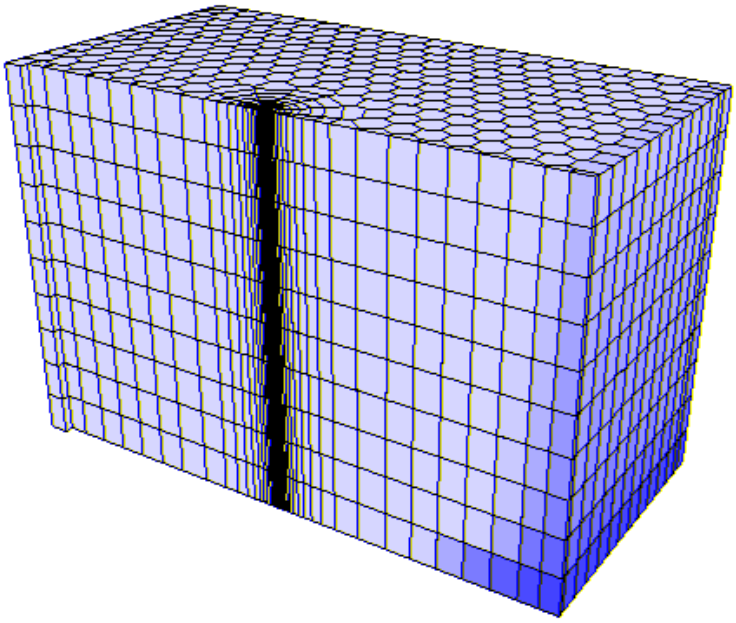

Figure 4.50 : 3D geometry plot.

The pressure and production rate for the second condition when the water breakthrough happened and the water cut is negligible is shown in **Figure 4.51.**

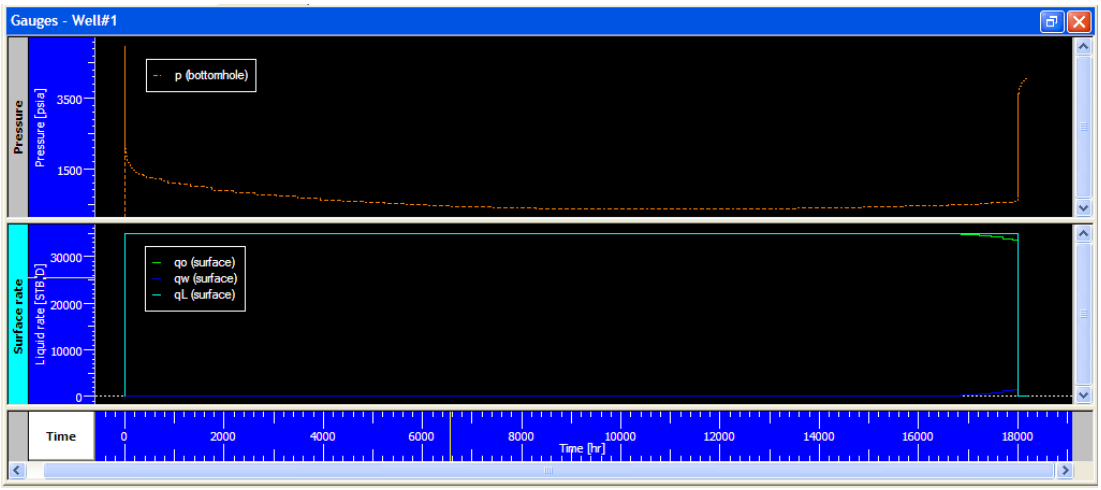

Figure 4.51 : Bottomhole pressure and surface production rate plot for t_p=18 000 hr.

The water cut in the second condition is 4%. The production time for second condition is 18 000 hr.

The buildup interpretation of the second condition is shown in **Figure 4.52**.

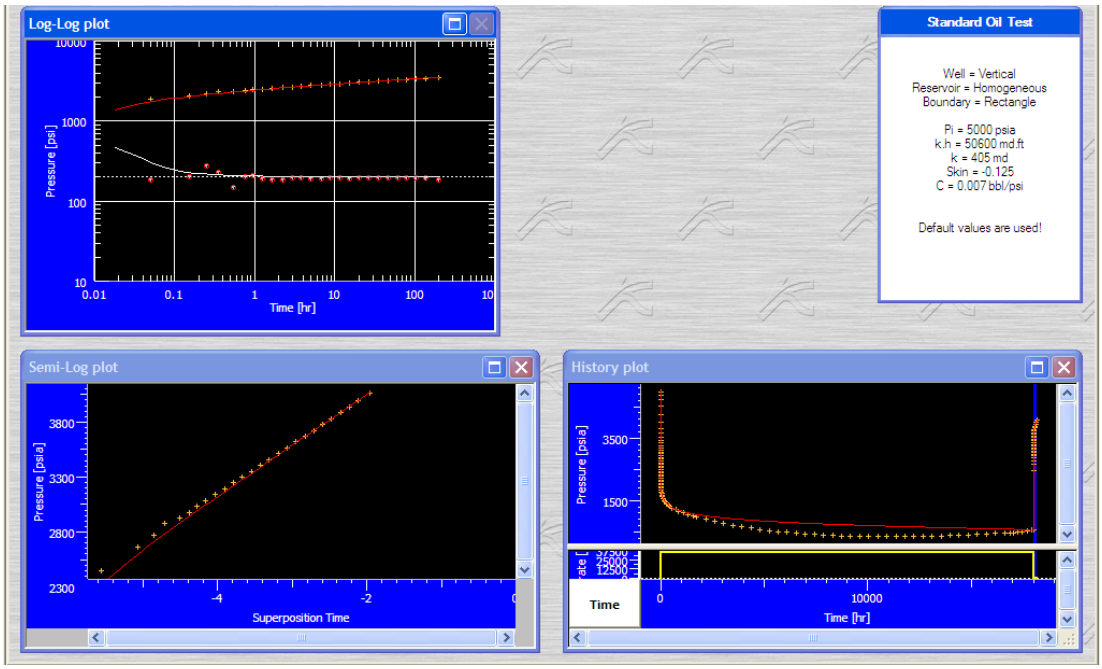

Figure 4.52 : Sapphire buildup analysis for t_p=18 000 hr.

As soon as water phase reached the well, the water production started. This phenomenon affects the permeability. The permeability increased and became 405 md. The cross sectional plot of this condition is given in **Figure 4.53**.

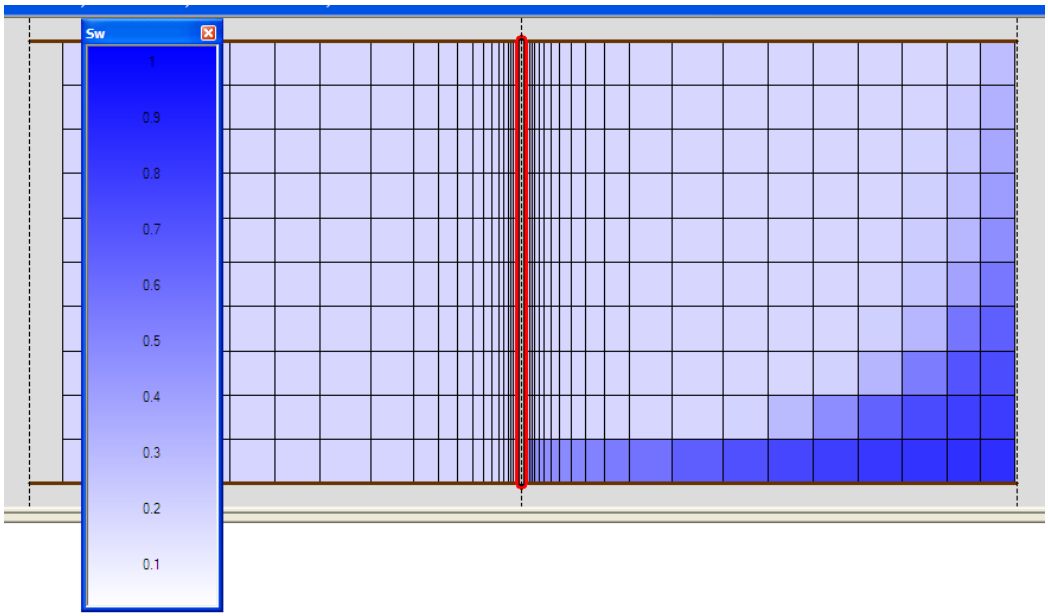

Figure 4.53 : The cross sectional plot of simulated model.

The 3D geometry plot of the second condition is given in **Figure 4.54.**

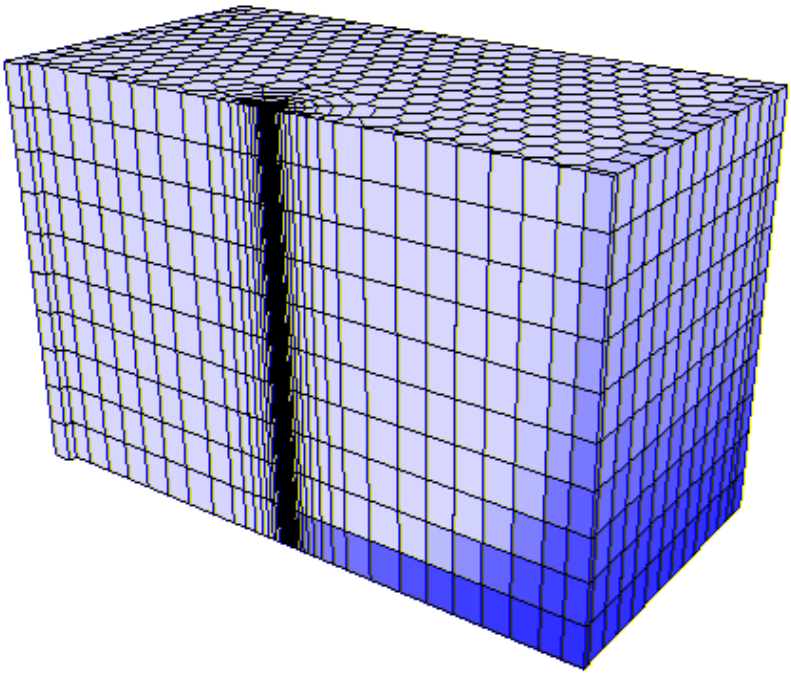

Figure 4.54 : 3D geometry plot.

Figure 4.55 shows the pressure and production rate data related to third condition, when the production time is 30 000 hr.

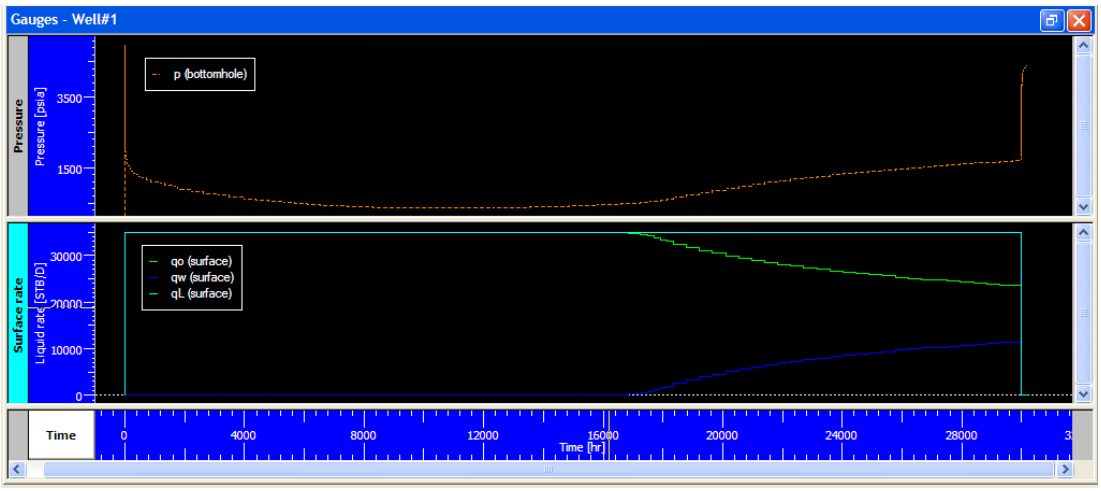

Figure 4.55 : Bottomhole pressure and surface production rate plot for t_p=30 000 hr.

The water production rate is 11 490 STB/D and the water cut increased and reached to 32.83%.

Sapphire interpretation analysis related to this condition is given in **Figure 4.56**.

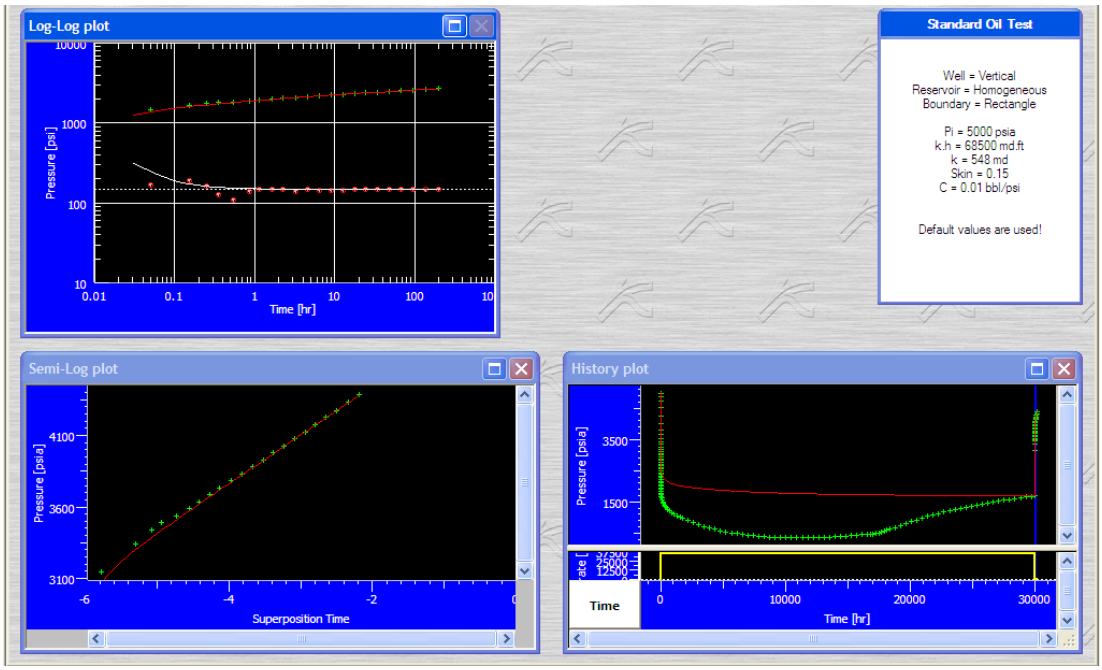

Figure 4.56 : Sapphire buildup analysis for t_p=30 000 hr.

From **Figure 4.56** we see that the permeability value increased and reached to 548 md when the water cut increased.

The cross sectional plot of this condition is given in **Figure 4.57**.

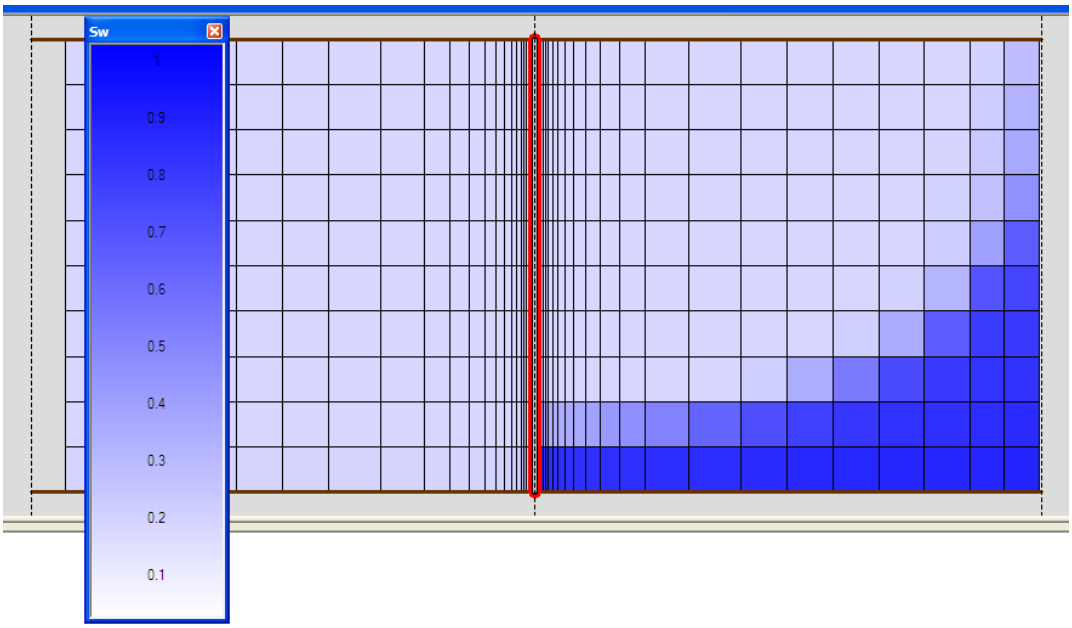

Figure 4.57 : The cross sectional plot of simulated model.

The 3D geometry plot of the second condition is given in **Figure 4.58**.

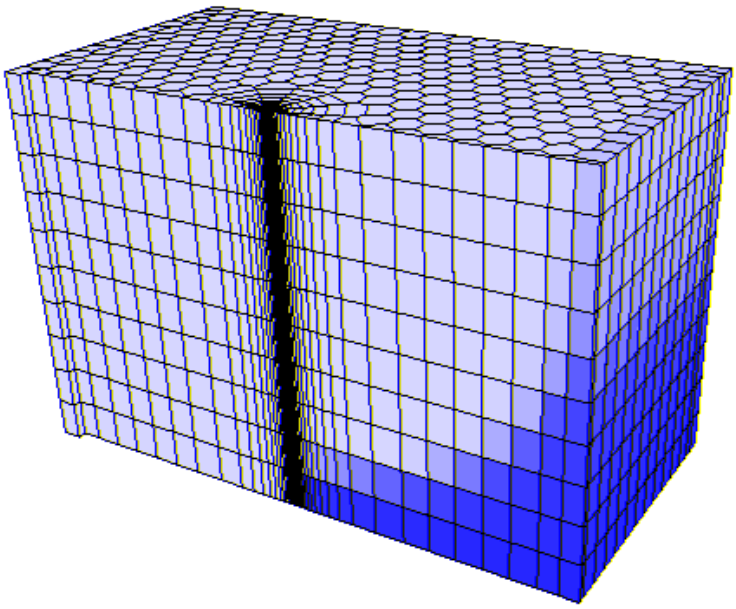

Figure 4.58 : 3D geometry plot.

Results obtained from Rubis simulation model and from Sapphire buildup interpretations are given in **Table 4.13**.

Table 4.13 : Data from Rubis model simulation and Sapphire analysis.

Production Time, t_p, hr	$P_{wf,\,s}$, psia	Water Production, q_w, STB/D	Initial Pressure, P_i, psia	Permeability-Thickness, kh, md-ft	Permeability, k, md	Skin, s	Wellbore Storage, C, bbl/psi
10 000	354.882	0	5000.01	50 000	400	-0.125	0.0085
18 000	570.139	1402	5000	50 600	405	-0.125	0.007
30 000	1696.43	11 490	5000	68 500	548	0.15	0.01

The permeability obtained from Sapphire buildup interpretation analysis is not input permeability. These permeability values are the total effective permeability data of the oil-water fluid mixture. To calculate the volumetric averaged total mobility values of our two phase system we use equation **(4.10).** As in section 4.2.1, here we also need to know water volume in system at corresponding time (W_w), cumulative water influx (W_e), initial water volume in the system (W_i), cumulative production (W_p), reservoir volume (V), oil zone (V_{oz}) and water invaded zone (V_{wz}) parameters. We have calculated W_i and V parameters in section 4.2.1. Using equation **(4.13)** we can find water volume in system at any time. **Table 4.14** shows the calculated W_w values. In the first condition (t_p=10 000 hr) the water invasion is 1/35 part of the reservoir. In the second condition (t_p=18 000 hr) the water invasion is 1/12 part and in the third condition (t_p=30 000 hr) the water invasion is 1/8 part of the reservoir.

Table 4.14 : Calculated W_w data.

Production Time, t_p, hr	Water Cut, %	Water Influx Value, W_e, MM ft^3	Cumulative Water Production, W_p, MM ft^3	Volume of Water At Corresponding Time, W_w, MM ft^3
10 000	0	51.13	0	58.99
18 000	4	116.9	0.286	139.5
30 000	32.83	218.9	22.4	230.9

Now we have all parameters that we need to use equation **(4.10)**.

The obtained volumetric averaged total mobility values for the piston-like displacement approach are given in **Table 4.15**.

Table 4.15 : Calculated volumetric averaged total mobility values for piston-like displacement.

Production Time, t_p, hr	Water Invaded Zone Volume, V_{wz}, MM ft^3	Oil Zone Volume, V_{oz}, MM ft^3	The Volumetric Averaged Total Mobility of Fluid Mixture, $\bar{\lambda}_t$, md/cp
10 000	268.12	12 232	122.369
18 000	634.23	11 866	152.913
30 000	1049.5	11 450	187.561

Table 4.16 shows the calculation results of equation **(4.15)** for each three conditions. Note that $(\bar{\lambda}_t)_{t=0}$=100 md/cp.

Table 4.16 : Calculation results of equation **(4.15)** for piston-like approach.

Production Time, t_p, hr	$\frac{(k)_t}{(k)_{t=0}}$	$\frac{(\bar{\lambda}_t)_t}{(\bar{\lambda}_t)_{t=0}}$
10 000	1	1.224
18 000	1.0125	1.529
30 000	1.37	1.876

As we see from the **Table 4.16** there is no equality between the ratios. So, that shows us the value of water relative permeability is less than one.

If we take $(k_{rw})_{\bar{s}_w}$=0.48, and apply the equation **(4.16)**, then the volumetric total averaged mobility will be below:

Table 4.17 : Calculated volumetric averaged total mobility values for $(k_{rw})_{\bar{s}_w}$=0.48.

Production Time, t_p, hr	The Volumetric Averaged Total Mobility of Fluid Mixture, $\bar{\lambda}_t$, md/cp
10 000	109.622
18 000	122.760
30 000	137.663

Then by applying equation **(4.15)**, the results will be as given in **Table 4.18** below:

Table 4.18 : Calculation results of equation **(4.15)** for $(k_{rw})_{\bar{s}_w}$=0.48.

Production Time, t_p, hr	$\frac{(k)_t}{(k)_{t=0}}$	$\frac{(\bar{\lambda}_t)_t}{(\bar{\lambda}_t)_{t=0}}$
10 000	1	1.096
18 000	1.0125	1.228
30 000	1.37	1.377

In **Table 4.18** the obtained ratios are better than the ratios in **Table 4.16**.

From **Table 4.10** we see the same track in between mobility and permeability values. Mobility values increase during the production time and the same track follows in **Table 4.18**. Another interesting fact associated with the difference in viscosity values between the phases. By the high difference viscosity we actually create difference in mobility values between the phases. Let's compare the third condition of both the section 4.2.1 and section 4.2.2. In section 4.2.1 when the water cut value reached to 33.62% the permeability in buildup analysis obtained 407 md. In section 4.2.2 when the water cut reaches to 32.83% the value of the permeability, which is from buildup analysis, is 548 md. So, from this fact we can come into a conclusion that in water-oil systems when there is high difference in viscosity values between the oil and water (μ_o=4 cp, μ_w=0.35 cp) phases, using the single phase interpretation method, the permeability value reaches to high values than the actual one.

5. CONCLUSIONS

A rectangular oil reservoir model is simulated by Ecrin Rubis software and the impact of water phase on the permeability of the reservoir is investigated in two cases. In literature single phase well test interpretation methods are well known. Although our simulated model is in two phase flow, by using Ecrin Sapphire software, we conducted interpretation using the single phase interpretation method. We studied two cases. In the first case the assumed rectangular model is bounded with no flow sealing boundaries. The study is conducted to investigate how the water saturation would affect the permeability obtained from the buildup tests. This investigation is conducted for two conditions. The first condition assumes that the viscosity difference between the phases were not high. Whereas the second condition assumes that the viscosity difference between the phases were high. As it is expected the permeability obtained from Sapphire buildup analysis that is based on single phase interpretation method, does not represent the real permeability of the multiphase system. These permeabilities represent the total effective permeability values of the oil-water fluid mixture of system. Our study showed that there is a relationship between the model total mobility and total effective fluid mixture permeability. Our analysis clearly indicated that the change in water saturation affects the permeability. The range of this change is clearly observed particularly when the viscosity difference between phases was high. The water phase becomes more mobile and impacts the permeability by increasing them considerably.

In the second case the simulated oil field model was bounded with aquifer from the east side. In the first part of this analysis the viscosity difference between the phases is assumed to be low, but in the second part it is taken to be high. Three conditions were investigated in each part. The first condition is the water from the aquifer has not reached to the well, in the second condition the water reached the well, but the water cut is small. In the last condition the water breakthrough has happened and the value of water cut reached to considerably high value. The buildup tests obtained from two phase flow data were analyzed by using the single phase flow interpretation method. Methods of calculating volumetric averaged total mobility concept are

shown. The relationship between the volumetric averaged total mobility values of model and the permeability from buildup tests is validated.

Results of this study clearly indicates that the change of permeability is directly proportional with the change of the total multiphase mobility. As Perrine approach suggested the total multiphase mobilities should be used to analyse the buildup data and the effective (or relative) permeability can be obtained from the relative permeability data by knowing the water saturation at that stage of the field history. Such conclusion is valid if the water saturation is uniform throught the reservoir.

If the oil field is patially supported by an aquifer, the pressure buildup analysis should be interpreted by using volumetric averaged total mobilities as suggested in this report. Since such a system consists of two zones, an oil zone with an initial water saturation and a water invaded zone with an average water saturation, using the volumetric averaged total mobility in pressure buildup analysis of the multiphase system is suggested.

REFERENCES

Al-Khalifah A.J., Horne R.N. and Aziz K. (1989). Multiphase Well Test Analysis: Pressure and Pressure-squared Methods. SPE California Regional Meeting, Bakersfield, California, April 6-7. SPE 18803.

Ayan C. and Lee W.J. (1988a). Multiphase Pressure Buildup Analysis: Field Examples. SPE California Regional Meeting held in Long Beach, California, March 23-25. SPE 17412.

Al-Khalifah, K. Aziz, and Horne R.N. (1987). A New approach to Multiphase Well Test Analysis. The 62nd Annual Technical Conference and Exhibition of the Society of Petroleum Engineers, Dallas, TX, September 27-30. SPE 16743.

Ayan C., Lee W.J. (1988b). The Effects of Multiphase Flow on the Interpretation of Pressure-Buildup Tests. SPE Formation Evaluation, June, 459-466.

Bourdet D. (2002). Well Test analysis-The Use of Advanced Interpretation Models. Elsevier, 2002.

Chu W-C., Reynolds A.C., Raghavan R. (1986). Pressure Transient Analysis of Two-Phase Flow Problems. SPE Formation Evaluation, April, 151-164.

C&C Reservoirs (2005). Field Evaluation Report. Azeri-Chirag-Gunashli Field Complex. South Caspian Basin, Azerbaijan, August.

Escobar F-H. and Montealegre-M. M. (2008). Application of TDS Technique to Multiphase Flow. CT&F – Ciencia, Tecnologia y Futuro – Vol. 3 Num. 4.

Horne R. N., (1995). Modern Well Test Analysis. A Computer-Aided Approach. Second Edition. Petroway, Inc., 1995.

Ibrahimov T., (2014). Personal Communication, BP, ACG Team Lider.

Kamal M. M. and Pan Y. (2010). Use of Transient Data to Calculate Absolute Permeability and Average Fluid Saturations. SPE Reservoir Evaluation & Engineering, April, 306-312.

Kamal M. M. and Pan Y. (2011). Pressure Transient Testing Under Multiphase Flow Conditions. SPE Middle East Oil and Gas Show and Conference, Manama, Bahrain, 25-28 September 2011. SPE 141572.

Martin J. C. (1959). Simplified Equations of Flow in Gas Drive Reservoirs and the Theoretical Foundation of Multiphase Pressure Buildup Analyses. Petroleum Transactions of AIME, 216, 321-323.

Perrine R.L. (1956). Analysis of Pressure-buildup Curves. Presented at the spring meeting of the Pacific Coast District, Division of Production, Los Angeles, May 1956.

Raghavan R. (1989). Well-Test Analysis for Multiphase Flow. SPE Formation Evaluation, December, 585-594.

Schilthuis, R.J. (1936). Active Oil and Reservoir Energy. Transactions of AIME, Vol. 118, 33-52.

Sharifi M., Ahmadi M. (2009). Two-Phase Flow in Volatile Oil Reservoir Using Two-Phase Pseudo-Pressure Well Test Method. Journal of Canadian Petroleum Technology, September 2009, Volume 48, No. 9.

Vo Dyung T. and Raghavan Rajagopal (1991). An Approximate Analysis Method for Multiphase Flow Data. SPE Formation Evaluation, March, 121-128.

Weller W. T. (1966). Reservoir Performance During Two-Phase Flow. Journal of Petroleum Technology, February, 240-246.

Wethington W. B., Reddick C., and Husseynov B. (2002). Development of a Super Giant, ACG Field, Offshore Azerbaijan: An Overview. AAPG Search and Discovery Article #90007©2002 AAPG Annual Meeting, Houston, Texas, March 1-13, 2002.

Zheng S. and Xu W. (2009). New Approaches for Analyzing Transient Pressure from Oil And Water Two-Phase Flowing Reservoir. 2009 Kuwait International Petroleum Conference and Exhibition, Kuwait City, Kuwait, 14-16 December 2009.

Url-1 <*http://www.bp.com*>, accessed 15.02.2014.

Url-2 <*http://www.wikimedia.org*>, accessed 18.02.2014

CURRICULUM VITAE

PHOTO

Name Surname: Gismat VALIYEV

Place and Date of Birth: Armenia, 14.03.1986

Address: Nizami district, E. Suleymanov Street 118, Baku, Azerbaijan

E-Mail: velili@live.com

B.Sc.: Azerbaijan State Oil Academy

Professional Experience and Rewards: Reward of Student Scientific Society in 56th Scientific Technical Conference of Azerbaijan State Oil Academy in 2007.